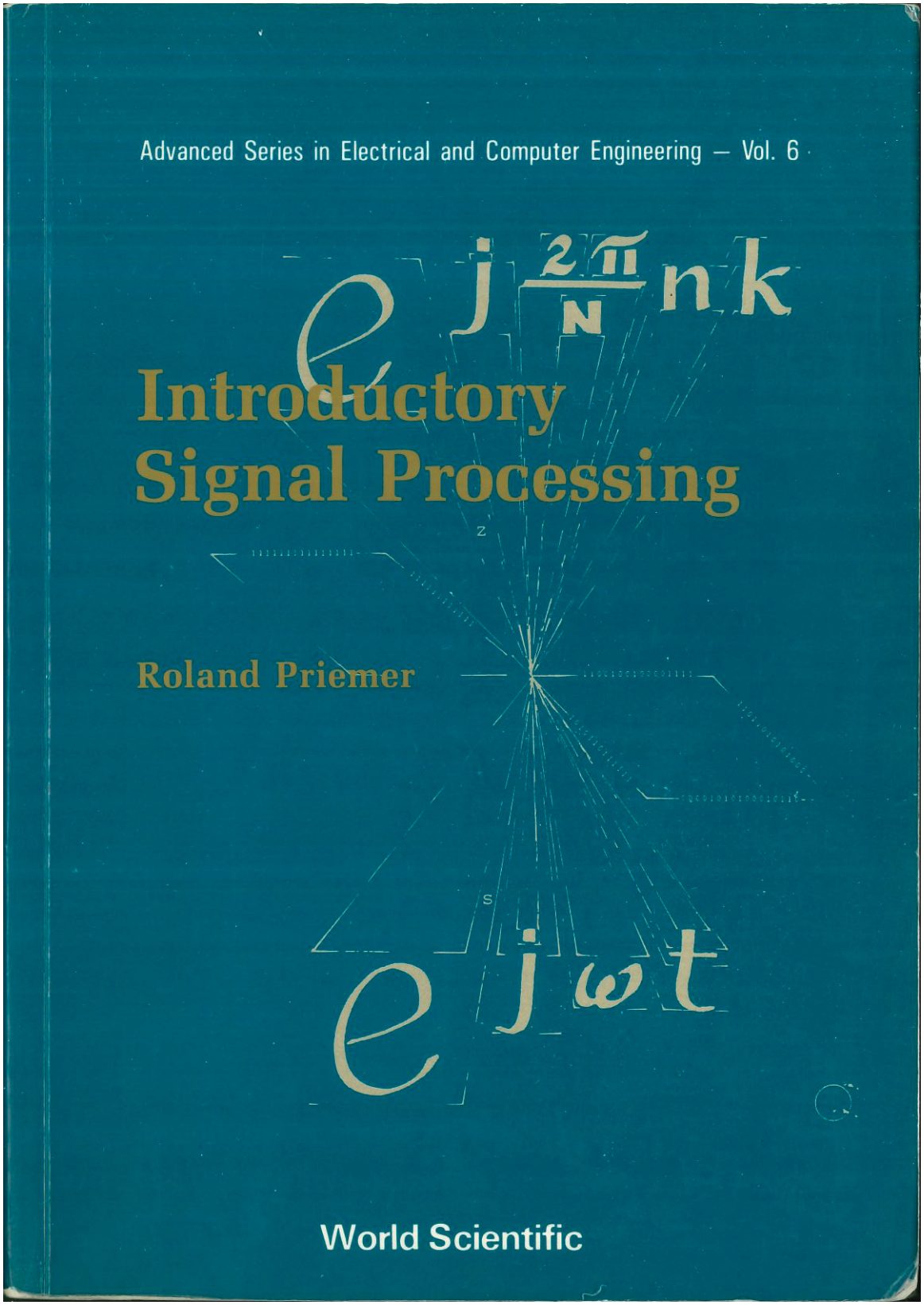
Advanced Series in Electrical and Computer Engineering – Vol. 6



Introductory Signal Processing

Roland Priemer

World Scientific

Comcast, Ex. 1141

Priemer
Introductory Signal Processing

Published by
World Scientific Publishing Co. Pte. Ltd.
P O Box 128, Farrer Road, Singapore 9128
USA office: 687 Hartwell Street, Teaneck, NJ 07666
UK office: 73 Lynton Mead, Totteridge, London N20 8DH

Library of Congress Cataloging-in-Publication data is available.

INTRODUCTORY SIGNAL PROCESSING

Copyright © 1991 by World Scientific Publishing Co. Pte. Ltd.

All rights reserved. This book, or parts thereof, may not be reproduced in any form or by any means, electronic or mechanical, including photocopying, recording or any information storage and retrieval system now known or to be invented, without written permission from the Publisher.

ISBN 9971-50-919-9
9971-50-920-2 (pbk)

Printed in Singapore by Loi Printing Pte. Ltd.

TABLE OF CONTENTS

Chapter Zero *Signals and Signal Processing* **1**

Chapter One *Basic Linear System Theory* **10**

1-1 Systems 10
1-1.1 System Properties 11
1-1.2 Linear Operator 31
1-2 Exponential Function 32
1-3 Response of LTI Systems to Complex Exponential Functions 37
1-3.1 Complete Response of a First Order System 37
1-3.2 Frequency Response 42
1-3.3 Complete Response of an n^{th} Order System 55
1-3.4 LTI System Stability 64
1-4 Impulse Response of LTI Systems 67
1-4.1 Impulse Function 68
1-4.2 Impulse Response 73
1-4.3 Continuity of Initial Conditions 78
1-5 Convolution 82
1-6 Bounded Input-Bounded Output Stability 86
1-7 Summary 87
REFERENCES 88
PROBLEMS 89
COMPUTER PROJECTS 95

Chapter Two ***Fourier Series*** **98**

2-1 Periodic Signals and Properties 98
2-2 Complex Exponential Fourier Series 102
2-3 Trigonometric Fourier Series 111
2-4 Properties of Fourier Series 116
2-5 Power Spectrum 117
2-6 Steady-State Response of LTI Systems to Periodic Signals 119
2-7 Fourier Series For Nonperiodic Signals 120
2-8 Summary 123
REFERENCES 124
PROBLEMS 125

Chapter Three ***Discrete Fourier Series*** **129**

3-1 Approximation For Fourier Series Coefficients 129
3-1.1 Discrete Fourier Transform 129
3-1.2 Inverse Discrete Fourier Transform 136
3-1.3 Aliasing Error and Sampling Requirements 137
3-2 Leakage Error and Data Windowing 143
3-3 Implementing the DFT Algorithm 148
3-3.1 Alternate Inverse DFT 149
3-3.2 DFT Program 149
3-3.3 DFT of Complex Signals 155
3-4 Summary 156
REFERENCES 156
PROBLEMS 158
COMPUTER PROJECTS 160

Chapter Four ***Fourier Transform and Applications*** **162**

4-1 Fourier Transform and Basic Properties 162
4-1.1 Fourier Transform 162
4-1.2 Some Applications 171
4-1.3 Transfer Function and Impulse Response 176
4-1.4 Fourier Transform Existence Conditions 179
4-2 Additional Fourier Transforms and Properties 182
4-2.1 Time Scaling Property 183
4-2.2 Energy Spectral Density 185
4-2.3 Symmetry Property 187
4-2.4 Time Shift Property 189
4-2.5 Modulation Property 191
4-2.6 Fourier Transform of a Periodic Signal 193
4-2.7 Time Convolution Property 194
4-2.8 Frequency Convolution Property 196
4-2.9 Time Derivative Property 198
4-2.10 Time Integration Property 198
4-2.11 Frequency Derivative Property 199

4-2.12 Some Examples 200
4-3 Further Remarks on Convolution 204
4-3.1 Graphical Convolution 205
4-3.2 Circular Convolution 212
4-4 Partial Fraction Expansion 215
4-5 Frequency Response Plots 220
4-5.1 Polar Plots 220
4-5.2 Bode Plots 223
4-6 Summary 233
REFERENCES 234
PROBLEMS 235

Chapter Five ***Discrete Fourier Transform*** **245**

5-1 Sampling Process and Sampling Theorem 245
5-1.1 Impulse Sampler Model For Sampling 245
5-1.2 Poisson Summation Formulas 252
5-1.3 Sampling Theorem 254
5-1.4 Data Reconstruction 255
5-1.5 Digital Signal Processing System 257
5-2 Discrete Fourier and Inverse Fourier Transform 258
5-2.1 Forward DFT 258
5-2.2 Data Windowing 261
5-2.3 Leakage Error Analysis 268
5-2.4 Inverse DFT 272
5-2.5 Frequency and Time Domain Aliasing Error Analysis 276
5-3 Discrete Fourier Transform Properties 277
5-3.1 Linearity Property 279
5-3.2 Time Shift Property 279
5-3.3 Circular Convolution Property 283
5-3.4 Parseval's Relation 285
5-3.5 Symmetry Property 285
5-4 Discrete Convolution 286
5-5 Summary 294
REFERENCES 295
PROBLEMS 296
COMPUTER PROJECTS 299

Chapter Six ***Fast Fourier Transform*** **303**

6-1 Decimation in Time FFT Algorithm 303
6-1.1 Radix Two FFT 304
6-1.2 In-Place Computation 312
6-1.3 Bit Reversing 314
6-1.4 Other Decimation in Time FFT Algorithms 316
6-2 Decimation in Frequency FFT Algorithm 318
6-3 Comparison of Computational Requirements 324
6-3.1 Convolution Computational Requirements 325

6-3.2 Overlap-Add Convolution 326
6-3.3 DFT of Partitioned Sequences 331
6-4 Summary 333
REFERENCES 333
PROBLEMS 335
COMPUTER PROJECTS 336

Chapter Seven ***Correlation*** **338**

7-1 Continuous Time Averaged Correlation 338
7-1.1 Autocorrelation 338
7-1.2 Crosscorrelation 345
7-1.3 Average Correlation 353
7-1.4 Least Error Squared Estimation 361
7-2 Correlation Over a Finite Time Interval 364
7-2.1 Autocorrelation 364
7-2.2 Crosscorrelation 367
7-2.3 Power Spectral Density Estimation 367
7-3 Discrete Time Averaged Correlation 371
7-3.1 Averaged Correlation Formulas 371
7-3.2 Application of the FFT For Correlation Analysis 372
7-4 Summary 383
REFERENCES 384
PROBLEMS 386
COMPUTER PROJECTS 389

Chapter Eight ***Laplace Transform and Applications*** **391**

8-1 Laplace Transform 391
8-1.1 Bilateral Laplace Transform 392
8-1.2 Unilateral Laplace Transform 397
8-1.3 Inverse Laplace Transform 398
8-2 Laplace Transforms and Properties 400
8-3 LTI System Analysis with the Laplace Transform 416
8-4 Block Diagrams 422
8-5 Introduction to State Variables 433
8-5.1 State Variable Description 433
8-5.2 Time Domain Solution of the State Equation 441
8-5.3 Frequency Domain Solution of the State Equation 446
8-6 Discretizing a Continuous Time System 453
8-7 Summary 464
REFERENCES 465
PROBLEMS 467
COMPUTER PROJECTS 476

Chapter Nine ***Z-Transform and Discrete Time Systems*** **477**

9-1 Z-Transform 477
9-1.1 Bilateral Z-Transform 477
9-1.2 Z-Transform Existence Condition 487
9-1.3 Inverse Z-Transform 488
9-1.4 Unilateral Z-Transform 491
9-2 Z-Transform and Properties 491
9-2.1 Linearity Property 491
9-2.2 Time Shift Property 492
9-2.3 Z-Transform Applications 493
9-2.4 Frequency Shift Property 500
9-3 Complete Response and Convolution 501
9-4 Stability Test 510
9-5 Frequency Response 511
9-6 Chirp Z-Transform 516
9-7 Block Diagrams and State Variables 522
9-8 Computer Algorithm For a Cascade Realization 533
9-9 Solution of the State Equation 536
9-9.1 Time Domain Solution 536
9-9.2 Frequency Domain Solution 538
9-10 Summary 542
REFERENCES 542
PROBLEMS 544
COMPUTER PROJECTS 553

Chapter Ten ***Digital Filter Design*** **557**

10-1 Digital Filter Properties 557
10-1.1 Review 557
10-1.2 Pole or Zero Reflection 561
10-1.3 Frequency Response Specifications 562
10-1.4 Transient Response Specifications 574
10-1.5 Digital Filter Advantages and Disadvantages 576
10-2 Finite Impulse Response Filter Design 578
10-2.1 Fourier Series Method 579
10-2.2 FIR Filter Symmetry Property 587
10-2.3 Frequency Sampling Method 591
10-3 Infinite Impulse Response Filter Design 597
10-3.1 Backward Difference Approximation 597
10-3.2 Forward Difference Approximation 599
10-3.3 Bilinear Transformation 601
10-3.4 Analog Prototypes 605
10-3.5 Analog Frequency Transformations 613
10-3.6 Impulse Invariant Method 618
10-3.7 Modified Impulse Invariant Method 621
10-3.8 Unit Step Invariant Method 622
10-3.9 Matched Z-Transform Method 623
10-3.10 Design Summary 623

10-3.11 Phase Equalization 624
10-4 Summary 630
REFERENCES 631
PROBLEMS 633
COMPUTER PROJECTS 641

Chapter Eleven ***Microprocessors for Signal Processing*** **645**

11-1 Microprocessors 646
11-2 Application of a General Purpose Microprocessor 647
11-3 Quantization Error 649
11-4 Application of Special Purpose Microprocessors 650
11-4.1 Intel 2920 Based Digital Filter 650
11-4.2 TI TMS32010 Based Digital Filter 655
11-4.3 AT&T DSP32 Based Digital Filter 661
11-5 Summary 664
REFERENCES 664

Appendix A ***Review of Complex Number Theory and Some Trigonometric Identities*** **665**

Appendix B ***Computer Programs For Discrete Fourier Series and Discrete Fourier Transform Analysis*** **670**

Appendix C ***AD/DA Conversion*** **678**

Appendix D ***Basic Matrix Algebra*** **692**

Appendix E ***Function Minimization Program*** **706**

Appendix F ***Answers To Selected Problems*** **713**

Index **724**

$$y(t) = K e^{-t} - 2e^{-t} + 2, \quad t > 0$$

as shown in Fig. 1.20 for $K = 0$ (the zero-state response) and 1 volt.

For $t > 0$, the transient response is $y_n(t) = Ke^{-t} - 2e^{-t}$, the steady-state response is $y_f(t) = 2$, the zero-input response is $y_{zi}(t) = Ke^{-t}$, and the zero-state response is $y_{zs}(t) = -2e^{-t} + 2$. The forced response is a constant, and, since s_n is a negative number, we have

$$\lim_{t \to \infty} y(t) = y_f(t) = 2$$

for any initial condition.

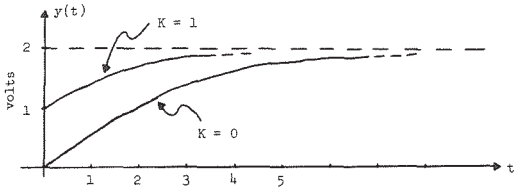


Fig. 1.20. Response of *RC* circuit in Example 1.14.

If the transient response quickly decays to zero, then for t large enough it becomes negligible compared to the forced (steady-state) response.

1-3.2 Frequency Response

When we consider the frequency response of a system it is implied that the input is a sinusoidal function or a linear combination of many sinusoidal functions with different frequencies, i.e.

$$x(t) = \sum_{i=1}^{N} A_i \cos(\omega_i t + \theta_i)$$

even as $N \to \infty$, where A_i is the zero-to-peak amplitude, ω_i is the real frequency, and θ_i is the phase angle of each sinusoid. As we shall soon see, the forced response of an LTI system is also a linear combination of sinusoids with the same frequencies as those of the input, but with different amplitudes and phase angles, i.e.

$$y_f(t) = \sum_{i=1}^{N} B_i \cos(\omega_i t + \phi_i)$$

Given $x(t)$, we want to determine $y_f(t)$. If the natural response decays to zero, then, for t large enough, the complete response becomes $y(t) = y_f(t)$, and the only unknowns are B_i and ϕ_i.

Consider again the RC circuit given in Fig. 1.18, and suppose that $RC = 1$. Let us find the forced response to $x(t) = A\cos\omega t$, where A is the zero-to-peak amplitude of $x(t)$ and ω is the frequency of $x(t)$, which we will not specify at this time. The governing differential equation is eq. 1.8. We are only interested in the steady-state response. Since s_n is negative, then, for every initial condition, the natural response decays to zero, and therefore, we can avoid the effort of finding the natural response.

We will find the forced response in two different ways, i.e., (1) by writing $x(t)$ as in eq. 1.5 and (2) by writing $x(t)$ as in eq. 1.7.

By eq. 1.5, the excitation can be decomposed into the sum of two complex conjugate exponential functions so that $x(t)$ is given by

$$x(t) = \frac{A}{2}e^{j\omega t} + \frac{A}{2}e^{-j\omega t}$$

We can think of $x(t)$ as the series connection of two voltage sources as shown in Fig. 1.21, where

$$x_1(t) = \frac{A}{2}e^{j\omega t}, \quad x_{-1}(t) = \frac{A}{2}e^{-j\omega t}$$

The subscript notation is used to distinguish the exponential function with $s = j\omega$ from the one with $s = -j\omega$.

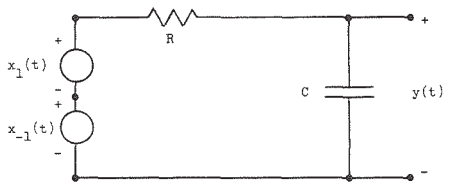


Fig. 1.21. *RC* circuit with a sinusoidal excitation.

By the superposition principle, we can find the forced response to $x_1(t)$ and $x_{-1}(t)$ separately, and then sum the two responses to obtain the forced response to $x(t)$. For $x_1(t)$, we write

$$x_1(t) = X_1 e^{s_1 t}, \quad X_1 = \frac{A}{2}, \quad s_1 = j\omega$$

and therefore, the forced response $y_1(t)$ to $x_1(t)$ is given by

$$y_1(t) = H(s)|_{s=s_1} X_1 e^{j\omega t} = Y_1 e^{j\omega t}$$

Substituting $s = s_1$ into $H(s)$ results in

$$H(j\omega) = \frac{1}{1+j\omega} = \frac{1}{\sqrt{1+\omega^2}\,e^{j\tan^{-1}(\omega)}} = \frac{1}{\sqrt{1+\omega^2}}e^{-j\tan^{-1}(\omega)}$$

and we have

$$\|H(j\omega)\| = \frac{1}{\sqrt{1+\omega^2}}, \quad \angle H(j\omega) = -\tan^{-1}(\omega)$$

Or, to identify the real and imaginary parts of $H(j\omega)$, we use

$$H(j\omega) = \frac{1}{1+j\omega}\frac{1-j\omega}{1-j\omega} = \frac{1-j\omega}{1+\omega^2}$$

and then

$$Re(H(j\omega)) = \frac{1}{1+\omega^2}, \quad Im(H(j\omega)) = \frac{-\omega}{1+\omega^2}$$

$H(j\omega)$ is a complex function of the real variable ω. Finally, $y_1(t)$ is given by

$$y_1(t) = \frac{1}{\sqrt{1+\omega^2}} e^{-j\tan^{-1}(\omega)} \frac{A}{2} e^{j\omega t}$$

For $x_{-1}(t)$, we write

$$x_{-1}(t) = X_{-1} e^{s_{-1}t}, \quad X_{-1} = \frac{A}{2}, \quad s_{-1} = -j\omega$$

and therefore, the forced response $y_{-1}(t)$ to $x_{-1}(t)$ is given by

$$y_{-1}(t) = H(s)|_{s=s_{-1}} X_{-1} e^{-j\omega t} = Y_{-1} e^{-j\omega t}$$

Substituting $s = s_{-1}$ into $H(s)$ results in

$$H(-j\omega) = \frac{1}{1-j\omega} = \frac{1}{\sqrt{1+\omega^2}\, e^{-j\tan^{-1}(\omega)}} = \frac{1}{\sqrt{1+\omega^2}} e^{j\tan^{-1}(\omega)} = H^*(j\omega)$$

Or, multiplying the numerator and denominator of $H(-j\omega)$ by the complex conjugate of the denominator results in

$$H(-j\omega) = \frac{1}{1-j\omega}\frac{1+j\omega}{1+j\omega} = \frac{1+j\omega}{1+\omega^2} = H^*(j\omega)$$

Finally, $y_{-1}(t)$ is given by

$$y_{-1}(t) = \frac{1}{\sqrt{1+\omega^2}} e^{j\tan^{-1}(\omega)} \frac{A}{2} e^{-j\omega t} = y_1^*(t)$$

Summing $y_1(t)$ and $y_{-1}(t)$ yields the forced response $y_f(t) = y_1(t) + y_{-1}(t)$ to $x(t)$. For t large enough, $y(t)$ is given by

$$y(t) = y_1(t) + y_{-1}(t), \quad t \gg 0$$

and then with Euler's identity we get

$$y(t) = \frac{1}{\sqrt{1+\omega^2}} A\cos(\omega t - \tan^{-1}(\omega)), \quad t \gg 0$$

Notice that $s_{-1} = s_1^*$, and therefore $H(s_{-1}) = H(s_1^*)$. Then, we found that $H(s_1^*) = H^*(s_1)$, which resulted in $y_{-1}(t) = y_1^*(t)$. Thus, it is not necessary to find $y_{-1}(t)$. After finding $y_1(t)$, we know that $y_f(t) = y_1(t) + y_1^*(t)$.

In terms of the transfer function magnitude and angle, the steady-state response to $x(t) = A\cos(\omega t)$ is given by

$$y(t) = \| H(j\omega) \| A\cos(\omega t + \angle H(j\omega))$$

The *RC* circuit performs a useful type of signal processing activity. This can be seen by considering the zero-to-peak amplitude of the response as compared to the zero-to-peak amplitude of the excitation (input signal), and

$$\frac{\text{amplitude of } y(t)}{\text{amplitude of } x(t)} = \| H(j\omega) \|$$

A plot of $\| H(j\omega) \|$ versus ω reveals how the system modifies the input amplitude to obtain the output amplitude for different frequencies of the input. Such a plot shows the **magnitude frequency response** of an LTI system, and for this *RC* circuit, the magnitude frequency response is given in Fig. 1.22a.

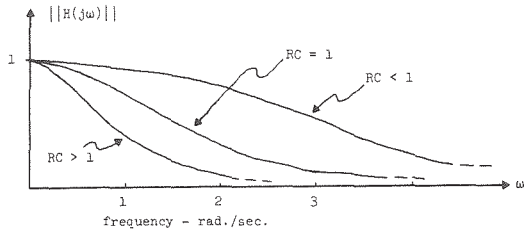


Fig. 1.22a. Magnitude frequency response of the *RC* circuit.

Notice further that the phase angle difference between the output and the input is determined by the angle of the transfer function, which is shown in Fig. 1.22b.

Figures 1.22 completely describe the frequency response of this system. The concept of a frequency response can be applied to any dynamic system, and for a linear and time invariant system the frequency response can be readily obtained.

If $x(t)$ consists of two sinusoids such as $x(t) = \cos\omega_a t + \cos\omega_b t$, where $\omega_a \ll \omega_b$, then the steady-state response $y(t)$ will also consist of two sinusoids $y_a(t)$ and $y_b(t)$ at the two frequencies ω_a and ω_b, respectively. However, the amplitude of $y_a(t)$ will be greater then the amplitude of $y_b(t)$

so that $y(t) \cong y_a(t)$. The RC circuit attenuates high frequency input signals. This behavior is referred to as **low-pass** (LP) **filtering**. The R and C values determine the specific low-pass filter characteristic of this circuit.

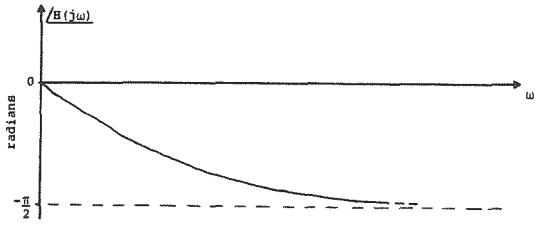


Fig. 1.22b. Phase angle frequency response of the RC circuit.

LP filters are commonly used for signal processing, and more elaborate circuits can be designed to approximate an ideal LP filter characteristic as shown in Fig. 1.23, where ω_c is called the **cut-off frequency** or **bandwidth** (BW) of the filter. If the goal of processing the signal $x(t)$ is to produce another signal $y(t)$ that is predominantly the part of $x(t)$ with frequency $\omega = \omega_a$, then we would design a circuit that approximates the ideal LP filter characteristic given in Fig. 1.23 such that $\omega_a < \omega_c < \omega_b$ and $\lim_{t \to \infty} y_n(t) = 0$. The resulting circuit will filter out the part of $x(t)$ with frequency $\omega = \omega_b$.

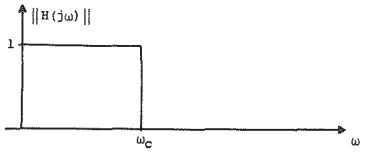


Fig. 1.23. Ideal LP filter magnitude frequency response.

A hi-fi amplifier with a treble control uses a low-pass filter. When we adjust the treble control, we are changing component values within the filter to vary the bandwidth ω_c of the LP filter. As the bandwidth of the filter is reduced, the high frequency components of a music signal are attenuated. We will discuss filtering concepts more extensively in later chapters.

Example 1.15. Find the forced response of the RC circuit shown in Fig. 1.18 to the input $x(t) = \sin t + \cos(10t + \pi/4)$, which is given in Fig. 1.24a.

For convenience, let $RC = 1$ so that $H(s) = 1/(s+1)$. For the sine term we write $\sin(t) = \cos(t - \pi/2)$. By the superposition principle, the steady-state response to $x(t)$ is given by

$$y(t) = \|H(j1)\| \cos(t - \pi/2 + \angle H(j1)) + \|H(j10)\| \cos(10t + \pi/4 + \angle H(j10))$$

Notice that subscript notation is not used here, because, for t large enough, this is the complete response. Evaluating the magnitudes and angles yields

$$y(t)=\frac{1}{\sqrt{2}}\cos(t-3\pi/4)+\frac{1}{\sqrt{101}}\cos(10t+\pi/4-\tan^{-1}(10))$$

which is shown in Fig. 1.24b.

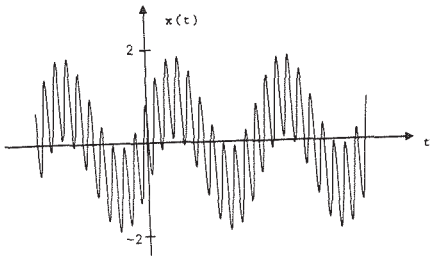


Fig. 1.24a. Sinusoidal input.

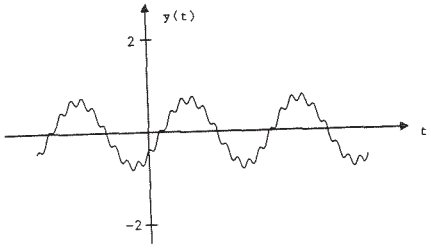


Fig. 1.24b. Steady-state output.

Although the input sinusoids have the same amplitude, the circuit has significantly attenuated the input sinusoid with frequency $\omega = 10$ rad/sec. By changing the R and/or C values we can control the extent to which the component of $x(t)$ with frequency $\omega = 10$ is attenuated. This filter is not an ideal LP filter, and the part of the input with frequency $\omega = 1$ is also slightly attenuated.

An alternative to the preceding analysis is based on eq. 1.7. Consider the following equation

$$\frac{dw}{dt}+w(t)=v(t) \tag{1.20}$$

With $RC = 1$, this is the same equation as eq. 1.8. Now suppose that

$$v(t)=A\,e^{j\omega t}$$

The input signal $x(t)$ is related to $v(t)$ by

$$Re(v(t))=A\cos\omega t=x(t)$$

where if, in general, we write $v(t)=V\,e^{st}$, then $V=A$ and $s=j\omega$. By our previous results, the forced response has the form

$$w_f(t) = W e^{j\omega t}$$

where W is given by

$$W = H(s)|_{s=j\omega} V = H(j\omega)A = \frac{1-j\omega}{1+\omega^2}A$$

With W, $w_f(t)$ becomes

$$w_f(t) = \frac{1-j\omega}{1+\omega^2}A(\cos(\omega t) + j\sin(\omega t))$$

After multiplication, the real part of $w_f(t)$ can be obtained, and we get

$$Re(w_f(t)) = \frac{A}{1+\omega^2}(\cos(\omega t) + \omega\sin(\omega t))$$

By a trigonometric identity (See Appendix A.)

$$Re(w_f(t)) = \frac{A}{1+\omega^2}\sqrt{1+\omega^2}\cos(\omega t - \tan^{-1}(\omega))$$

and then it becomes apparent that the forced response to $Re(v(t))$ is given by

$$Re(w_f(t)) = y(t)$$

The above procedure is a simpler method for finding $y(t)$ than the method based on eq. 1.5. However, for obtaining the response of a linear system to almost arbitrary input signals, we will see in Chapters Two and Four that the method based on eq. 1.5 can be more conveniently extended.

The rationale for the method based on eq. 1.7 stems from writing $v(t)$ and $w_f(t)$ as

$$v(t) = v_R(t) + jv_I(t)$$

$$w_f(t) = w_R(t) + jw_I(t)$$

where $v_R(t)$ and $w_R(t)$ are the real parts of $v(t)$ and $w_f(t)$, respectively, and $v_I(t)$ and $w_I(t)$ are the imaginary parts of $v(t)$ and $w_f(t)$, respectively. Substituting $v(t)$ and $w_f(t)$ into eq. 1.20 yields

$$\frac{d}{dt}(w_R + jw_I) + (w_R + jw_I) = v_R + jv_I$$

After equating real and imaginary parts, we have

$$\frac{dw_R}{dt} + w_R = v_R$$

$$\frac{dw_I}{dt} + w_I = v_I$$

and the real and imaginary parts of $w_f(t)$ separately are the forced response of the system to the real and imaginary parts of $v(t)$.

Let us apply the concept of a linear operator to eq. 1.11, which is repeated here for convenience, i.e.

$$\frac{dy_{zs}}{dt} + y_{zs}(t) = x(t), \quad RC = 1$$

Here, we assume that the system is initially at rest, so that $y(t) = y_{zs}(t)$. This is a linear system. Operating on both sides of the equation with some linear operator L yields

$$L\left(\frac{dy_{zs}}{dt} + y_{zs}(t)\right) = L(x(t))$$

Since L is a linear operator, then we have

$$L\left(\frac{dy_{zs}}{dt}\right) + L(y_{zs}(t)) = L(x(t))$$

Now, suppose we define L to be a time invariant differential operator, i.e.

$$L(\cdot) = c_i \frac{d^i(\cdot)}{dt^i} + \cdots + c_1 \frac{d(\cdot)}{dt} + c_0(\cdot)$$

for some nonnegative integer i, where $c_0, c_1, \cdots, c_i$ are arbitrary constants. Then L and the linear operation differentiation can be reversed, and we get

$$\frac{d}{dt}(L(y_{zs}(t))) + L(y_{zs}(t)) = L(x(t))$$

Therefore, if $y_{zs}(t)$ is the zero-state response to $x(t)$, then $L(y_{zs}(t))$ is the zero-state response to $L(x(t))$. Furthermore, if $y_f(t)$ is the forced response to $x(t)$, then $L(y_f(t))$ is the forced response to $L(x(t))$.

Example 1.16. We just found the response $y_f(t)$ of the circuit in Fig. 1.18 to $x(t) = A\cos(\omega t)$. Let us find the forced response of this circuit to $z(t) = A\sin(\omega t)$. But, $x(t)$ and $z(t)$ can be related through an appropriate linear operator, which in this case is

$$L(x(t)) = -\frac{1}{\omega}\frac{d}{dt}(x(t)) = z(t)$$

Therefore, the forced response to $z(t)$ is given by $L(y_f(t))$, which is

$$L(y_f(t)) = -\frac{1}{\omega}\frac{d}{dt}(y_f(t)) = \frac{A}{\sqrt{1+\omega^2}}\sin(\omega t - \tan^{-1}(\omega))$$

The reader should obtain this same result based on writing $z(t)$ as $z(t) = Im(A\, e^{j\omega t})$.

Example 1.17. To illustrate another kind of frequency selective behavior, consider the circuit given in Fig. 1.25, where the voltage $v(t)$ is the input and the loop current $i(t)$ is the desired response.

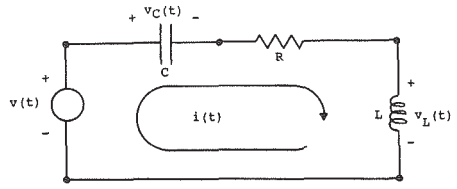


Fig. 1.25. A series *RLC* circuit.

By KVL and the $v-i$ relationships for the components we have for $t > 0^-$

$$Ri(t)+L\frac{di}{dt}+\frac{1}{C}\int_{0^-}^{t} i(\tau)d\tau+v_C(0^-)-v(t)=0 \tag{1.21}$$

Differentiating once yields

$$L\frac{d^2i}{dt^2}+R\frac{di}{dt}+\frac{1}{C}i(t)=\frac{dv}{dt} \tag{1.22}$$

Using $R=6\,\Omega, L=1\,\text{H}, C=1/25\,\text{F}$, the homogeneous equation yields the characteristic equation given by

$$s_n^2+6s_n+25=0$$

and the natural frequencies are $s_1=-3+j4$ and $s_2=-3-j4$. These are complex natural frequencies with negative real parts, and the natural response $i_n(t)$ is an exponentially decaying sinusoid given by

$$i_n(t)=I_1e^{-3t}e^{j4t}+I_1^*e^{-3t}e^{-j4t}=2\|I_1\|\,e^{-3t}\cos(4t+\angle I_1),\quad I_1=\|I_1\|\,e^{j\angle I_1}$$

so that $\lim_{t\to\infty} i_n(t)=0$. I_1 can be found by applying initial conditions at $t=0^+$ to the complete response $i(t)$. Here, we are only concerned with the frequency response of this circuit, and since $\lim_{t\to\infty} i_n(t)=0$, then the steady-state response is $i_f(t)$.

If $v(t)=A\cos(\omega t+\theta)$, then we must find the forced response to $v(t)=Ve^{st}+(Ve^{st})^*$, where $s=j\omega$ and $V=\frac{A}{2}e^{j\theta}$. For the purpose of investigating the frequency response of this circuit, we need only find the forced response $i_f(t)$ to $v(t)$. Denote the response to Ve^{st} by Ie^{st}, where $I=H(s)V$, and therefore $i_f(t)=Ie^{st}+(Ie^{st})^*$.

Substituting Ie^{st} and Ve^{st} into eq. 1.23 results in

$$Ls^2I + RsI + \frac{1}{C}I = sV$$

or

$$LsI + RI + \frac{1}{Cs}I = V \tag{1.23}$$

and, for $H(s)$, we get

$$H(s) = \frac{1}{Ls + R + \frac{1}{Cs}} = \frac{1}{L}\frac{s}{s^2 + \frac{R}{L}s + \frac{1}{LC}} = \frac{P(s)}{Q(s)}$$

where $P(s)$ is the numerator polynomial of $H(s)$ and $Q(s)$ is the denominator polynomial of $H(s)$.

Before continuing with this example, let us consider again the $v - i$ relationships for the components when either the voltage or current is an excitation that is a complex exponential function.

For an inductor the $v - i$ relationship is given by

$$v_L(t) = L\frac{di_L}{dt}$$

If $i_L(t) = I_L e^{st}$, then $v_L(t) = V_L e^{st} = LsI_L e^{st}$, and $V_L = LsI_L$.

For a resistor we have

$$v_R(t) = Ri_R(t)$$

If $i_R(t) = I_R e^{st}$, then $v_R(t) = V_R e^{st} = RI_R e^{st}$, and $V_R = RI_R$.

And, for a capacitor the $v - i$ relationship is given by

$$i_C(t) = C\frac{dv_C}{dt}$$

If $v_C(t) = V_C e^{st}$, then $i_C(t) = I_C e^{st} = CsV_C e^{st}$, and $V_C = \frac{1}{Cs}I_C$.

The relationships between the complex amplitudes of the voltage and the complex amplitudes of the current for an inductor, resistor, and capacitor, i.e.

$$V_L = LsI_L$$

$$V_R = RI_R$$

$$V_C = \frac{1}{Cs}I_C$$

are called **Ohm's law**. By Ohm's law we can relate the complex voltage amplitudes and the complex current amplitudes of the components through the quantities Ls, R, and $1/Cs$, which are called the **impedance** of an inductor, resistor, and capacitor, respectively.

If we are only interested in the forced response, then we can omit writing time domain equations such as eq. 1.21, skip the steps from eq. 1.21 to eq. 1.23, and immediately apply KVL in terms of complex amplitudes and impedances to obtain frequency domain equations such as eq. 1.23, where LsI is the complex amplitude of the voltage across the inductor, RI is the complex amplitude of the voltage across the resistor, and I/Cs is the complex amplitude of the voltage across the capacitor. By KVL, the sum of these complex voltage amplitudes equals the complex amplitude of the input (See eq. 1.23.).

Now, with $s = j\omega$, write $H(j\omega)$ in polar form, i.e.

$$H(j\omega) = \| H(j\omega) \| \, e^{j\angle H(j\omega)}$$

Since $I = H(j\omega)V$, $i_f(t)$ is given by

$$i_f(t) = \| H \| \, e^{j\angle H} \frac{A}{2} e^{j\theta} e^{j\omega t} + \| H \| \, e^{-j\angle H} \frac{A}{2} e^{-j\theta} e^{-j\omega t}$$

After combining exponential terms and using Euler's identity we get

$$i_f(t) = \| H(j\omega) \| \, A \cos(\omega t + \theta + \angle H(j\omega))$$

With the component values of the RLC circuit we have

$$\| H(j\omega) \| = \frac{|\omega|}{((25 - \omega^2)^2 + 36\omega^2)^{1/2}}$$

and the magnitude frequency response of the circuit is shown in Fig. 1.26.

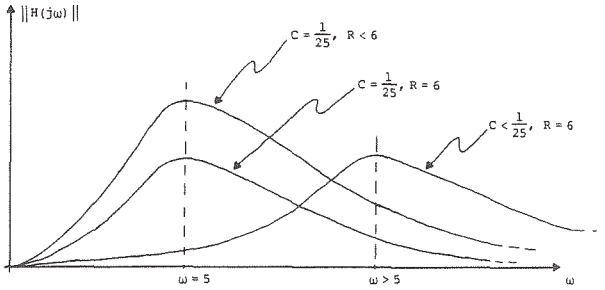


Fig. 1.26. Magnitude frequency response for Example 1.17.

If $v(t)$ consists of the sum of sinusoids at many different frequencies, then $i_f(t)$ also consists of a sum of sinusoids at these frequencies. However, from Fig. 1.26 we see that input sinusoids with frequencies significantly below and above $\omega = 5$ rad/sec are attenuated. This circuit exhibits the frequency selective behavior of a **band-pass** (BP) **filter**. A more elaborate circuit is necessary

to approximate the ideal BP characteristic shown in Fig. 1.27, where ω_1 and ω_2 are called the **lower and upper cut-off frequencies**, respectively, and $(\omega_2 - \omega_1)$ is called the **bandwidth** (BW) of the BP filter.

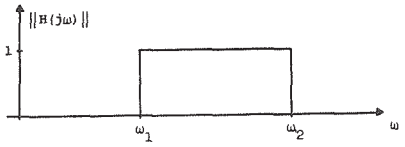


Fig. 1.27. Ideal BP filter.

By varying component values, such as the capacitor value, the range of frequencies of input sinusoidal functions that are passed by this circuit can be changed as shown in Fig. 1.26. This is the basis of the kind of signal processing activity that first occurs in a TV or radio receiver. The intent is to allow the remainder of the receiver to process only one of the many incoming signals. Tuning in a particular transmitting station can be done by adjusting component values in a band-pass filter circuit until the frequency response of the filter peaks about the frequencies of signals transmitted by a desired station.

For any linear and time invariant system with transfer function $H(s)$, if the $\lim_{t\to\infty} y_n(t) = 0$, then the steady-state response to the input

$$x(t) = A\cos(\omega t + \theta)$$

is given by

$$y(t) = \|H(j\omega)\| A\cos(\omega t + \theta + \angle H(j\omega))$$

The complex function $H(j\omega)$ of the real variable ω determines how an LTI system processes an input sinusoidal function to produce an output sinusoidal function.

Example 1.18. Let us write KCL equations in terms of forced response amplitudes for the circuit given in Fig. 1.28, and determine its frequency response.

Again, we assume that the input is given by $v(t) = Ve^{st} + (Ve^{st})^*$. Consequently, the forced responses for the node voltages v_1 and v_2 are $v_1(t) = V_1e^{st} + (V_1e^{st})^*$ and $v_2(t) = V_2e^{st} + (V_2e^{st})^*$. Now, instead of writing time domain equations similar to eq. 1.21, we will write equations, which are called **frequency domain equations**, similar to eq. 1.23. Applying KCL by summing the complex amplitudes of currents leaving nodes (1) and (2) results in

$$\frac{V_1 - V}{R_1} + Cs\,V_1 + \frac{V_1 - V_2}{R_2} = 0$$

$$\frac{V_2 - V_1}{R_2} + \frac{V_2}{Ls} = 0$$

and we have two coupled linear algebraic equations instead of two coupled time domain differential equations. Rearranging these two equations in two unknowns results in

$$\left(Cs + \frac{1}{R_1} + \frac{1}{R_2}\right)V_1 - \frac{1}{R_2}V_2 = \frac{1}{R_1}V$$

$$-\frac{1}{R_2}V_1 + \left(\frac{1}{Ls} + \frac{1}{R_2}\right)V_2 = 0$$

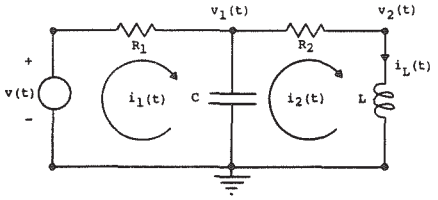


Fig. 1.28. A two loop *RLC* circuit.

If $v_1(t)$ is the desired output, then by **Cramer's rule** (See Appendix D.) we can solve for V_1 to obtain

$$V_1 = \frac{Ls + R_2}{R_1 LC\, s^2 + (L + R_1 R_2 C)s + R_1 + R_2}V = \frac{P_1(s)}{Q(s)}V$$

which also identifies the transfer function $H_1(s)$ from V to V_1. With the transfer function we can write the differential equation that relates $v_1(t)$ and $v(t)$. Furthermore

$$V_2 = \frac{Ls}{R_1 LC\, s^2 + (L + R_1 R_2 C)s + R_1 + R_2}V = \frac{P_2(s)}{Q(s)}V$$

which identifies the transfer function $H_2(s)$ from V to V_2.

The characteristic equation for the natural frequencies can be identified from the denominator of either $H_2(s)$ or $H_1(s)$. Remember, regardless of which quantity we choose to find, the natural frequencies will be the same.

Now assume that $v(t) = A\cos(\omega t + \theta)$ so that $V = \frac{A}{2}e^{j\theta}$ and $s = j\omega$. Then, with $H_1(s)$ we can find the forced response $v_1(t)$ to $v(t)$, and with $H_2(s)$ we can find the forced response $v_2(t)$ to $v(t)$. If $v_1(t)$ is the desired output, then a plot of $\|H_1(j\omega)\|$ versus ω will reveal the frequency selective behavior of this circuit.

We have been analyzing linear and time invariant systems, which, for a single input $x(t)$ and single output $y(t)$, can be represented in the frequency domain as shown in Fig. 1.29, where X is the complex amplitude of the input and Y is the complex amplitude of the output.

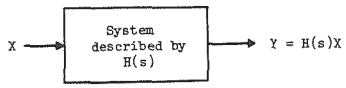


Fig. 1.29. Frequency domain representation of an LTI system.

1-3.3 Complete Response of an nth Order System

In the analysis of the circuit given in Fig. 1.18 we introduced various salient terms and procedures that are involved in the analysis of any LTI system. Before we consider an n^{th} order system, let us repeat this analysis procedure, but without the intermediate details.

Example 1.19. Find the complete solution of the differential equation given by

$$2\frac{d^2y}{dt^2}+10\frac{dy}{dt}+12y(t)=3\frac{dx}{dt}+12x(t) \tag{1.24}$$

for $t>0$. The input $x(t)$ is assumed to have the form $x(t)=X\,e^{st}$ for $t>0$ and $x(t)=0$ for $t<0$. To solve for $y(t)$, we need two conditions on $y(t)$, and suppose they are $y(0^+)=1$ and $\dot{y}(0^+)=0$. Since $x(t)$ has only a finite discontinuity at $t=0$, then $y(t)$ is continuous at $t=0$. In Section 1-4 we will consider issues regarding the continuity of the solution of a linear differential equation. Now, let us proceed as before. The complete response has the form as in eq. 1.9.

From the homogeneous equation, the characteristic equation is

$$2s_n^2+10s_n+12=2(s_n+2)(s_n+3)=0$$

This second order polynomial equation in s_n has two roots, which are $s_1=-2$ and $s_2=-3$. These are the natural frequencies of this system. Each natural frequency generates an exponential function that satisfies the homogeneous equation. Therefore, $y_n(t)$, as given by

$$y_n(t)=Y_1e^{-2t}+Y_2e^{-3t}$$

also satisfies the homogeneous equation. Try it. The constants Y_1 and Y_2 will be found by applying the conditions given for the complete solution.

To find the forced response $y_f(t)=Y_fe^{st}$, we need the transfer function $H(s)$, which is

$$H(s)=\frac{3s+12}{2s^2+10s+12}=\frac{3}{2}\frac{s+4}{s^2+5s+6}=\frac{P(s)}{Q(s)}$$

CHAPTER TEN

DIGITAL FILTER DESIGN

Basically, a discrete time system or digital signal processor executes an algorithm that operates on an input number sequence to produce an output number sequence. We have already seen through several examples that a discrete time system can exhibit frequency selective behavior, and consequently the term digital filter is also used when we refer to a discrete time system. In the previous chapter the Z-transform was presented, and we found that it is a useful tool for the analysis of LTI (linear and time invariant) discrete time systems. And, we developed several ways by which a discrete time system can be described and realized. In this chapter we shall be concerned with the design or synthesis of LTI digital filters to achieve a prescribed frequency response. Then, in the next chapter, we will consider the application of some commercially available special purpose microprocessors for implementing a digital filter.

SECTION 10-1 Digital Filter Properties

To design a digital filter, we must provide a specification of the desired performance of the filter. Filter specifications must be consistent with design procedures. Therefore, we must satisfy some particular discrete time system properties as we impose filter performance requirements. Before we develop some digital filter design procedures, let us review some LTI discrete time system properties to see how they affect a design specification.

10-1.1 Review

A single input $u(k)$ and single output $y(k)$ LTI digital filter can be described by a scalar difference equation, i.e.

$$y(k+n)+a_{n-1}y(k+(n-1))+\cdots+a_0y(k)=b_mu(k+m)+b_{m-1}u(k+(m-1))+\cdots+b_0u(k)$$

This is an n^{th} order difference equation. We assume that $u(k)=0$ for $k<0$. Since the filter is time invariant (shift invariant), we can write

$$y(k)=b_mu(k-(n-m))+b_{m-1}u(k-(n-m+1))+\cdots+b_1u(k-(n-1))+b_0u(k-n)$$
$$-a_{n-1}y(k-1)-\cdots-a_1y(k-(n-1))-a_0y(k-n)$$

or

$$y(k)=\sum_{i=0}^{m}b_{m-i}u(k-(n-m)-i)-\sum_{i=1}^{n}a_{n-i}y(k-i) \qquad \textbf{(10.1a)}$$

for $k = 0, 1 \cdots$. To run eq. 10.1a requires the initial conditions, $y(-i)$, $i = 1, 2, \cdots, n$. If the filter is to be causal, then the present output $y(k)$ cannot depend on future inputs, and therefore, from the term $u(k-(n-m))$, we require that $(n-m) \geq 0$, or $n \geq m$.

We saw in the previous chapter that there are innumerable other ways, which preserve the input-output relationship, for describing a digital filter. Through a definition of n state variables, a causal filter can always be represented with

$$x(k+1) = Ax(k) + Bu(k) \tag{10.1b}$$

$$y(k) = Cx(k) + Du(k) \tag{10.1c}$$

where x is an n component state vector. To run eq. 10.1b requires the initial condition $x(0)$. We can run either description given in eqs. 10.1 to obtain the response $y(k)$ to an input $u(k)$, for $k = 0, 1, \cdots$.

A digital filter is also described by its unit pulse response $h(k)$, and for a causal system, $h(k) = 0$ for $k < 0$. The response to an input $u(k)$, $k = 0, 1, \cdots$, can be found with the convolution operation, and we have

$$y(k) = \sum_{i=0}^{k} h(k-i)u(i) = \sum_{i=0}^{k} h(i)u(k-i) \tag{10.2a}$$

By taking the Z-transform of eq. 10.1a and assuming zero initial conditions, the transfer function of the filter is given by

$$H(z) = \frac{\sum_{i=0}^{m} b_i z^i}{z^n + \sum_{i=0}^{n-1} a_i z^i} = \frac{P(z)}{Q(z)} \tag{10.3a}$$

$$H(z) = H_0 \frac{\prod_{i=1}^{m} (z - z_i)}{\prod_{i=1}^{n} (z - p_i)} \tag{10.3b}$$

If the filter is to be causal, i.e., $m \leq n$, then $H(z)$ must be a **proper** function. Assuming that $H(z)$ is **irreducible**, the poles of $H(z)$ are the roots of the characteristic equation, i.e., $Q(z) = 0$ or $|zI - A| = 0$, which are called the **natural frequencies** of the filter. If the filter is to be stable, then all the poles p_i of $H(z)$ must be inside the unit circle, i.e., $\| p_i \| < 1$, $i = 1, 2, \cdots, n$. However, without some other specification, the zeros z_i can be anywhere in the z-plane.

With the convolution property we have that $Y(z) = H(z)U(z)$, and $H(z) = Z(h(k))$. Therefore, $y(k)$ in eq. 10.2a can also be found with

$$y(k) = Z^{-1}(H(z)U(z)) \tag{10.2b}$$

From an input-output viewpoint we can represent a digital filter as shown in Fig. 10.1. It is important to remember that eqs. 10.2 yield the **complete response** under **zero initial conditions**.

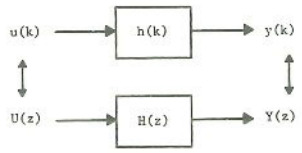


Fig. 10.1. Time and frequency domain representations for a digital filter.

If any a_i, $i = 0, 1, \cdots, (n-1)$, in eq. 10.1a, is not zero, then there is **feedback** in the filter, i.e., the present output depends on past outputs. Such a filter is said to be a **recursive filter**, and any finite duration input will cause an infinite duration response. This is an **IIR** filter.

Example 10.1. Let us consider the relationship between the behavior of the unit pulse response and the pole locations of a filter with $h(k)$ given by

$$h(k) = \gamma^k \cos(\omega_0 kT + \psi) u_{-1}(k)$$

If $|\gamma| < 1$, then $h(k)$ is an exponentially decreasing sinusoid. The transfer function $H(z)$ is given by

$$Z(h(k)) = H(z) = \frac{\cos(\psi)z^2 - \gamma\cos(\omega_0 T - \psi)z}{z^2 - 2\gamma\cos(\omega_0 T)z + \gamma^2}$$

and the difference equation relating $y(k)$ and $u(k)$ is given by

$$y(k) = b_2 u(k) + b_1 u(k-1) - a_1 y(k-1) - a_0 y(k-2)$$

where $b_2 = \cos(\psi)$, $b_1 = -\gamma\cos(\omega_0 T - \psi)$, $a_1 = -2\gamma\cos(\omega_0 T)$, and $a_0 = \gamma^2$. This is a recursive filter.

The poles of $H(z)$ are $p_1 = \gamma e^{+j\omega_0 T}$ and $p_2 = \gamma e^{-j\omega_0 T}$. Notice that the magnitudes of the poles determine the exponential decay rate of $h(k)$. Therefore, the closer the poles are to the unit circle, the longer it will take for the filter response to reach steady-state conditions. Furthermore, the angles of the poles determine the frequencies of the natural response. For example, if $f_s = 8$ samples/sec, and the poles are given by

$$p_{1,2} = \gamma e^{\pm j\pi/6}$$

then $\omega_0 T = \pi/6$ so that $\omega_0 = 4\pi/3$ rad/sec.

If the a_i, for $i = 0, \cdots, (n-1)$, in eq. 10.1a are zero, then $H(z)$ becomes

$$H(z) = \frac{\sum_{i=0}^{m} b_i z^i}{z^n} = \sum_{i=0}^{m} b_i z^{-(n-i)} \qquad \textbf{(10.4a)}$$

so that

$$y(k) = b_m u(k-(n-m)) + b_{m-1} u(k-(n-m+1)) + \cdots + b_1 u(k-(n-1)) + b_0 u(k-n)$$

and we have a **nonrecursive filter**, which is also called a **transversal** or **tapped delay line filter**. The response of a nonrecursive filter depends only on the input, and therefore the response to a finite duration input also has a finite duration. This is an **FIR** filter. If it is a causal filter, then the response depends only on the present and past inputs.

The unit pulse response of a nonrecursive filter is given by

$$h(k) = Z^{-1}(H(z)) = \sum_{i=0}^{m} b_i u_0(k-(n-i)) = \sum_{i=n-m}^{n} b_{n-i} u_0(k-i)$$

$$= \sum_{i=0}^{n} b_{n-i} u_0(k-i) \tag{10.5}$$

where, if $m < n$, then we set $b_{m+1} = 0, \cdots, b_n = 0$. Therefore, $h(k) = b_{n-k}$, $k = 0, 1, \cdots, n$. Since the n poles of a nonrecursive filter are all at $z = 0$, a nonrecursive (FIR) filter is **unconditionally stable**. And, $H(z)$ is simply given by

$$H(z) = \sum_{k=0}^{n} h(k) z^{-k} \tag{10.4b}$$

which has the structure shown in Fig. 10.2.

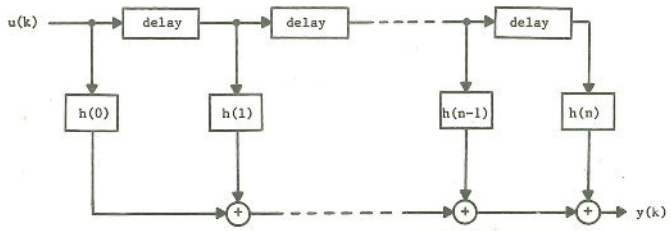


Fig. 10.2. A causal FIR filter.

Since the unit pulse response $h(k)$ of eq. 10.1a is a real time function, then the coefficients in the polynomials $P(z)$ and $Q(z)$ are also real, and therefore we have

$$H(z^*) = \frac{P(z^*)}{Q(z^*)} = \frac{P^*(z)}{Q^*(z)} = H^*(z) \tag{10.6}$$

The steady-state response $y(kT)$ to $u(kT) = A\cos(\omega kT + \theta)u_{-1}(kT)$ of a stable LTI digital filter is given by $y(kT) = M(\omega)A\cos(\omega kT + \theta + \phi(\omega))$, where

$$M(\omega) = \| H(e^{j\omega T}) \| \tag{10.7a}$$

$$\phi(\omega) = \angle H(e^{j\omega T}) \tag{10.7b}$$

Therefore, the amplitude and phase angle of the response depend on the frequency of the input and the nature of the digital filter.

Writing $H(e^{j\omega T})$ in polar form results in

$$H(e^{j\omega T}) = M(\omega)e^{j\phi(\omega)} \tag{10.8a}$$

and by eq. 10.6 we get

$$H(e^{-j\omega T}) = H^*(e^{j\omega T})$$

$$M(-\omega)e^{j\phi(-\omega)} = M(\omega)e^{-j\phi(\omega)} \tag{10.8b}$$

Therefore, $M(-\omega) = M(\omega)$, and $M(\omega)$ is an **even** function, and $\phi(-\omega) = -\phi(\omega)$, and $\phi(\omega)$ is an **odd** function. Furthermore, by Euler's identity we can write

$$H(e^{j\omega T}) = M(\omega)\cos\phi(\omega) + jM(\omega)\sin\phi(\omega) \tag{10.9}$$

and the real (imaginary) part of $H(e^{j\omega T})$ is also an even (odd) function. Consequently, to achieve real coefficients in the design of a digital filter as described in eqs. 10.1, we must choose $H(z)$ such that the magnitude (and real part) of $H(e^{j\omega T})$ is an even function, and such that the phase angle (and imaginary part) of $H(e^{j\omega T})$ is an odd function.

We have already shown that $H(e^{j\omega T})$ is a periodic function of ω, with period ω_s, the sampling frequency. This means that if $h(k)$ and the response to any real input are to be real, then $M(\omega)$ (and the real part of $H(e^{j\omega T})$) must be an **even periodic** function, and $\phi(\omega)$ (and the imaginary part of $H(e^{j\omega T})$) must be an **odd periodic** function.

10-1.2 Pole or Zero Reflection

It is possible to replace any pole or zero of $H(z)$ in eq. 10.3b by its reciprocal without changing the shape of $M(\omega)$. By eqs. 10.8 we have

$$M^2(\omega) = H(e^{j\omega T})H(e^{-j\omega T}) = H(z)H(z^{-1})\,|_{z=e^{j\omega T}} \tag{10.10}$$

Notice that if $(z - p_i)$ is a factor in the denominator of $H(z)$ in eq. 10.3b, then $(z^{-1} - p_i)$ is a factor in the denominator of $H(z^{-1})$, and $z = 1/p_i$ is a pole of $H(z^{-1})$. Similarly, $z = 1/z_i$ is zero of $H(z^{-1})$.

With eq. 10.3b, $M(\omega)$ is given by

$$M(\omega) = |H_0| \frac{\prod_{i=1}^{m} \| e^{j\omega T} - z_i \|}{\prod_{i=1}^{n} \| e^{j\omega T} - p_i \|} \tag{10.11}$$

Consider any factors due to a complex conjugate pole pair, and we have

$$\|e^{j\omega T}-p_i\|\,\|e^{j\omega T}-p_i^*\| = \|(e^{j\omega T}-p_i)^*\|\,\|(e^{j\omega T}-p_i^*)^*\| = \|e^{-j\omega T}-p_i^*\|\,\|e^{-j\omega T}-p_i\|$$

$$= \left\| p_i^*\left(\frac{1}{p_i^*}-e^{j\omega T}\right)e^{-j\omega T}\right\| \left\| p_i\left(\frac{1}{p_i}-e^{j\omega T}\right)e^{-j\omega T}\right\| = \|p_i\|^2\left\|e^{j\omega T}-\frac{1}{p_i^*}\right\|\left\|e^{j\omega T}-\frac{1}{p_i}\right\| \qquad (10.12)$$

Eq. 10.12 shows that the shape of the magnitude frequency response is not changed if in $H(z)$, any real poles (or zeros) or any complex conjugate pair of poles (or zeros) are replaced by their reciprocals. The resulting magnitude frequency response is only scaled by a constant. This means that if in the design of a digital filter $H(z)$, we obtain an unstable filter because p_i and p_i^* are outside the unit circle, then if we are only concerned with achieving a desired $M(\omega)$ shape, the factors $(z-p_i)(z-p_i^*)$ can be replaced with $(z-1/p_i)(z-1/p_i^*)$. The resulting $H(z)$ will be stable, since $1/p_i$ and $1/p_i^*$ are inside the unit circle.

10-1.3 Frequency Response Specifications

Example 10.2. Let us investigate the frequency response of the filter given in Example 10.1 with $\psi=-\pi/2$, $\omega_0=4\pi/3$, and $T=1/8$, so that

$$H(z)=\frac{\frac{1}{2}\gamma z}{(z-\gamma e^{j\pi/6})(z-\gamma e^{-j\pi/6})}$$

$$h(k)=\gamma^k \sin\left(\frac{\pi}{6}k\right)u_{-1}(k)$$

$H(e^{j\omega T})$ is periodic, and here, the period is $\omega_s=\frac{2\pi}{T}=16\pi$ rad/sec.

Assume the input is $u(kT)=\cos(\omega kT+\theta)u_{-1}(k)$. With $|\gamma|<1$, the complete response will consist of a transient term similar to $h(k)$ plus a sinusoidal term. For some $0<\gamma=\gamma_a<1$ and $0<\gamma=\gamma_b<1$, where $\gamma_b>\gamma_a$, $M(\omega)$ is shown in Fig. 10.3.

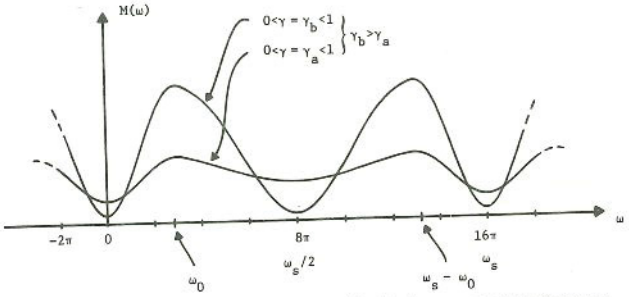


Fig. 10.3. Band-pass filter magnitude frequency response.

By eq. 10.11 we see that $M(\omega)$ should peak at or in the vicinity of $\omega = \omega_0$. This is because the factor $\| e^{j\omega T} - p_1 \|$ in the denominator of $M(\omega)$ takes on its minimum value as $\omega \to \omega_0$. This $M(\omega)$ does peak at $\omega = \pm\omega_0$.

Since $H(e^{j\omega T}) = H(e^{j(\omega + r\omega_s)T})$ for any integer $r = \pm 1, \pm 2, \cdots$, the amplitude and phase angle of the steady-state response for $\omega = \omega_a$ and $\omega = \omega_b = \omega_a + \omega_s$ will be the same. For example, suppose $\omega_a = 2\pi$ ($f_a = 1$ Hz), so that $\omega_b = 18\pi$ ($f_b = f_a + f_s = 9$ Hz). The input for ω_a and for ω_b is shown in Fig. 10.4.

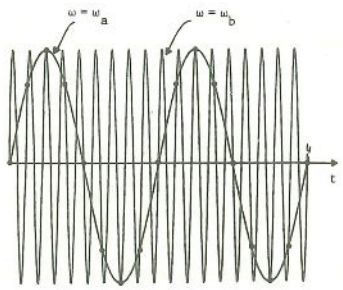


Fig. 10.4. Input for $f_a = 1$ Hz and $f_b = 9$ Hz.

Notice that at the sample time points $t = kT$, the same number sequence $u(kT)$ occurs, and the filter cannot distinguish between inputs at these two frequencies. To uniquely determine the frequency of the output, we must limit the input frequency range to $0 \le \omega < \omega_s/2$.

For this $H(z)$, $M(\omega)$ is small for low frequencies and high frequencies (up to $\omega_s/2$). Therefore, this $H(z)$ exhibits the characteristic of a **band-pass** (BP) filter. If the input consists of a sum of equal amplitude sampled sinusoids with frequencies in the range $0 \le \omega < \omega_s/2$, then the steady-state response will also consist of a linear combination of sinusoids at these frequencies. However, the response sinusoids with frequencies significantly above and below $\omega = \omega_0$ will have small amplitudes (the input sinusoids are attenuated) compared to sinusoids with frequencies in the vicinity of $\omega = \omega_0$.

To be more specific about the nature of a BP filter, we refer to the frequency range $\omega_1 \le \omega \le \omega_2$, where $M^2(\omega) \ge \frac{1}{2} M^2_{\text{peak}}$ as the **pass-band** of the filter, and $(\omega_2 - \omega_1)$ as the **bandwidth** (BW) of the filter, i.e., $BW = \omega_2 - \omega_1$, where ω_1 and ω_2 are called the **lower** and **upper**, respectively, **cut-off frequencies**. Therefore, at the cut-off frequencies we have

$$10 \log\left(\frac{M^2(\omega = \omega_1 \text{ or } \omega_2)}{M^2_{\text{peak}}}\right) = 10 \log\left(\frac{1}{2}\right) \cong -3dB$$

Since this $M(\omega)$ peaks at $\omega = \omega_0$, the cut-off frequencies are found with $M^2(\omega_1) = M^2(\omega_2) = \frac{1}{2}M^2(\omega_0)$. Notice that $\omega = \omega_0$ is not necessarily the arithmetic average $(\omega_1 + \omega_2)/2$ of ω_1 and ω_2. If an input with unity amplitude has the frequency $\omega = \omega_0$, then the amplitude of the steady-state response is $M(\omega_0)$, and the average power of the sinusoidal steady-state response is given by $\frac{1}{2}M^2(\omega_0)$. If the input frequency is $\omega = \omega_1$, then the average power of the steady-state response is given by $\frac{1}{2}M^2(\omega_1) = \frac{1}{2}\left(\frac{1}{2}M^2(\omega_0)\right)$. Therefore, $\omega = \omega_1$ and $\omega = \omega_2$ are also referred to as the **half power** points.

A sketch of the characteristic of a BP filter is shown in Fig. 10.5a. In specifying the desired characteristics of a band-pass filter, which is to be designed, ω_1 and ω_2 are usually given.

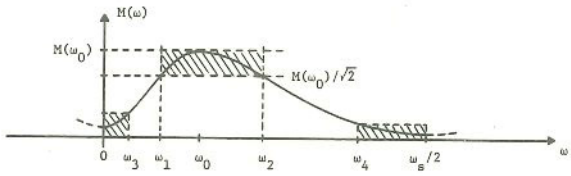


Fig. 10.5a. A BP filter magnitude characteristic.

Furthermore, we must also specify some frequencies $\omega = \omega_3 < \omega_1$, $\omega = \omega_4 > \omega_2$, and the extent to which $M(\omega)$ is to decrease as ω is decreased from ω_1 to ω_3 and increased from ω_2 to ω_4. Our design goal is to determine an $H(z)$ such that $M(\omega)$ meets the bandwidth requirement, and $M(\omega) \le M(\omega_3)$ for $0 \le \omega \le \omega_3$ and $M(\omega) \le M(\omega_4)$ for $\omega_4 \le \omega \le \omega_s/2$. The frequency ranges $0 \le \omega \le \omega_3$ and $\omega_4 \le \omega \le \omega_s/2$ are called **stop-bands**, while the ranges $\omega_3 < \omega < \omega_1$ and $\omega_2 < \omega < \omega_4$ are called **transition-bands**. Once ω_1, ω_2, ω_3, $M(\omega_3)$, ω_4, and $M(\omega_4)$ are given, we must determine an $H(z)$ such that $M(\omega)$ remains within the cross-hatched area shown in Fig. 10.5a.

An ideal BP filter magnitude characteristic $M_{BP}(\omega)$ is given by

$$M_{BP}(\omega) = \begin{cases} 0, & 0 \le \omega < \omega_1 \\ 1, & \omega_1 < \omega < \omega_2 \\ 0, & \omega_2 < \omega < \omega_s/2 \end{cases} \qquad \textbf{(10.13a)}$$

and since $M(\omega)$ must also be an even periodic function, then the $M_{BP}(\omega)$ shown in Fig. 10.5b results.

If the input to an ideal BP filter consists of a linear combination of sinusoids with frequencies in the range $0 \le \omega < \omega_s/2$, then the steady-state response will only consist of sinusoids with frequencies within the pass-band of the filter, and their amplitudes are the same as the corresponding input amplitudes. Those input sinusoids with frequencies within the stop-bands are perfectly attenuated. If $M(\omega)$ is not a constant within the pass-band, then the input wave shape corresponding

to sinusoids with frequencies within the pass-band is not preserved in the output. This is called **magnitude distortion**. As we shall see, it is possible to design an $H(z)$ with an $M(\omega)$ that comes as close to $M_{BP}(\omega)$ as we desire.

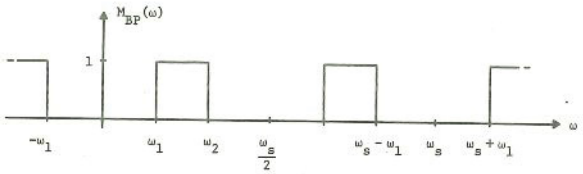


Fig. 10.5b. An ideal BP filter magnitude characteristic.

With any $H(z)$ that has been designed to achieve desired specifications on $M(\omega)$, the resulting phaseshift $\phi(\omega)$ determines how the filter modifies the phase angles of input sinusoids to obtain the phase angles of the output sinusoids. Suppose the filter in Fig. 10.1 is an ideal BP filter, and that the input consists of

$$u(kT) = \cos(\omega_a kT)u_{-1}(k) + \cos(\omega_b kT)u_{-1}(k)$$

where ω_a and ω_b are within the pass-band of the filter. If in the steady-state response, the input wave shape is to be preserved, then the filter should do no more than delay the input by some delay time T_d, so that

$$y(kT) = u(kT - T_d) = \cos(\omega_a(kT - T_d)) + \cos(\omega_b(kT - T_d))$$

$$= \cos(\omega_a kT - \omega_a T_d) + \cos(\omega_b kT - \omega_b T_d)$$

Here, we have that $M_{BP}(\omega_a) = M_{BP}(\omega_b) = 1$, and to equally delay each sinusoidal input, it is necessary that $\phi(\omega_a) = -\omega_a T_d$ and $\phi(\omega_b) = -\omega_b T_d$. For an ideal BP filter we require that

$$\phi_{BP}(\omega) = -T_d\omega \qquad \textbf{(10.13b)}$$

for $-\omega_s/2 < \omega < \omega_s/2$, which is a linear function of ω. Since $\phi(\omega)$ must also be an odd periodic function, then the $\phi_{BP}(\omega)$ shown in Fig. 10.5c results. Notice that for a causal filter the slope of $\phi_{BP}(\omega)$ cannot be positive.

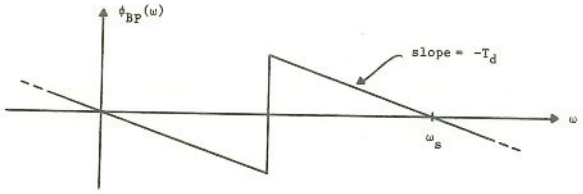


Fig. 10.5c. An ideal BP filter phaseshift characteristic.

If $\phi(\omega)$ is not a linear function of ω, then the input wave shape is not preserved in the output. This is called **phase distortion.**

A commonly used alternative to describe the phaseshift characteristic of a filter is the **group delay** $\tau(\omega)$, which is defined by

$$\tau(\omega) = -\frac{d}{d\omega}\phi(\omega) \tag{10.14}$$

and for an ideal BP filter we have the constant $\tau_{BP}(\omega) = T_d$ secs. Since $H(z)$ is a ratio of polynomials in z, we generally do not expect that $\phi(\omega)$ will be a linear function of ω, which, as we shall see in the next section, only occurs under special circumstances. Instead, a design specification should require that $\tau(\omega)$ remain within some range over the pass-band of the filter as shown by the cross-hatched area in Fig. 10.5d.

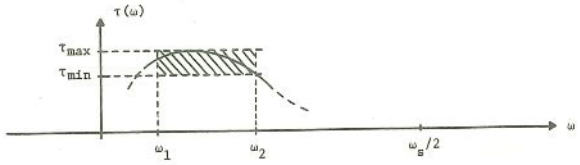


Fig. 10.5d. A BP filter group delay characteristic.

In general, we are not free to independently use any function form for $M(\omega)$ and $\phi(\omega)$, which are related through $H(z)$. Furthermore, $H(z) = P(z)/Q(z)$ should be the transfer function of a real, causal, and stable digital filter, where we would like that n, which is the order of the filter, be as small as filter specifications allow. Therefore, a filter specification is usually given in terms of bounds as shown in Figs. 10.5a and 10.5d. Even then, it may not be easy (or possible) to find an acceptable $H(z)$, which meets both of the bound conditions shown in Figs. 10.5a and 10.5d, if these conditions are too stringent. Usually, $H(z)$ is determined based only on conditions imposed on $M(\omega)$, and then the resulting $\phi(\omega)$ is evaluated to see if any phase distortion or delay is acceptable within the context of the intended application.

Example 10.3. For $H(z)$ given in Example 10.2, $M^2(\omega)$, $\phi(\omega)$ and $\tau(\omega)$ are given, respectively, by

$$M^2(\omega) = \frac{\gamma^2\cos^2(\omega_0 T - \psi)}{(1+\gamma^2-2\gamma\cos((\omega-\omega_0)T))(1+\gamma^2-2\gamma\cos((\omega+\omega_0)T))}$$

$$\phi(\omega) = -\omega T - \tan^{-1}\left(\frac{\gamma\sin((\omega-\omega_0)T)}{1-\gamma\cos((\omega-\omega_0)T)}\right) - \tan^{-1}\left(\frac{\gamma\sin((\omega+\omega_0)T)}{1-\gamma\cos((\omega+\omega_0)T)}\right)$$

$$\tau(\omega) = T\left(1 - \frac{\gamma^2-\gamma\cos((\omega-\omega_0)T)}{1+\gamma^2-2\gamma\cos((\omega-\omega_0)T)} - \frac{\gamma^2-\gamma\cos((\omega+\omega_0)T)}{1+\gamma^2-2\gamma\cos((\omega+\omega_0)T)}\right)$$

and one period is defined for $-8\pi < \omega < 8\pi$. The reader should verify these expressions. Notice that $\phi(-\omega) = -\phi(\omega)$. For $\gamma = 0.95$, these functions are plotted in Fig. 10.6, where the more conventional dB value of $M^2(\omega)$ is shown.

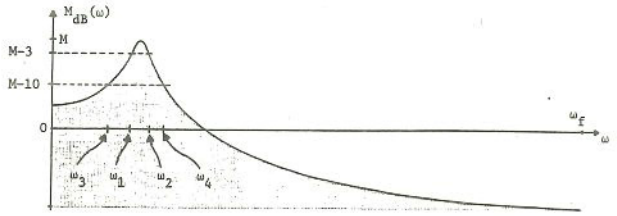


Fig. 10.6a. Magnitude response.

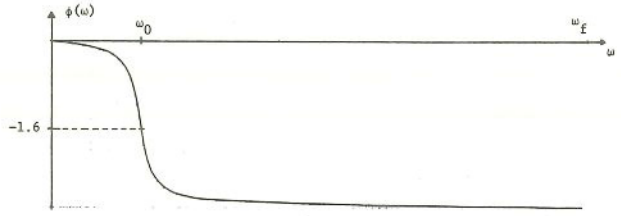


Fig. 10.6b. Phase response.

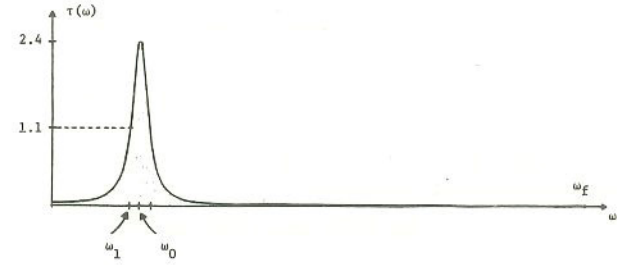


Fig. 10.6c. Group delay response.

In Fig. 10.6a we see that the gain $M(\omega)$ is down 3 dB from the peak value at $\omega_1 = 3.75$ and $\omega_2 = 4.55$ rad/sec, so that the bandwidth is BW = 0.8 rad/sec. If this is the desired pass-band, and it is sufficient that the gain is down 10 dB from the peak value at $\omega_3 \cong 2.7$ and $\omega_4 \cong 5.3$, then the difference equation given in Example 10.1 can be used to realize this band-pass filter. On the other hand, we may want the gain to be down more than 10 dB at ω_3 and ω_4 or some other values for ω_3 and ω_4, which are closer to ω_1 and ω_2, respectively. We shall develop design techniques to achieve such goals.

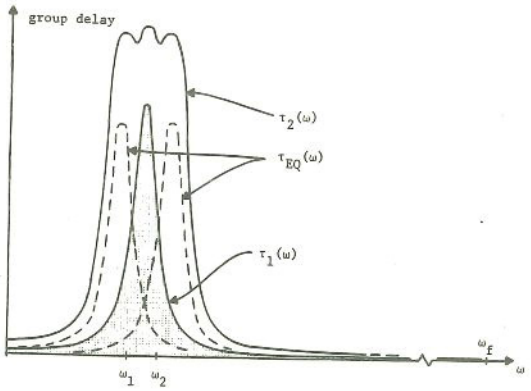


Fig. 10.6d. Equalized group delay.

Now, let us see how this BP filter responds to the input $u(kT) = \sin(\omega kT)u_{-1}(k)$, which is shown in Fig. 10.7a for $\omega = \omega_0$. For $\omega = \omega_0$, ω_3, and ω_4, the outputs are shown in Figs. 10.7b, c, and d, respectively.

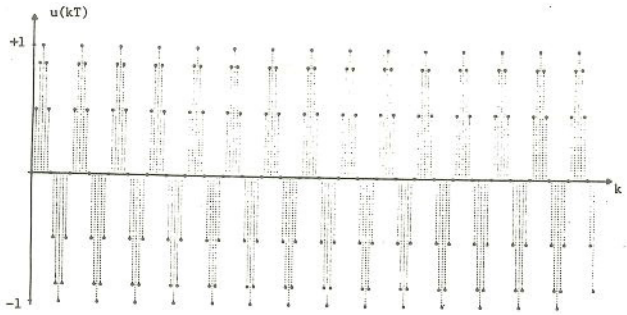


Fig. 10.7a. Input with $\omega = \omega_0$.

This filter was realized with the algorithm described in Fig. 9.25, and a subroutine, which executes this algorithm, is given in Fig. 10.8.

From the outputs, which are shown in Fig. 10.7, we see that after steady-state conditions have been reached, the filter has significantly attenuated the input for the frequencies $\omega = \omega_3$ and $\omega = \omega_4$. Notice that the input with frequency $\omega = \omega_0$ has been phase shifted by $\phi(\omega_0) \cong -1.6$ rad. (See Fig. 10.6b.), or delayed by $\tau(\omega_0) \cong 2.4$ secs. (See Fig. 10.6c.). From Fig. 10.6c we see that the group delay is not a constant within the pass-band, but instead varies over the range 1.1 secs. to 2.4 secs. An improved group delay is shown in Fig. 10.6d, which will be explained in a short while.

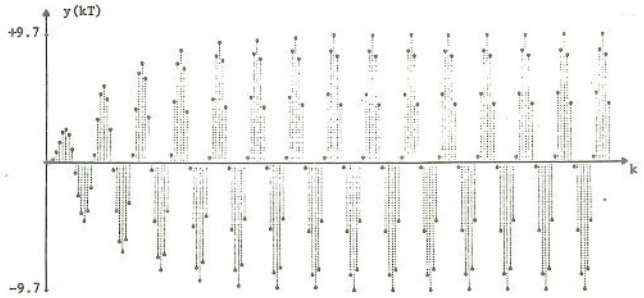


Fig. 10.7b. Output with $\omega = \omega_0$.

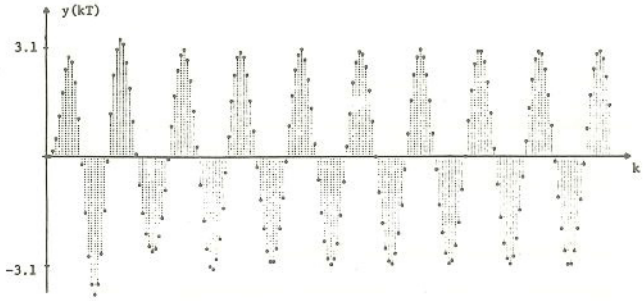


Fig. 10.7c. Output with $\omega = \omega_3$.

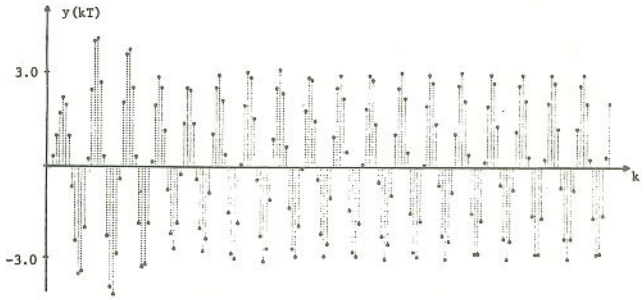


Fig. 10.7d. Output with $\omega = \omega_4$.

```
DIMENSION C(48),Y(48),Y0(512),YI(512),TIME(512)
DATA PI/3.1415926/,W3/2.7/,W4/5.3/
GAMMA=.95
W0=4.*PI/3.
T=.125
```

```
      PSI=-PI/2.
      B2=COS(PSI)
      B1=-GAMMA*COS(W0*T-PSI)
      B0=0.
      A1=-2.*GAMMA*COS(W0*T)
      A0=GAMMA**2
      C(1)=B0
      C(2)=B1
      C(3)=B2
      C(4)=-A0
      C(5)=-A1
      I=1
      NY=6*I
      DO 1 M=1,NY
    1 Y(M)=0.
      W=W0
      N=512
      DO 2 K=1,N
      TIME(K)=(K-1)*T
      AD=SIN(W*TIME(K))
      Y0(K)=AD
      CALL FILTER(I,C,Y,AD,DA)
    2 YI(K)=DA
      CALL PLOT('------FILTER-INPUT------',N,
     1 Y0,'--------',TIME,'--SECS.-')
      CALL PLOT('------FILTER-OUTPUT-----',N,
     1 YI,'--------',TIME,'--SECS.-')
      STOP
      END

      SUBROUTINE FILTER(I,C,Y,AD,DA)
C     EXECUTES THE FILTER ALGORITHM GIVEN IN FIG. 9.25B
      DIMENSION C(1),Y(1)
      Y(3)=AD
      INDEX=0
      DO 1 ISECT=1,I
      INDEX=INDEX+1
      SUM=0.
      DO 2 M=1,5
      SUM=SUM+C(INDEX)*Y(INDEX)
    2 INDEX=INDEX+1
      Y(INDEX)=SUM
      IF(ISECT.EQ.I) GO TO 3
    1 Y(INDEX+3)=Y(INDEX)
    3 DA=Y(INDEX)
      DO 4 M=2,INDEX
    4 Y(M-1)=Y(M)
      RETURN
      END
```

Fig. 10.8. Main program and subroutine for running a cascade structure filter.

A design specification may require that within the pass-band of the filter, $\tau(\omega)$ should not deviate by more than, for example, $\pm 10\%$ from some constant value. Since in general, there is no direct design procedure that can simultaneously achieve arbitrary specifications on both $M(\omega)$ and

$\phi(\omega)$, we first determine an $H(z)$ that satisfies the requirement for $M(\omega)$. Let us denote the resulting $H(z)$ by $H_1(z)$. We then can cascade $H_1(z)$ with an all-pass filter $H_{EQ}(z)$ that consists of a product of terms each having the form

$$\frac{(1-pz)(1-p^*z)}{(z-p^*)(z-p)} = \frac{1-(p+p^*)z+\|p\|^2z^2}{z^2-(p+p^*)z+\|p\|^2} \tag{10.15a}$$

for complex poles, or $(1-pz)/(z-p)$ for real poles. Therefore, the zeros of $H_{EQ}(z)$ are the reciprocals of the poles of $H_{EQ}(z)$, and by eq. 10.12, $M_{EQ}(\omega)=1$. Let us denote the overall transfer function by $H_2(z)$, and we have

$$H_2(z) = H_1(z)H_{EQ}(z)$$

$$M_2(\omega) = M_1(\omega)M_{EQ}(\omega) = M_1(\omega)$$

$$\phi_2(\omega) = \phi_1(\omega) + \phi_{EQ}(z)$$

$$\tau_2(\omega) = \tau_1(\omega) + \tau_{EQ}(\omega)$$

Since an all-pass filter does not alter the magnitude response of $H_1(z)$, it is commonly used for **phase equalization**, which means that the poles of $H_{EQ}(z)$ must be positioned such that for a given $\phi_1(\omega)$ (or $\tau_1(\omega)$), $\phi_2(\omega)$ (or $\tau_2(\omega)$) satisfies the specifications imposed on $\phi(\omega)$ (or $\tau(\omega)$). $H_{EQ}(z)$ must also be a stable filter, and if in eq. 10.15a we write $p=\alpha e^{j\beta}$, then $\alpha<1$.

If $H_{EQ}(z)$ were to consist of just one term as given in eq. 10.15a, then $\tau_{EQ}(\omega)$ is given by

$$\tau_{EQ}(\omega) = 2T\left(1-\frac{\alpha^2-\alpha\cos(\omega T-\beta)}{1+\alpha^2-2\alpha\cos(\omega T-\beta)}-\frac{\alpha^2-\alpha\cos(\omega T+\beta)}{1+\alpha^2-2\alpha\cos(\omega T+\beta)}\right) \tag{10.15b}$$

which, like $\tau(\omega)$ given in Example 10.3, peaks at $\omega=\pm\beta/T$. The extent of the peak is determined by α. If an equalizer for $\tau_1(\omega)$ shown in Fig. 10.6c is needed, then it is likely that at least two terms as given in eq. 10.15a are required in $H_{EQ}(z)$. For one term, the group delay should peak near ω_1, and for the other term, the group delay should peak near ω_2. This is illustrated in Fig. 10.6d, where we have simply used guess and try values for $p=p_1=\alpha_1e^{j\beta_1}$ and $p=p_2=\alpha_2e^{j\beta_2}$. Later in this chapter we shall develop a method for finding suitable values for p_1 and p_2, or the poles of any other phase equalizer we may want to try.

At this point, the reader should realize that LTI filter design is mainly an approximation problem, where a causal (for real-time operation), real, and stable discrete time system, which meets prescribed filtering behavior, must be determined. This becomes even more apparent if we consider the time domain behavior of an ideal BP filter. For $-\omega_s/2<\omega<\omega_s/2$, eqs. 10.13 become

$$H_{BP}(e^{j\omega T}) = \begin{cases} e^{-j\omega T_d}, & -\omega_2<\omega<-\omega_1,\quad \omega_1<\omega<\omega_2 \\ 0, & -\omega_s/2<\omega<-\omega_2,\ -\omega_1<\omega<\omega_1,\ \omega_2<\omega<\omega_s/2 \end{cases} \tag{10.16}$$

By eq. 9.16, the unit pulse response $h_{BP}(k)$ is given by

$$h_{BP}(k) = Z^{-1}(H_{BP}(z)) = \frac{1}{2\pi j}\oint_{\Gamma} H_{BP}(z) z^{k-1} dz$$

where the path Γ must be within the annulus of convergence of $Z(h_{BP}(k))$. Since the filter must be stable, the annulus of convergence includes the unit circle, which we will use as the path Γ. Therefore, along the path Γ, let $z = e^{j\omega T}$ for $-\pi \le \omega T < \pi$, and $h_{BP}(k)$ becomes

$$h_{BP}(k) = \frac{1}{2\pi j}\int_{-\omega_s/2}^{\omega_s/2} H_{BP}(e^{j\omega T}) e^{j\omega T(k-1)} jT e^{j\omega T} d\omega$$

$$= \frac{T}{2\pi}\left(\int_{-\omega_2}^{-\omega_1} e^{-j\omega T_d} e^{j\omega kT} d\omega + \int_{\omega_1}^{\omega_2} e^{-j\omega T_d} e^{j\omega kT} d\omega\right)$$

$$h_{BP}(k) = \frac{T}{2\pi}\left(\left(\frac{e^{j(kT-T_d)\omega}}{j(kT-T_d)}\right)\Big|_{-\omega_2}^{-\omega_1} + \left(\frac{e^{j(kT-T_d)\omega}}{j(kT-T_d)}\right)\Big|_{\omega_1}^{\omega_2}\right)$$

$$= \frac{\omega_2 T}{\pi}\frac{\sin(\omega_2(kT-T_d))}{\omega_2(kT-T_d)} - \frac{\omega_1 T}{\pi}\frac{\sin(\omega_1(kT-T_d))}{\omega_1(kT-T_d)} \qquad (10.17)$$

For the cut-off frequencies of Example 10.3, the unit pulse response of an ideal BP filter is shown in Fig. 10.9, with $T_d = 0$.

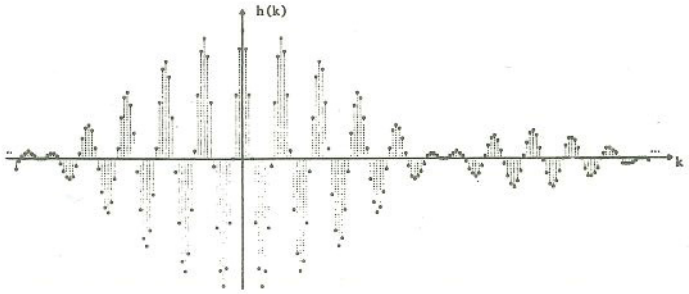


Fig. 10.9. Unit pulse response of an ideal BP filter.

From eq. 10.17 or Fig. 10.9 we see that $h_{BP}(k) \neq 0$ for $k < 0$, and therefore an ideal filter can only be achieved with a noncausal system, regardless of the value of T_d. However, suppose we use a large enough positive value for T_d, which would shift, for example, the $h_{BP}(k)$ shown in Fig. 10.9 to the right, and then define $h(k) = h_{BP}(k)u_{-1}(k)$, which is causal. With this $h(k)$,

$H(z) = Z(h(k)) \rightarrow H_{BP}(z)$ as $T_d \rightarrow \infty$. For $T_d = 128T$, $\| H(e^{j\omega T}) \|$ is shown in Fig. 10.10, which was obtained by taking the DFT of $h(k)$ for $k = 0, 1, \cdots, (N-1)$, where $N = 512$, which is large enough for a negligible leakage error, was used.

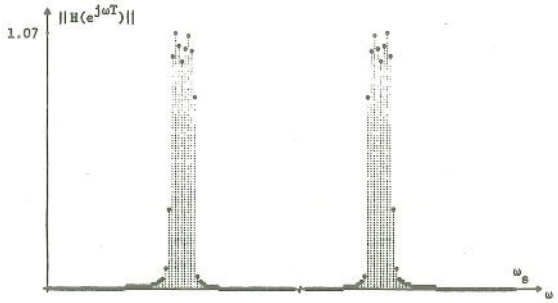


Fig. 10.10. Approximation for an ideal BP filter magnitude response.

Although we can come close to the ideal BP filter characteristic by increasing T_d, we cannot exactly achieve it. Nevertheless, the $h(k)$ values could be used as the weights for the FIR filter structure given in Fig. 10.2.

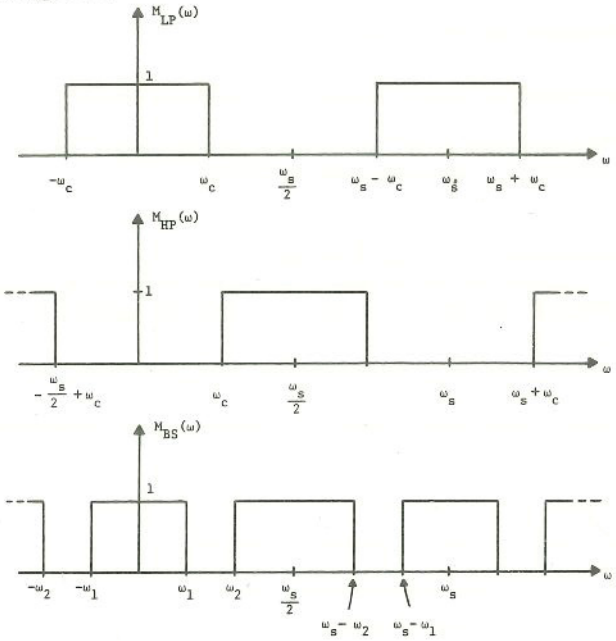


Fig. 10.11. Ideal characteristic for LP, HP, and BS filters.

There are several other common types of filters. These are the **low-pass** (LP), **high-pass** (HP), and **band-stop** (BS) filters, the ideal magnitude characteristics of which are shown in Fig. 10.11.

For $H_{LP}(z)$ and $H_{HP}(z)$, ω_c is referred to as the **cut-off frequency**, and the bandwidth is ω_c and $(\omega_s/2 - \omega_c)$, respectively. For $H_{BS}(z)$, ω_1 and ω_2 are the **lower** and **upper**, respectively, cut-off frequencies, and the frequency range ω_1 to ω_2 is referred to as the **stop-band**. The ideal phaseshift characteristic for each of these filters is the same as that shown in eq. 10.13b.

Achieving an ideal filter characteristic is a typical digital (or analog) filter design goal. However, there are other design goals that we may want to achieve. We have already considered one example, which was to design a digital filter to perform phase equalization. Similarly, suppose some system has an undesirable magnitude frequency response $M_1(\omega)$. Then, we would consider the design of a cascaded filter $H_{EQ}(z)$ that performs **magnitude equalization**, such that the overall magnitude response $M_2(\omega) = M_1(\omega)M_{EQ}(\omega)$ meets required specifications.

We may also want to design a discrete time system to perform operations such as differentiation or integration. By describing the desired performance of an LTI discrete time system in terms of its frequency response we have a goal for the design of a digital filter. As we develop several digital filter design techniques, we will see examples of the design of discrete time systems which perform various activities.

10-1.4 Transient Response Specifications

So far, all of our discussion concerning digital filters has focused on the steady-state sinusoidal response. In some applications, we must also be concerned about the transient response, which depends on the natural frequencies of the filter. In fact, as the bandwidth of a filter is decreased, it will take longer for the filter to reach steady-state conditions.

Example 10.4. Let us use a specific filter to illustrate the relationship between bandwidth and transient response duration. In Fig. 10.7b we see that we must wait a while before we can discern how the filter has processed the input. Suppose we want a more frequency selective filter. This can be accomplished by moving the poles closer to the unit circle. For $\gamma = 0.975$, the magnitude frequency response is shown in Fig. 10.12a, and we have obtained a filter with a smaller bandwidth than with $\gamma = 0.95$.



Fig. 10.12a. Magnitude response with $\gamma = 0.975$.

From the response to $\sin(\omega_0 kT)u_{-1}(k)$ shown in Fig. 10.12b we see that we must wait even longer to discern the steady-state response.

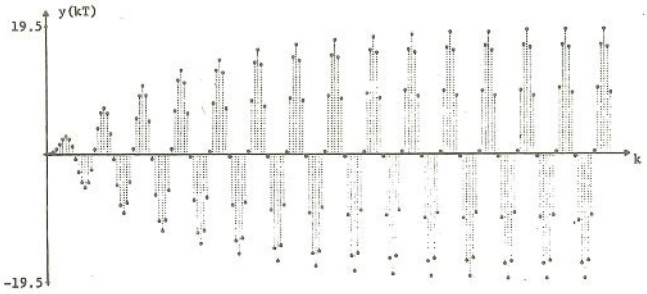


Fig. 10.12b. Output with $\omega = \omega_0$.

A better indication of a filter's transient behavior can be obtained from a unit step response, which is commonly used for such purposes, and it is shown in Fig. 10.13.

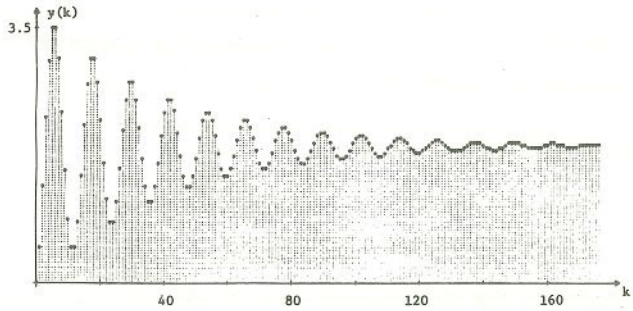


Fig. 10.13. Unit step response of the BP filter.

An indicator of transient behavior is the **rise time** t_r, which is commonly defined as the time it takes for the response in its initial rise to go from 10% to 90% of the peak value. Another commonly used parameter is the **settling time** t_s, which is the time required for the response to reach and then remain within a range ±5% about the steady-state value. Since the transient response depends on initial conditions, the parameters t_r and t_s are obtained under zero initial conditions, and thereby the transient behavior of different filters can be compared. In this example we see that as the BW of the filter is made smaller, the settling time is increased. Also of concern is the amount the response in its initial rise overshoots the steady-state value.

We have seen in previous examples that there are numerous trade-offs to consider between transient and steady-state filter performance. Generally, the settling time is inversely proportional to the bandwidth. This can be established for a particular case by considering the unit pulse response $h(k)$ of a filter with transfer function $H(z) = Z(h(k))$. If the input is a unit step, i.e., $u(k) = u_{-1}(k)$, then the response is $Y(z) = H(z)/(1 - z^{-1})$, and therefore we have

$$y(k) = h(k) + y(k-1) \tag{10.18}$$

The unit step response, which is the solution of eq. 10.18, can be found by running this equation. If $h(k)$ is causal, then we start eq. 10.18 at $k = 0$, with $y(-1) = 0$, and if $h(k)$ is not causal, as in eq. 10.17, then we must start eq. 10.18 at $k = -\infty$, with $y(-\infty) = 0$. Through eq. 10.18, we can relate the settling time to the duration of $h(k)$. Since the filter is stable, then for some large enough $k_s T \equiv t_s$, $h(k) \equiv 0$ for $k > k_s$, and for $k > k_s$, eq. 10.18 becomes $y(k) \equiv y(k-1)$, i.e., steady-state conditions have been reached.

Let us determine the settling time of an ideal LP filter. In eq. 10.17 set $\omega_1 = 0$, so that the BP filter becomes an LP filter with $\mathrm{BW} = \omega_c = \omega_2$. The LP filter unit pulse response is given by

$$h_{\mathrm{LP}}(k) = \frac{\omega_c T}{\pi} \frac{\sin(\omega_c(kT - T_d))}{\omega_c(kT - T_d)}$$

which is zero or crosses zero at the time points determined by $\omega_c(kT - T_d) = i\pi$, $i = \pm 1, \pm 2, \cdots$. Suppose we use the zero crossing points of $h_{\mathrm{LP}}(k)$ closest to $kT \equiv T_d$ to specify the duration of $h_{\mathrm{LP}}(k)$. For $i = -1$ we get $kT \equiv -\frac{\pi}{\omega_c} + T_d$, and for $i = +1$ we get $kT \equiv \frac{\pi}{\omega_c} + T_d$. The length of this time interval is $2\pi/\omega_c$, and we see that the duration of $h_{\mathrm{LP}}(k)$ or the settling time is inversely proportional to the bandwidth. For any other duration, and even for any other filter, only the proportionality constant will change. Thus, as we decrease the bandwidth of a filter, the transient response will last longer.

10-1.5 Digital Filter Advantages and Disadvantages

In the design of a digital filter, we want to achieve ideal filtering characteristics as given in eqs. 10.13 and Fig. 10.11, and good transient performance, i.e., little overshoot and minimum settling time. However, these are opposing requirements. Instead, a digital filter design is usually based on an $M(\omega)$ specification. These same issues and subsequent compromises arise in the design of analog (continuous time) filters. However, digital filters have some practical advantages over analog filters, such as:

(a) digital filters can be perfectly duplicated, without the concern about maintaining component value tolerances as with analog filters;

(b) they are programmable, so that the same hardware can be used to realize different filtering characteristics;

(c) they can be fabricated in small packages with low power consumption through the use of integrated circuit (IC) technology;

(d) digital filters are less susceptible to environmental influences, because filter parameters are numbers stored in digital hardware memory and filter operation is determined by the activity of digital hardware;

(e) they can achieve any desired accuracy of operation.

A limiting factor on the application of digital filters is the speed at which digital hardware can execute the arithmetic of a discrete time system. To run a digital filter in real-time, data acquisition and all of the arithmetic must be executed within the time duration of one sample time increment T. **Real-time processing** is illustrated in Fig. 10.14.

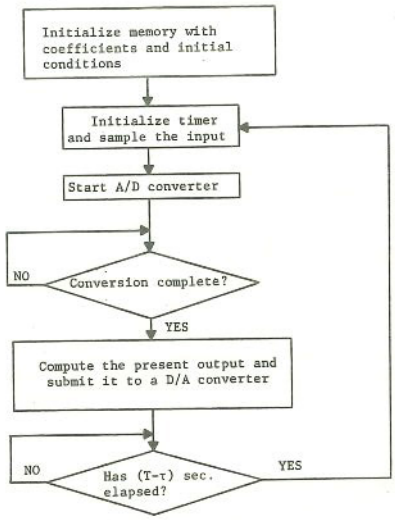


Fig. 10.14. Real-time processing flowchart.

There are many trade-offs to consider. For data acquisition, we must decide on the number of bits necessary in A/D conversion based on an acceptable signal to quantization error (noise) ratio. This along with A/D converter cost constraints will determine A/D conversion time. Then, the number of binary digits used to represent coefficients, the time it takes to perform multiply, add, and store operations for a required precision, the order of the filter, and the realization (structure) that is used all determine the minimum possible value τ (For example, see Fig. 9.25.) for T. Consequently, the bandwidth of a signal that can be processed in real-time by a digital filter must be less than $1/(2\tau)$ Hz. On the other hand, if $\tau \ll T$, then the same digital hardware can be used to process up to L analog signals, if $L\tau \leq T$. This can be accomplished with either a digital multiplexer or an analog multiplexer as shown in Fig. 10.15. In fact, by using different sets of filter coefficients, which are all stored in computer memory, each signal can be processed by a different filter with the same hardware.

If $\tau > T$, then real-time processing is not possible. However, **off-line processing** may still be possible. This is accomplished by first acquiring and storing a sequence of input signal samples, and then the sequence of recorded samples can be processed by a filter algorithm that is not necessarily a causal filter. For off-line processing, the signal bandwidth is only limited by the time required to perform an A/D conversion and to store a sample value.

Now that we have described some time and frequency domain attributes of a digital filter, we are ready to develop some design techniques.

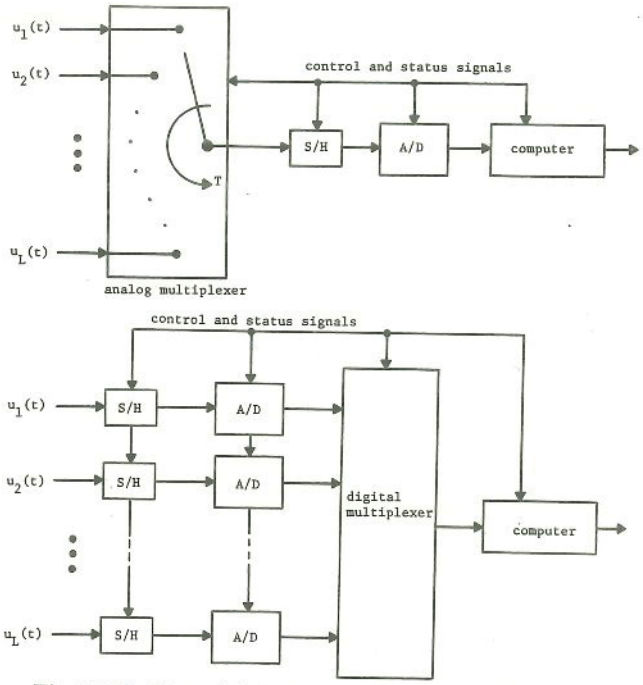


Fig. 10.15. Time division multiplexed data acquisition.

SECTION 10-2 Finite Impulse Response Filter Design

In the design of a causal finite impulse response (FIR) filter we want to obtain a discrete time system with a transfer function given by

$$H(z) = \sum_{i=0}^{I-1} h(i) z^{-i} \tag{10.19}$$

where I is a finite integer. The filter is described by the I coefficients, $h(i)$, $i = 0, \cdots, (I-1)$. The unit pulse response has a finite duration, i.e., $h(k) = 0$ for $k < 0$ and $k \geq I$.

If the unit pulse response $h_{IIR}(k) = Z^{-1}(H_{IIR}(z))$ of a stable and recursive digital filter, which has a transfer function $H_{IIR}(z)$ as given in eq. 10.3a, is known, then, through the convolution summation, the filter can be approximated with a nonrecursive form. Since $h_{IIR}(k) \to 0$ as $k \to \infty$, select an I such that $h_{IIR}(k) \cong 0$, for $k \geq I$. Then, eq. 10.2a becomes

$$y(k) \equiv \sum_{i=0}^{I-1} h_{\text{IIR}}(i)u(k-i)$$

Or, in eq. 10.19 use

$$h(k) = h_{\text{IIR}}(k)w(k) \tag{10.20}$$

where $w(k)$ is a window function such that $w(k) = 0$ for $k < 0$ and $k \geq I$. Thus, we obtain $H(z)$ of eq. 10.19, and depending on I and the window function $w(k)$ that is used we can achieve

$$H(e^{j\omega T}) \equiv H_{\text{IIR}}(e^{j\omega T})$$

Issues concerned with the choice for I and $w(k)$ are discussed in Chapter Five. With eq. 10.20, even a recursive filter can be implemented with a nonrecursive structure as given in Fig. 10.2. Some recursive filter design methods will be given in Section 10-3.

We will now develop two design methods to directly obtain an $H(z)$ as given in eq. 10.19 that approximates a desired frequency response $M_d(\omega)$ and $\phi_d(\omega)$.

10-2.1 Fourier Series Method

This design method is based on the property that $H(e^{j\omega T}) = M(\omega)e^{j\phi(\omega)}$ is a periodic function of ω with period ω_s, where $M(\omega)$ is an even function and $\phi(\omega)$ is an odd function. Let us specify a desired frequency response $H_d(e^{j\omega T})$ that satisfies these properties. Therefore, $H_d(e^{j\omega T})$ can be written as a Fourier series as given by

$$H_d(e^{j\omega T}) = \sum_{i=-\infty}^{\infty} h_i e^{-ji\frac{2\pi}{\omega_s}\omega} \tag{10.21}$$

where the Fourier series coefficients h_i are determined with

$$h_i = \frac{1}{\omega_s}\int_{-\omega_s/2}^{\omega_s/2} H_d(e^{j\omega T})e^{ji\frac{2\pi}{\omega_s}\omega}\, d\omega \tag{10.22}$$

While we may only be accustomed to writing a Fourier series representation for a real periodic time function, we can obtain a Fourier series for this complex periodic function of the real variable ω. Essentially, the only requirement is that the Fourier series coefficients exist.

Using Euler's identity and noting that $2\pi/\omega_s = T$, results in

$$h_i = \frac{1}{\omega_s}\int_{-\omega_s/2}^{\omega_s/2} M_d(\omega)\,(\cos\phi_d(\omega) + j\sin\phi_d(\omega))\,(\cos(iT\omega) + j\sin(iT\omega))d\omega \tag{10.23}$$

Since $\phi_d(\omega)$ is an odd function, we have that $\cos(\phi_d(-\omega)) = \cos(-\phi_d(\omega)) = \cos(\phi_d(\omega))$ and $\sin(\phi_d(-\omega)) = \sin(-\phi_d(\omega)) = -\sin(\phi_d(\omega))$, and therefore, $\cos(\phi_d(\omega))$ is an even function, while $\sin(\phi_d(\omega))$ is an odd function. And, since $M_d(\omega)$ is an even function, eq. 10.23 reduces to

$$h_i = \frac{1}{\omega_s}\int_{-\omega_s/2}^{\omega_s/2} M_d(\omega)\,(\cos\phi_d(\omega)\cos(iT\omega) - \sin\phi_d(\omega)\sin(iT\omega))\,d\omega \tag{10.24a}$$

$$= \frac{1}{\omega_s}\int_{-\omega_s/2}^{\omega_s/2} M_d(\omega)\cos(iT\omega + \phi_d(\omega))\,d\omega \tag{10.24b}$$

which shows that the h_i are real numbers. Furthermore, if we specify a real $H_d(e^{j\omega T})$, i.e., $\phi_d(\omega) = 0$, then $\sin\phi_d(\omega) = 0$, and by eq. 10.24a, $h_i = h_{-i}$, so that h_i is an **even** function of i. And, if we specify an imaginary $H_d(e^{j\omega T})$, i.e., $\phi_d(\omega) = \pm\pi/2$, for $0 < \omega < \omega_s/2$ and $\phi_d(\omega) = \mp\pi/2$, for $-\omega_s/2 < \omega < 0$, then $\cos\phi_d(\omega) = 0$, and by eq. 10.24a, $h_i = -h_{-i}$, so that h_i is an **odd** function of i. In any case, the h_i, as determined with eq. 10.22 (10.24b), are real, and the integration range can be any interval of duration ω_s.

Now, let us consider eq. 10.21. To obtain an FIR filter for which I is finite we must truncate the series in eq. 10.21, and instead of $H_d(e^{j\omega T})$ we have

$$\hat{H}(e^{j\omega T}) = \sum_{i=-K}^{K} \hat{h}_i e^{-ji T\omega} = \hat{M}(\omega)e^{j\hat{\phi}(\omega)} \tag{10.25}$$

where $\hat{h}_i = h_i$ and as the limit $K \to \infty$, $\hat{H}(e^{j\omega T}) \to H_d(e^{j\omega T})$. However, if $H_d(e^{j\omega T})$ has any discontinuities, then $\hat{H}(e^{j\omega T})$ will exhibit Gibbs' oscillation about any points of discontinuity. From our experience with Fourier series representations of real, finite, and periodic time functions we do expect that $h_i \to 0$ as $i \to \pm\infty$ (See Problem 2.18.), and for some summation limit K, $h_i \equiv 0$ for $|i| > K$. In a short while, we will illustrate this with an example.

Now, let eq. 10.25 come from the frequency response of a discrete time system with a transfer function given by

$$\hat{H}(z) = \sum_{i=-K}^{K} \hat{h}_i z^{-i} \tag{10.26}$$

This noncausal system can be changed to a causal system by delaying the unit pulse response by K sample time increments. The causal system transfer function is $(z^{-K})\hat{H}(z)$, or

$$z^{-K}\hat{H}(z) = \sum_{i=-K}^{K} \hat{h}_i z^{-(i+K)} = \sum_{i=0}^{2K} \hat{h}_{i-K} z^{-i} \tag{10.27}$$

Comparing eqs. 10.19 and 10.27 completes the **Fourier series** FIR filter design method. Setting $I - 1 = 2K$, and using

$$h(i) = \hat{h}_{i-K} = h_{i-K} \tag{10.28}$$

for $i = 0, 1, \cdots, 2K$, results in

$$H(z) = z^{-K}\hat{H}(z) = \sum_{i=0}^{2K} \hat{h}_{i-K} z^{-i} \tag{10.29a}$$

$$h(k) = \sum_{i=0}^{2K} \hat{h}_{i-K} u_0(k-i) \tag{10.29b}$$

$$M(\omega) = \| e^{-jKT\omega} \| \hat{M}(\omega) = \hat{M}(\omega) \tag{10.30a}$$

$$\phi(\omega) = -KT\omega + \hat{\phi}(\omega) \tag{10.30b}$$

By choosing K large enough, $M(\omega) \equiv M_d(\omega)$, and $\phi(\omega) \equiv -KT\omega + \phi_d(\omega)$.

Now, we can point out a very useful result. Recall that in the design of a filter, as described in eq. 10.16 and Fig. 10.11, we wish to achieve a linear phaseshift characteristic. A linear phaseshift characteristic can be exactly achieved, if we initially specify that $\phi_d(\omega) = 0$. Then, $h_i = h_{-i}$, $\hat{\phi}(\omega) = 0$, and $\phi(\omega)$ is exactly given by $\phi(\omega) = -KT\omega$. And, in eq. 10.29b we see that the unit pulse response is **symmetrical** about the point $k = K = \frac{I-1}{2}$, i.e., $h(k) = h(I-1-k)$, for $k = 0, 1, \cdots, (I-3)/2$, so that $h(0) = h(I-1)$, $h(1) = h(I-2)$, $\cdots$, $h\left(\frac{I-3}{2}\right) = h\left(\frac{I+1}{2}\right)$, and $h\left(\frac{I-1}{2}\right) = h_0$ has no matching point. In fact, only with an FIR filter, where the unit pulse response is symmetrical about the point $k = \frac{I-1}{2}$, can a linear phaseshift characteristic ($-KT\omega$) be exactly achieved.

Example 10.5. Suppose a signal $u(t)$ is bandlimited to 1000 Hz, and we want to low-pass filter it with an FIR filter for which BW $= f_c = 500$ Hz. Let $f_s = 2000$ Hz. For a linear phaseshift characteristic, set $\phi_d(\omega) = 0$, and the desired frequency response becomes $H_d(e^{j\omega T}) = M_d(\omega)$, which is shown in Fig. 10.16.

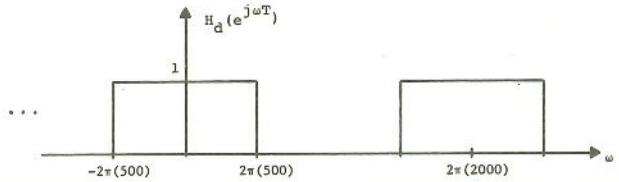


Fig. 10.16. Ideal LP filter characteristic.

By eq. 10.22 we get

$$h_i = \frac{1}{\omega_s}\int_{-\omega_s/4}^{\omega_s/4} e^{jiT\omega} d\omega = \frac{1}{\omega_s}\frac{1}{jiT}\left(e^{jiT\omega_s/4} - e^{-jiT\omega_s/4}\right) = \frac{1}{2}\frac{\sin(i\pi/2)}{(i\pi/2)}$$

Setting $i = 0$ before taking the integral, we get $h_0 = \frac{1}{2}$. The FIR filter transfer function is given by

$$H(z) = \sum_{i=0}^{2K} \frac{1}{2} \frac{\sin((i-K)\pi/2)}{(i-K)\pi/2} z^{-i}$$

and for $K = 20$ ($I = 41$), the unit pulse response is shown in Fig. 10.17.

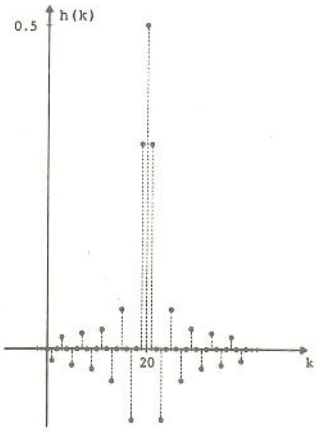


Fig. 10.17. LP filter unit pulse response.

Notice the symmetry about $k = K = \frac{I-1}{2} = 20$. Since $\phi_d(\omega) = 0$, the linear phaseshift of $H(e^{j\omega T})$ occurs because of the z^{-K} term in eq. 10.29a. Therefore, let us plot $\hat{H}(e^{j\omega T})$, which is real, and it is shown in Fig. 10.18.

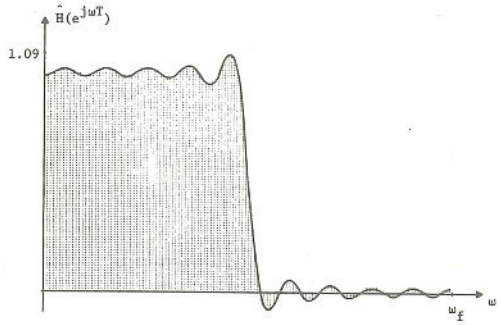


Fig. 10.18. FIR LP filter approximation.

Of course, $M(\omega) = \hat{M}(\omega)$. However, because of Gibbs' oscillation, $\hat{H}(e^{j\omega T})$ is not always positive. When $\hat{H}(e^{j\omega T})$ is negative, the phaseshift of $H(e^{j\omega T})$ changes from $\phi(\omega) = -KT\omega$ to $\phi(\omega) = -KT\omega - \pi$, which, strictly speaking, is not a linear phaseshift characteristic. Since this occurs for frequencies within the stop-band, it may not be a practical issue.

We can improve how well $M(\omega)$ approximates $M_d(\omega)$ by increasing K. However, this would only concentrate the oscillation about the discontinuity of $M_d(\omega)$, and it would not diminish the peak amplitude of the oscillation. By simply truncating the Fourier series given in eq. 10.21 we have actually achieved $H(e^{j\omega T}) = \pm\hat{M}(\omega)e^{-jKT\omega}$. In a short while, we will consider a remedy for Gibbs' oscillation.

Gibbs' oscillation occurs because $M_d(\omega)$ has discontinuities. This can be avoided by initially specifying an $M_d(\omega)$ with narrow transition bands instead of discontinuities.

When a specified $H_d(e^{j\omega T})$ is imaginary, we have already shown that $h_i = -h_{-i}$, which requires that $h_0 = 0$. Then, $h(k) = -h(I-1-k)$, for $k = 0, 1, \cdots, (I-3)/2$, and it is said that $h(k)$ is **anti-symmetrical** about the point $k = (I-1)/2$, where $h\left(\frac{I-1}{2}\right) = h_0 = 0$.

Recall that the imaginary part of any $H(e^{j\omega T})$ must be an odd periodic function of ω. Therefore, if we specify an imaginary $H_d(e^{j\omega T})$, then it must be zero at the frequencies $\omega = 0$ and $\omega = \pm\omega_s/2$.

Example 10.6. Let us obtain an FIR filter that approximates the transfer function $H_d(e^{j\omega T}) = j\omega$ for $-\omega_s/2 < \omega < \omega_s/2$. This is the transfer function of a differentiator for input signals bandlimited to $\omega_s/2$.

By eq. 10.22 we have

$$h_i = \frac{1}{\omega_s}\int_{-\omega_s/2}^{\omega_s/2} j\omega e^{jiT\omega} d\omega = -\frac{1}{\omega_s}\int_{-\omega_s/2}^{\omega_s/2} \omega \sin(iT\omega) d\omega$$

where $h_0 = 0$, and it turns out that $h_i = (-1)^i/iT$ for $i \neq 0$. The FIR filter transfer function is given by

$$H(z) = \sum_{\substack{i=0 \\ i\neq K}}^{2K} \frac{(-1)^{i-K}}{(i-K)T} z^{-i}$$

and for $K = 20$ and $T = 1/8$, the unit pulse response is shown in Fig. 10.19a.

Notice the antisymmetry about $k = \frac{I-1}{2} = 20$. For this $H_d(e^{j\omega T})$, $\phi_d(\omega) = \pi/2$ for $0 < \omega < \omega_s/2$ and $\phi_d(\omega) = -\pi/2$ for $-\omega_s/2 < \omega < 0$, and $\hat{H}(e^{j\omega T})$ is imaginary, so that $\phi(\omega) = -KT\omega + \phi_d(\omega)$. $\hat{H}(e^{j\omega T})/j$ is shown in Fig. 10.19b, and Gibbs' oscillation has occurred.

Let us view truncating the Fourier series given in eq. 10.21 to obtain eq. 10.25 as the result of using $\hat{h}_i = w(i)h_i$, where $w(i)$ is a rectangular window function $w_R(i) = 1$ for $i = -K, -K+1, \cdots, K-1, K$. We will now consider using window functions other than $w_R(i)$ to

diminish Gibbs' oscillation in $\hat{H}(e^{j\omega T})$. Recall that we already used various window functions in Chapters Three and Five to reduce leakage error in approximating the spectrum of a time function with the DFT.

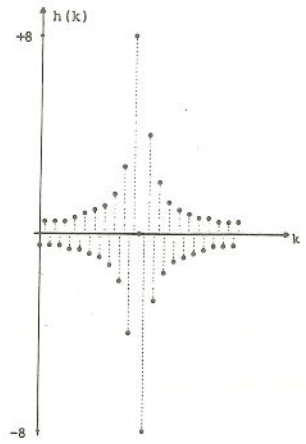


Fig. 10.19a. Antisymmetrical FIR filter unit pulse response.

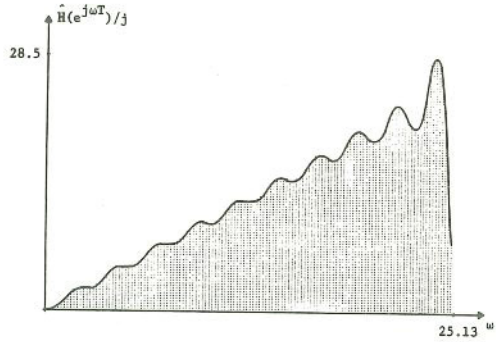


Fig. 10.19b. FIR filter differentiator approximation.

$H_d(e^{j\omega T})$ and $\hat{H}(e^{j\omega T})$ are both periodic functions. In eq. 4.42a we obtained the Fourier series coefficients of the result of a circular convolution of two periodic functions. Since $\hat{h}_i = w(i)h_i$, then by eq. 4.42a, $\hat{H}(e^{j\omega T})$ can be expressed as the result of a circular convolution of two periodic functions, i.e.

$$\hat{H}(e^{j\omega T}) = \frac{1}{\omega_s} W(e^{j\omega T}) \otimes H_d(e^{j\omega T}) \qquad (10.31)$$

where

$$W(e^{j\omega T}) = \sum_{i=-K}^{K} w(i)e^{-jiT\omega}$$

which is a real function, and with eq. 10.31 we get

$$\hat{H}(e^{j\omega T}) = \frac{1}{\omega_s}\int_{-\omega_s/2}^{\omega_s/2} \sum_{i=-K}^{K} w(i)e^{-jiT(\omega-\Omega)} \sum_{m=-\infty}^{\infty} h_m e^{-jmT\Omega} d\Omega \qquad \textbf{(10.32a)}$$

$$= \sum_{i=-K}^{K} h_i w(i) e^{-jiT\omega} \qquad \textbf{(10.32b)}$$

Eq. 10.32a can also be obtained by using the frequency convolution property in Table 9.2 with $\lambda = e^{j\Omega T}$ defining the integration path Γ.

From the term $w(i)e^{-jiT\omega}$ in eq. 10.32b we see that Gibbs' oscillation, which is due to the high frequency components in $\hat{H}(e^{j\omega T})$, can be diminished if we use a $w(i)$, which also determines the amplitudes of the frequency components of $\hat{H}(e^{j\omega T})$, that decreases as $|i| \to K$. As long as $w(i)$ is an even function, the symmetry or antisymmetry property of h_i is preserved in $\hat{h}_i$, and therefore we can achieve a linear phaseshift FIR filter with any symmetrical $w(i)$. Ideally, we would like $w(i)$ to be a function for which $W(e^{j\omega T})$ is an impulse train, because then by eq. 10.31, $\hat{H}(e^{j\omega T}) = H_d(e^{j\omega T})$. But, this is only possible if $w(i) = 1$ and $K \to \infty$. Since K must be finite, we prefer a $w(i)$ for which the main lobe of $W(e^{j\omega T})$ is as narrow as possible with side lobe amplitudes that are as small as possible.

Example 10.7. Let us try using the Hann window (See Fig. 5.22.), which is given by

$$w_3(i) = \frac{1}{2}\left(1 + \cos\left(\frac{i}{K}\pi\right)\right)$$

for $i = -K, -K+1, \cdots, K$. This was obtained by shifting $w_3(t)$ in Fig. 5.22 to the left by $T_0/2 = KT$. Truncating the Fourier series for the LP filter given in Example 10.5 with the Hann window results in $h(i) = w_3(i-K)h_{i-K}$, for $i = 0, 1, \cdots, 2K$, and, for $K = 20$, $\hat{H}(e^{j\omega T})$ is shown in Fig. 10.20.

Gibbs' oscillation has been reduced, but compared to Fig. 10.18, the transition band has been widened. However, we can improve the frequency response by increasing K.

The specified $H_d(e^{j\omega T})$ for the LP filter is not negative for any ω, and $\hat{H}(e^{j\omega T})$ can take on negative values if $W(e^{j\omega T})$ becomes negative. To achieve an exact linear phaseshift, even in the stop-band, $W(e^{j\omega T})$ must be nonnegative for all ω. This is possible with the Bartlett window, which is given by (See Fig. 5.22.)

$$w_5(i) = \frac{K - |i|}{K}$$

for $i = -K, -K+1, \cdots, 0, 1, \cdots, K$. Since $W_5(e^{j\omega T})$ is nonnegative for all ω (See Problem 5.5.), $\hat{H}(e^{j\omega T})$, which is shown in Fig. 10.21 for $K = 20$, will not be negative for any ω, and $\phi(\omega) = -KT\omega$ for all ω in the range $\omega_s/2 < \omega < \omega_s/2$.

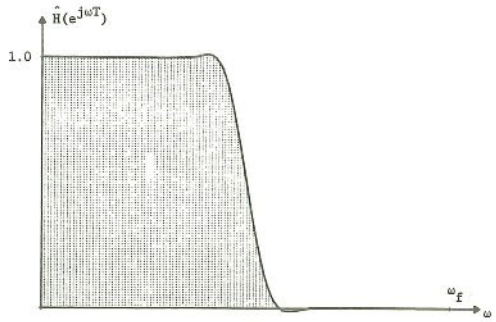


Fig. 10.20. FIR LP filter with the Hann window.

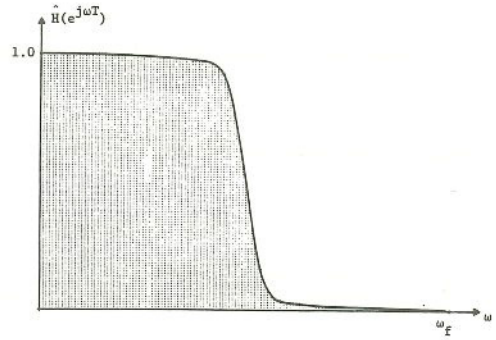


Fig. 10.21. FIR LP filter with the Bartlett window.

However, with the Bartlett window we must use a larger K to achieve the stop-band attenuation as obtained with the Hann window. Of course, we can try other window functions to achieve goals such as small transition bandwidth, large stop-band attenuation, linear phaseshift, and little magnitude distortion. Needless to say, there are many trade-offs to consider.

Using the Hann window to truncate the Fourier series for the differentiator approximation of Example 10.6 results in $\hat{H}(e^{j\omega T})/j$ shown in Fig. 10.22. By reducing Gibbs' oscillation we have increased the frequency range for which this $H(z)$ is a useful differentiator approximation.

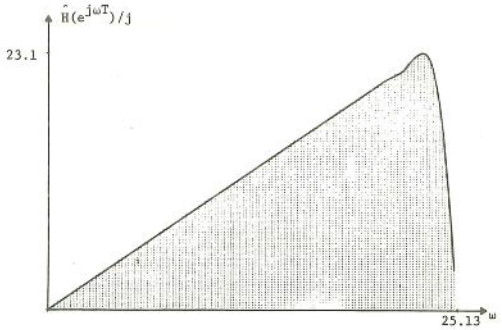


Fig. 10.22. FIR filter differentiator with the Hann window.

10-2.2 FIR Filter Symmetry Property

Without regard to how $h(k)$ is obtained, let us develop some properties of an FIR filter with transfer function $H(z)$, as given in eq. 10.19, that are due to symmetry properties of $h(k)$.

Assume that I in eq. 10.19 is an odd integer and that $h(k)$ is symmetrical about $k = (I-1)/2$, i.e.

$$h(k) = h(I-1-k), \quad k = 0, 1, \cdots, (I-3)/2$$

where $h\left(\frac{I-1}{2}\right)$ has no matching point. Expanding eq. 10.19 results in

$$H(z) = \sum_{i=0}^{\frac{I-3}{2}} h(i)z^{-i} + h\left(\frac{I-1}{2}\right)z^{-\frac{I-1}{2}} + \sum_{i=\frac{I+1}{2}}^{I-1} h(i)z^{-i} \tag{10.33}$$

Changing the summation index of the second summation from i to $l = I-1-i$ yields

$$\sum_{i=\frac{I+1}{2}}^{I-1} h(i)z^{-i} = \sum_{l=0}^{\frac{I-3}{2}} h(I-1-l)z^{-(I-1-l)}$$

By the symmetry condition, $h(k) = h(I-1-k)$, eq. 10.33 becomes

$$H(z) = h\left(\frac{I-1}{2}\right)z^{-\frac{I-1}{2}} + \sum_{i=0}^{\frac{I-3}{2}} h(i)\left(z^{-i} + z^{-(I-1-i)}\right) \tag{10.34}$$

Thus, the filter is described by only $(I+1)/2$ coefficients.

Example 10.8. If $I=7$, then by the symmetry condition we have $h(0)=h(6)$, $h(1)=h(5)$, $h(2)=h(4)$, and $h(3)$ can have any value. This filter can be realized with the structure shown in Fig. 10.23. This almost halves the required number of multiplications required by the structure shown in Fig. 10.2.

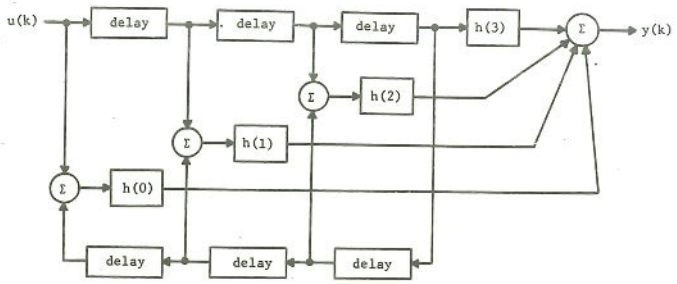


Fig. 10.23. A symmetrical FIR filter.

Removing $z^{-\frac{I-1}{2}}$ from each term in eq. 10.34 results in

$$H(z)=z^{-\frac{I-1}{2}}\left[h\left(\frac{I-1}{2}\right)+\sum_{i=0}^{\frac{I-3}{2}}h(i)\left(z^{\frac{I-1}{2}}z^{-i}+z^{-\frac{I-1}{2}}z^{i}\right)\right] \tag{10.35a}$$

and using $z=e^{j\omega T}$ for the frequency response yields

$$H(e^{j\omega T})=e^{-j\frac{I-1}{2}T\omega}\left[h\left(\frac{I-1}{2}\right)+\sum_{i=0}^{\frac{I-3}{2}}2h(i)\cos\left(\left(\frac{I-1}{2}-i\right)T\omega\right)\right] \tag{10.36a}$$

Denote the term in brackets by $\hat{H}(e^{j\omega T})$, so that

$$H(e^{j\omega T})=e^{-j\frac{I-1}{2}T\omega}\hat{H}(e^{j\omega T}),\quad M(\omega)=|\hat{H}(e^{j\omega T})|$$

Since $\hat{H}(e^{j\omega T})$ is real, we have that

$$\angle H(e^{j\omega T})=\begin{cases}-\dfrac{I-1}{2}T\omega, & \hat{H}>0,\quad -\omega_s/2<\omega<\omega_s/2\\ -\dfrac{I-1}{2}T\omega-\pi, & \hat{H}<0,\quad 0<\omega<\omega_s/2\\ -\dfrac{I-1}{2}T\omega+\pi, & \hat{H}<0,\quad -\omega_s/2<\omega<0\end{cases} \tag{10.37a}$$

Thus, if I is an odd integer and $h(k)$ is symmetrical about $k=\frac{I-1}{2}$, then $H(z)$ has a linear phaseshift characteristic.

If $h(k)$ is antisymmetrical about $k=(I-1)/2$, so that

$$h(k)=-h(I-1-k), \quad k=0,1,\cdots,(I-3)/2$$

which requires that $h\left(\frac{I-1}{2}\right)=0$, then the term $(z^{-i}+z^{-(I-1-i)})$ in eq. 10.34 becomes $(z^{-i}-z^{-(I-1-i)})$, and the transfer function can be written as

$$H(z)=z^{-\frac{I-1}{2}}\left[\sum_{i=0}^{\frac{I-3}{2}} h(i)\left(z^{\frac{I-1}{2}}z^{-i}-z^{-\frac{I-1}{2}}z^{i}\right)\right] \tag{10.35b}$$

Here, the FIR filter is described by only $(I-1)/2$ coefficients. The frequency response is given by

$$H(e^{j\omega T})=j\,e^{-j\frac{I-1}{2}T\omega}\left[\sum_{i=0}^{\frac{I-3}{2}} 2h(i)\sin\left(\left(\frac{I-1}{2}-i\right)T\omega\right)\right] \tag{10.36b}$$

Notice that by eq. 10.36b we have $H(e^{j\omega T})=0$ for $\omega=0$ and $\pm\omega_s/2$. Denote the term in brackets by $\hat{H}(e^{j\omega T})$, so that

$$H(e^{j\omega T})=j\,e^{-j\frac{I-1}{2}T\omega}\hat{H}(e^{j\omega T}), \quad M(\omega)=|\hat{H}(e^{j\omega T})|$$

Since $\hat{H}(e^{j\omega T})$ is real, we get

$$\angle H(e^{j\omega T})=\begin{cases} -\dfrac{I-1}{2}T\omega+\dfrac{\pi}{2}, & \hat{H}>0, \quad 0<\omega<\omega_s/2 \\ -\dfrac{I-1}{2}T\omega-\dfrac{\pi}{2}, & \hat{H}<0, \quad 0<\omega<\omega_s/2 \end{cases} \tag{10.37b}$$

Thus, if $h(k)$ is antisymmetrical, then the FIR filter has a constant group delay.

The Fourier series method for the design of FIR filters is one way to obtain a symmetrical or antisymmetrical $h(k)$ such that $H(z)$ approximates a desired frequency response, and eqs. 10.36 and 10.37 can be used to evaluate the resulting frequency response. This is illustrated in Examples 10.5 and 10.6.

The poles and zeros of $H(z)$ are found from

$$H(z)=\frac{h(0)z^{I-1}+h(1)z^{I-2}+\cdots+h(I-1)}{z^{I-1}}=\frac{P(z)}{Q(z)}$$

The $(I-1)$ poles are all located at $z=0$, and they do not affect the magnitude frequency response. The $(I-1)$ zeros are the roots of $P(z)=0$. If $h(k)$ is symmetrical, then the form for $H(z)$ given in eq. 10.35a can be used to find the zeros of $H(z)$. Notice that if in the summation of eq. 10.35a we replace z by $1/z$, then we get the same summation back. Therefore, if $z=z_i$ is a zero of $H(z)$, then $z=1/z_i$ is also a zero of $H(z)$. If $h(k)$ is antisymmetrical, then by eq. 10.35b z_i and $1/z_i$ are zeros of $H(z)$.

If a symmetrical or antisymmetrical FIR filter $H(z)$ has a complex conjugate pair of zeros z_i and z_i^* not on the unit circle, then it must also have the zeros $1/z_i$ and $1/z_i^*$. If z_i is a zero on the unit circle, but not $z_i = \pm 1$, then only z_i and z_i^* are necessary zeros, since $1/z_i = z_i^*$. If $H(z)$ has a real zero z_i, where $z_i \neq \pm 1$, then $1/z_i$ must also be a zero of $H(z)$. Finally, if $H(z)$ has a zero at $z_i = \pm 1$, then $1/z_i$ is also a zero of $H(z)$, and $H(z)$ can have any number of zeros at $z_i = \pm 1$. In any case, since I is an odd integer, $H(z)$ has an even number of poles and zeros.

Now, let us consider the case for which I in eq. 10.19 is an even integer. Expanding $H(z)$ results in

$$H(z) = \sum_{i=0}^{\frac{I}{2}-1} h(i)z^{-i} + \sum_{i=\frac{I}{2}}^{I-1} h(i)z^{-i}$$

Changing the summation index of the second summation from i to $l = I - 1 - i$ results in

$$\sum_{i=\frac{I}{2}}^{I-1} h(i)z^{-i} = \sum_{l=0}^{\frac{I}{2}-1} h(I-1-l)z^{-(I-1-l)}$$

If $h(k)$ is symmetrical about $t = \frac{I-1}{2}T$, so that

$$h(k) = h(I-1-k), \quad k = 0, 1, \cdots, \frac{I}{2} - 1$$

then $H(z)$ is given by

$$H(z) = \sum_{i=0}^{\frac{I}{2}-1} h(i)\left(z^{-i} + z^{-(I-1-i)}\right) = z^{-\frac{I-1}{2}}\left[\sum_{i=0}^{\frac{I}{2}-1} h(i)\left(z^{\frac{I-1}{2}}z^{-i} + z^{-\frac{I-1}{2}}z^{i}\right)\right]$$

Notice that this $h(k)$ is symmetrical about the time point midway between $\left(\frac{I}{2}-1\right)T$ and $\frac{I}{2}T$, and this filter is described by only $I/2$ coefficients. Using $z = e^{j\omega T}$ for the frequency response yields

$$H(e^{j\omega T}) = e^{-j\frac{I-1}{2}T\omega}\left[\sum_{i=0}^{\frac{I}{2}-1} 2h(i)\cos\left(\left(\frac{I-1}{2} - i\right)T\omega\right)\right] \tag{10.38a}$$

Denote the term in brackets by $\hat{H}(e^{j\omega T})$, and we again get the linear phaseshift characteristic of eq. 10.37a.

If $h(k)$ is antisymmetrical about $t = \frac{I-1}{2}T$, so that

$$h(k) = -h(I-1-k), \quad k = 0, 1, \cdots, \frac{I}{2} - 1$$

then $H(z)$ can be written as

$$H(z)=\sum_{i=0}^{\frac{I}{2}-1}h(i)\left(z^{-i}-z^{-(I-1-i)}\right)=z^{-\frac{I-1}{2}}\left[\sum_{i=0}^{\frac{I}{2}-1}h(i)\left(z^{\frac{I-1}{2}}z^{-i}-z^{-\frac{I-1}{2}}z^{i}\right)\right]$$

which is also described by $I/2$ coefficients. And, the frequency response is given by

$$H(e^{j\omega T})=j\,e^{-j\frac{I-1}{2}T\omega}\left[\sum_{i=0}^{\frac{I}{2}-1}2h(i)\sin\left(\left(\frac{I-1}{2}-i\right)T\omega\right)\right] \tag{10.38b}$$

Notice that by eq. 10.38b we have $H(e^{j\omega T})=0$ for $\omega=0$ and $\pm\omega_s/2$. Denote the term in brackets by $\hat{H}(e^{j\omega T})$, and we again get the phaseshift characteristic of eq. 10.37b.

If I is even, then $H(z)$ has an odd number of zeros, the locations of which must satisfy the same requirements as for the case I odd.

10-2.3 Frequency Sampling Method

A very simple way to filter a real signal $u(t)$ is to obtain N samples for a duration of $T_0=NT$ secs., compute $U(n/T_0)=\mathrm{DFT}(u(kT))$, multiply $U(n/T_0)$ by a desired frequency response characteristic $H_d(n/T_0)$ to obtain $Y(n/T_0)$, and then take the inverse DFT of $Y(n/T_0)$ to obtain $y(kT)$. If $y(kT)$ is to be real, then $H_d(n/T_0)$ must satisfy the property

$$H_d\left(n\frac{1}{T_0}\right)=H_d^*\left((N-n)\frac{1}{T_0}\right)$$

which means that $M_d(n/T_0)$ and $\phi_d(n/T_0)$ must be even and odd, respectively, periodic functions with period ω_s. Here, $H_d(n/T_0)$ is obtained by sampling a desired continuous frequency response characteristic $H_d(e^{j\omega T})$ at the frequencies

$$\omega=\omega_n=\frac{2\pi n}{T_0},\quad n=0,1,\cdots,(N-1) \tag{10.39}$$

To obtain an FIR filter as given in eq. 10.19, we note that with $h(i)=\mathrm{DFT}^{-1}(H_d(n/T_0))$, $i=0,1,\cdots,(N-1)$, where $I=N$, we will get an $H(z)$ for which $H(e^{j\omega T})=H_d(e^{j\omega T})$ at the frequencies $\omega=\omega_n$, for $n=0,1,\cdots,(N-1)$. Since $\mathrm{DFT}(h(i))=H_d(n/T_0)$, we will at least match $H_d(e^{j\omega T})$ at the points $\omega=\omega_n$. Thus, by using the uniformly spaced frequencies ω_n given in eq. 10.39, we can use the inverse DFT operation to find the $h(i)$. This FIR filter design procedure is called the **frequency sampling** method.

Let us consider an alternative to eq. 10.19 for implementing this FIR filter. Now, $H(z)$ is given by

$$H(z)=\sum_{i=0}^{N-1}h(i)z^{-i} \tag{10.4}$$

$$=\sum_{i=0}^{N-1}\left(\frac{1}{N}\sum_{n=0}^{N-1}H_d\left(\frac{n}{T_0}\right)e^{j\frac{2\pi}{N}ni}\right)z^{-i}$$

$$H(z)=\frac{1}{N}\sum_{n=0}^{N-1}H_d\left(\frac{n}{T_0}\right)\sum_{i=0}^{N-1}(z^{-1}e^{j\frac{2\pi}{N}n})^i \tag{10.4}$$

The inner summation of eq. 10.41 is a geometric series that evaluates to

$$\sum_{i=0}^{N-1}\left(z^{-1}e^{j\frac{2\pi}{N}n}\right)^i=\frac{1-(z^{-1}e^{j\frac{2\pi}{N}n})^N}{1-z^{-1}e^{j\frac{2\pi}{N}n}}=\frac{1-z^{-N}}{1-e^{j\frac{2\pi}{N}n}z^{-1}}$$

so that $H(z)$ becomes

$$H(z)=\frac{1-z^{-N}}{N}\sum_{n=0}^{N-1}H_d\left(\frac{n}{T_0}\right)\frac{1}{1-e^{j\frac{2\pi}{N}n}z^{-1}}=H_1(z)H_2(z) \tag{10.42}$$

where $H_1(z)=(1-z^{-N})/N$, and $H_2(z)$ consists of the summation terms. We can realize $H(z)$ with a nonrecursive structure as shown in Fig. 10.2, which is based on eq. 10.40, or with a recursive structure as shown in Fig. 10.24, which is based on eq. 10.42.

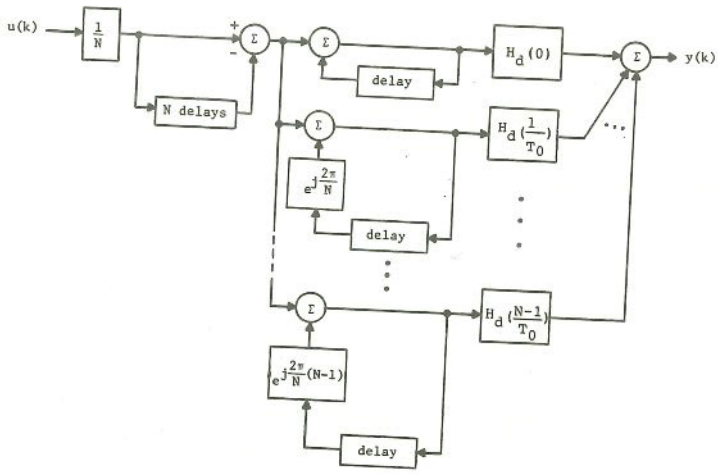


Fig. 10.24. Recursive realization of an FIR filter.

Here we have realized a nonrecursive filter with a cascade connection of $H_1(z)$ and $H_2(z)$. In fact, any FIR filter can be approximated with such a recursive form by using $H_d(n/T_0) = \text{DFT}(h(i))$ in eq. 10.42. Notice that the N poles of $H_2(z)$ at $z = e^{j2\pi n/N}$ cancel with the N zeros of $H_1(z)$, and therefore the $(N-1)$ zeros of $H(z)$ are $(N-1)$ zeros of $H_2(z)$, and the $(N-1)$ poles of $H(z)$ are $(N-1)$ poles of $H_1(z)$ at $z = 0$.

Generally, eq. 10.40 is preferred over eq. 10.42, because $H(z)$ in eq. 10.40 is unconditionally stable, while, in an implemented version of eq. 10.42, the pole-zero cancellations may not occur due to coefficient multiplier realization errors. Moreover, since the summation term poles in eq. 10.42 are on the unit circle, care must be taken to avoid implementing an unstable filter. However, to implement the filter, eq. 10.42 can require much less arithmetic than does eq. 10.40.

To avoid complex arithmetic, corresponding complex conjugate terms in eq. 10.42 can be combined. For example, referring to Fig. 10.24, we have that $H_d(N-1)/T_0) = H_d^*(1/T_0)$ and $e^{j2\pi(N-1)/N} = e^{-j2\pi/N} = (e^{j2\pi/N})^*$.

If N is an even integer, then eq. 10.42 can be rewritten as

$$H(z) = \frac{1-z^{-N}}{N}\left[H_d(0)\frac{1}{1-z^{-1}} + H_d\left(\frac{N}{2}\frac{1}{T_0}\right)\frac{1}{1+z^{-1}} + \sum_{n=1}^{K} H_n(z)\right] \tag{10.43a}$$

where $K = \frac{N}{2} - 1$, and, with $H_d((N-n)/T_0) = H_d^*(n/T_0) = M_d(n/T_0)e^{-j\phi_d(n/T_0)}$, the $H_n(z)$ are given by

$$H_n(z) = 2M_d\left(\frac{n}{T_0}\right)\frac{\cos\phi_d\left(\frac{n}{T_0}\right) - \cos\left(\phi_d\left(\frac{n}{T_0}\right) - \frac{2\pi}{N}n\right)z^{-1}}{1 - 2\cos\left(\frac{2\pi}{N}n\right)z^{-1} + z^{-2}} \tag{10.44}$$

$H_d(0)$ must be real, and since $\phi_d(n/T_0)$ must be an odd periodic function, $\phi_d\left(\frac{N}{2}\frac{1}{T_0}\right) = 0$.

If N is an odd integer, then eq. 10.42 can be rewritten as

$$H(z) = \frac{1-z^{-N}}{N}\left[H_d(0)\frac{1}{1-z^{-1}} + \sum_{n=1}^{K} H_n(z)\right] \tag{10.43b}$$

where $K = (N-1)/2$.

If our design goal is to achieve an ideal filter characteristic as given in eq. 10.13 or Fig. 10.11, then $M_d(n/T_0) = 1$ or 0, and many of the $H_n(z)$ in eqs. 10.43 will be zero. Consequently, the arithmetic requirements of running the filter based on eqs. 10.43 can be considerably less than those incurred by using eq. 10.40.

Now, we will obtain conditions to achieve a linear phaseshift characteristic. The possibilities are that $h(k)$ is symmetrical and N is an even or odd integer.

If $h(k)$ is symmetrical about $t = \frac{N-1}{2}T$, then, for N an odd or an even integer, we found by eqs. 10.36a (N odd) and 10.38a (N even) that

$$\phi(e^{j\omega T}) = -\frac{N-1}{2}T\omega$$

Now we know how to specify $\phi_d(e^{j\omega T})$ to obtain a real symmetrical unit pulse response FIR filter by the frequency sampling method, i.e.

$$\phi_d\left(n\frac{1}{T_0}\right) = -\frac{N-1}{2}T\omega_n = -\frac{N-1}{2}T\frac{2\pi}{NT}n = -\frac{N-1}{N}\pi n, \quad n = 0, 1, \cdots, K \tag{10.45a}$$

$$\phi_d\left((N-n)\frac{1}{T}\right) = -\phi_d(n/T_0), \quad n = 1, 2, \cdots, K \tag{10.45b}$$

where K is given by

$$K = \begin{cases} \dfrac{N-1}{2}; & N \text{ odd} \\ \dfrac{N}{2} - 1, & N \text{ even} \end{cases} \tag{10.46}$$

With $\phi_d(n/T_0)$ of eqs. 10.45, the $H_n(z)$, for $n = 1, \cdots, K$, in eq. 10.44 become

$$H_n(z) = 2M_d\left(\frac{n}{T_0}\right)\frac{(-1)^n \cos\left(\frac{\pi}{N}n\right)(1 - z^{-1})}{1 - 2\cos\left(\frac{2\pi}{N}n\right)z^{-1} + z^{-2}} \tag{10.47}$$

Finally, regarding $M_d(n/T_0)$, we know that it must be an even periodic function. However, if N is even and $h(k)$ is to be symmetrical, which is required for a linear phaseshift, then $H(e^{j\omega T})$ as in eq. 10.38a yields $H(e^{j\omega_{N/2}T}) = 0$. For N even, we must specify that $H_d\left(\frac{N}{2}\frac{1}{T_0}\right) = 0$, and thereby the second term in brackets in eq. 10.43a is eliminated.

Example 10.9. Let us obtain an LP filter, as specified in Example 10.5, by the frequency sampling method. First, let us try $N = 8$, so that $K = 3$, and we can specify

$$M_d\left(\frac{n}{8}f_s\right) = \begin{cases} 1, & n = 0, 1, 7 \\ 0.5, & n = 2, 6 \\ 0, & n = 3, 4, 5 \end{cases} \tag{10.48a}$$

$$\phi_d\left(\frac{n}{8}f_s\right) = \begin{cases} -\dfrac{7}{8}\pi n, & n = 0, 1, 2, 3 \\ 0, & n = 4 \\ \dfrac{7}{8}\pi(8-n), & n = 5, 6, 7 \end{cases} \tag{10.48b}$$

The inverse DFT of $H_d(n/T_0)$ as specified by eqs. 10.48 yields $h(k)$ as shown in Fig. 10.25a. Notice that $h(k)$ is symmetrical about $t = \frac{N-1}{2}T$. A plot of the amplitude frequency response (using eq. 10.38a) is shown in Fig. 10.25b.

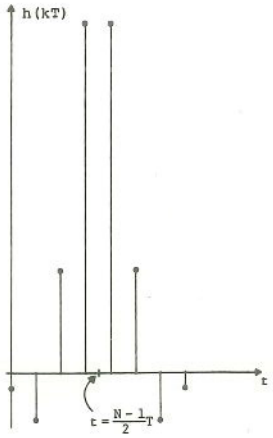


Fig. 10.25a. FIR LP filter unit pulse response for $N = 8$.

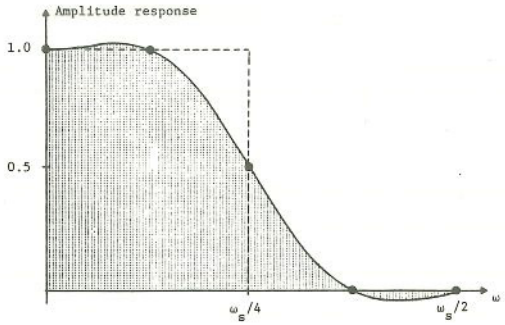


Fig. 10.25b. Amplitude response for $N = 8$.

Now, let us try $N = 9$, so that $K = 4$, and we can specify

$$M_d\left(\frac{n}{9}f_s\right) = \begin{cases} 1, & n = 0, 1, 2, 7, 8 \\ 0, & n = 3, 4, 5, 6 \end{cases} \qquad \textbf{(10.49a)}$$

$$\phi_d\left(\frac{n}{9}f_s\right)=\begin{cases}-\frac{8}{9}\pi n, & n=0,1,2,3,4\\ \frac{8}{9}\pi(9-n), & n=5,6,7,8\end{cases} \tag{10.49b}$$

A plot of the amplitude frequency response (using eq. 10.36a) is shown in Fig. 10.26a.

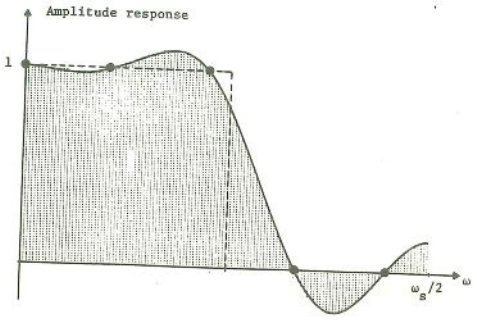


Fig. 10.26a. Amplitude response for $N=9$.

Notice that for N even (Fig. 10.25b) or odd (Fig. 10.26a) the amplitude response is oscillatory about points of discontinuity in the desired frequency response $H_d(e^{j\omega T})$. The extent of these oscillations can be reduced by introducing a transition band. For example, if we change eq. 10.49a to $M_d(n=2)=M_d(n=7)=0.75$ and $M_d(n=3)=M_d(n=6)=0.25$, then we obtain the amplitude frequency response shown in Fig. 10.26b, which has a wider transition band than the response shown in Fig. 10.26a. By guess and try we can arrive at a transition band, which diminishes the oscillations of $\hat{H}(e^{j\omega T})$.

Typically, N is chosen larger than the values used in Example 10.9. If N is a power of two, then a radix two FFT algorithm can be used to determine the $h(i)$ in eq. 10.40.

If $h(k)$ is antisymmetrical about $t=\frac{N-1}{2}T$, then, for N an odd or an even integer, we found by eqs. 10.36b (N odd) and 10.38b (N even) that $\phi(e^{j\omega T})=-\frac{N-1}{2}T\omega+\frac{\pi}{2}$ for $0<\omega<\omega_s/2$. Thus, with the results of Section 10-2.2 we can determine how to specify an $H_d(e^{j\omega T})$ at the frequencies given by eq. 10.39 to realize this FIR filter with a nonrecursive form or a recursive form. The details of this are left for the reader to develop (See Problems 10.25 and 10.26.).

Now we can realize an FIR filter either by eq. 10.40 or eqs. 10.43. If the recursive form is used, then it would be better to move the poles of $H_2(z)$ slightly inward from the unit circle. The resulting filter will be stable, and the discrepancy between the frequency response of the realized filter and a specification such as eqs. 10.48 or eqs. 10.49 in Example 10.9 will be small.

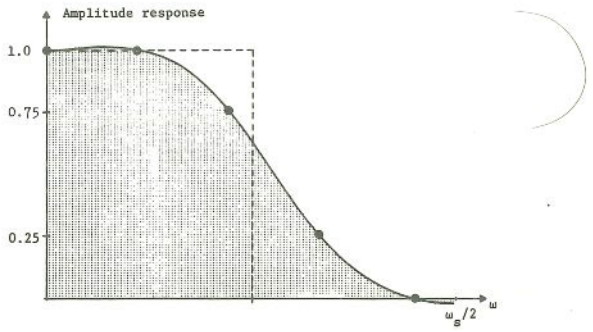


Fig. 10.26b. Amplitude response for $N = 9$ with a transition band.

SECTION 10-3 Infinite Impulse Response Filter Design

Mostly, infinite impulse response (IIR) or recursive digital filter design techniques involve transforming an analog filter transfer function $G(s)$ into a digital filter transfer function $H(z)$. This approach is used because there are an abundance of methods for finding a satisfactory $G(s)$ given a specification such as in Fig. 10.5a. The transformation procedure must yield a digital filter for which the frequency response is a good approximation of the frequency response of the corresponding analog filter.

10-3.1 Backward Difference Approximation

A simple discretization method (analog to digital filter transformation procedure) is to use a backward difference approximation for differentiation.

Example 10.10. Let us obtain a digital filter based on the analog filter

$$G(s) = \frac{1}{s^2 + \sqrt{2}s + 1} \tag{10.50}$$

Notice that $G(j0) = 1$, and that $\| G(j1) \|^2 = 1/2$. This is an LP filter with BW = 1 rad/sec. The input $u(t)$ to output $y(t)$ relationship is given by

$$\frac{d^2y}{dt^2} + \sqrt{2}\frac{dy}{dt} + y(t) = u(t) \tag{10.51}$$

Approximating the derivative operation with a **backward difference** formula yields

$$\dot{y}(t = kT) \cong \frac{y(kT) - y((k-1)T)}{T} \tag{10.52}$$

$$\ddot{y}(t=kT) \cong \frac{\dot{y}(kT)-\dot{y}((k-1)T)}{T} = \frac{y(kT)-2y((k-1)T)+y((k-2)T)}{T^2} \tag{10.53}$$

At $t=kT$, we can substitute eqs. 10.52 and 10.53 into eq. 10.51 to obtain a difference equation, from which $H(z)$ can be determined. Or, from a frequency domain viewpoint we see that by eq. 10.52, the derivative operation s is replaced by $(1-z^{-1})/T$. Similarly, by eq. 10.53 the second derivative operation s^2 is replaced by $(1-2z^{-1}+z^{-2})/T^2 = ((1-z^{-1})/T)^2$. In general, we have

$$H(z) = G(s)\big|_{s=(1-z^{-1})/T} \tag{10.54}$$

for any $G(s)$, which is a rational function of s with real coefficients. For $G(s)$ in eq. 10.50, the backward difference approximation yields

$$H(z) = \frac{1}{\left(\frac{1-z^{-1}}{T}\right)^2 + \sqrt{2}\left(\frac{1-z^{-1}}{T}\right)+1} = \frac{T^2z^2}{(1+T\sqrt{2}+T^2)z^2-(2+T\sqrt{2})z+1} \tag{10.55}$$

There are some basic issues to consider in employing this or any other discretization method. The resulting $H(z)$ must be a rational function of z with real coefficients, have its poles inside the unit circle, and to obtain a causal digital filter, $H(z)$ must be a proper function. In addition to these basic requirements, we must determine whether or not $H(z)$ exhibits the characteristics of the desired digital filter.

To obtain the frequency response of the digital filter, we evaluate $H(e^{j\omega T})$ as ω varies over the range $0 \le \omega \le \omega_f$, where $\omega_f = \omega_s/2$ is the folding frequency. Or, we can use

$$H(e^{j\omega T}) = G(s)\big|_{s=(1-e^{-j\omega T})/T} \tag{10.56}$$

From eq. 10.56 we see that $H(e^{j\omega T})$ takes on the values of $G(s)$ as s varies along a path defined by

$$s = \frac{1-e^{-j\omega T}}{T} = \frac{1-\cos\omega T}{T} + j\frac{\sin\omega T}{T}$$

in the s-plane, which is shown in Fig. 10.27a. Since this path is close to the s-plane imaginary axis only for small ω, $H(e^{j\omega T})$ can approximate the analog filter frequency response only for small ω.

We are using the symbol ω for the frequency of the digital filter input. To distinguish this frequency from points along the s-plane imaginary axis, we shall use $s = j\Omega$ to refer to the s-plane imaginary axis. Consequently, the symbol Ω will be used for the frequency of the analog filter input. Since $H(e^{j\omega T}) \cong G(j\Omega)$ only for small ω, the backward difference transformation is only useful for transforming LP analog filters.

By eq. 10.54, the poles of $H(z)$ can be found through

$$z = \frac{1}{1 - sT} = \frac{1}{(1 - Re(s)T) - jIm(s)T} \tag{10.57}$$

and if $G(s)$ is stable, i.e., $Re(p_i)$ for every pole $s = p_i$ of $G(s)$ is negative, then by eq. 10.57 the resulting poles of $H(z)$ will be inside the unit circle. Eq. 10.57 maps the s-plane onto the z-plane as shown in Fig. 10.27b, and we see that eq. 10.54 always results in a stable $H(z)$ given a stable $G(s)$.

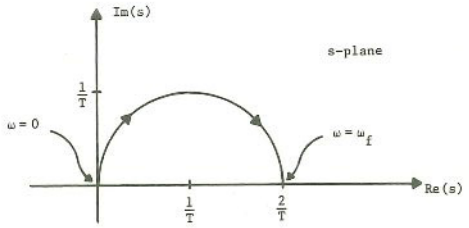


Fig. 10.27a. The s-plane frequency response path.

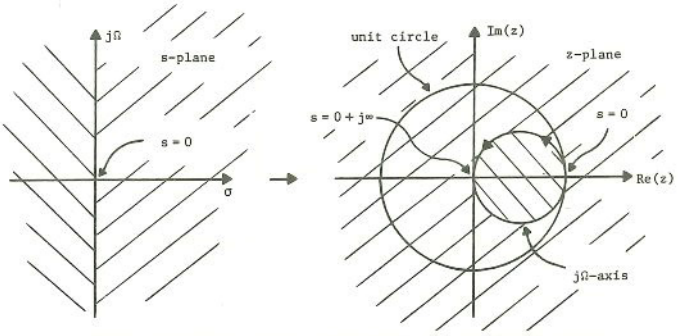


Fig. 10.27b. Backward difference approximation s-plane to z-plane mapping.

10-3.2 Forward Difference Approximation

Let us try a **forward difference** approximation for differentiation, i.e.

$$\dot{y}(t = kT) \cong \frac{y((k+1)T) - y(kT)}{T} \tag{10.58}$$

$$s \to \frac{z - 1}{T}$$

$$\ddot{y}(t=kT) \cong \frac{\dot{y}((k+1)T)-\dot{y}(kT)}{T} = \frac{y((k+2)T)-2y((k+1)T)+y(kT)}{T^2} \tag{10.59}$$

$$s^2 \rightarrow \left(\frac{z-1}{T}\right)^2$$

and, in general, $H(z)$ is obtained with

$$H(z) = G(s)|_{s=(z-1)/T} \tag{10.60}$$

Example 10.10 (continued). For $G(s)$ given in eq. 10.50, the forward difference approximation yields

$$H(z) = \frac{1}{\left(\frac{z-1}{T}\right)^2 + \sqrt{2}\frac{z-1}{T} + 1} = \frac{T^2}{z^2 - (2-T\sqrt{2})z + (1-T\sqrt{2}+T^2)} \tag{10.61}$$

By eq. 10.60, $H(e^{j\omega T})$ takes on the values of $G(s)$ as s varies along a path defined by

$$s = \frac{1}{T}(e^{j\omega T} - 1) = \frac{-1+\cos\omega T}{T} + j\frac{\sin\omega T}{T}$$

which is shown in Fig 10.28.

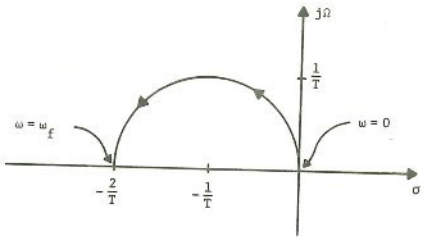


Fig. 10.28. The s-plane frequency response path.

In this figure we see that the forward difference transformation is also only useful for transforming LP analog filters. Furthermore, by eq. 10.60, the poles of $H(z)$ can be found through

$$z = 1 + sT = (1 + Re(s)T) + jIm(s)T \tag{10.62}$$

If $G(s)$ is stable, then $H(z)$ will be stable only if T is chosen such that for $Re(p_i)$ and $Im(p_i)$ of every pole $s = p_i$ of $G(s)$, T satisfies

$$(1+Re(p_i)T)^2 + (Im(p_i)T)^2 < 1 \quad \rightarrow \quad T < \frac{2|Re(p_i)|}{\|p_i\|^2} \tag{10.63}$$

and thereby, the poles of $H(z)$ will be inside the unit circle. Thus, if the sampling frequency is too small, then a forward difference approximation will yield an unstable discrete time system.

10-3.3 Bilinear Transformation

An $H(z)$ for which $H(e^{j\omega T})$ is a better approximation of $G(j\Omega)$ than with the backward or forward difference transformation results by using the **trapezoidal integration rule** to approximate integration.

Suppose we have

$$\frac{dy}{dt} = u(t) \quad \rightarrow \quad Y(s) = \frac{1}{s}U(s)$$

For any two time points $t = t_1$ and $t = t_2$, where $t_2 > t_1$, $y(t_2)$ is given by

$$y(t_2) = \int_{t_1}^{t_2} u(t)dt + y(t_1)$$

Let $t_2 = (k+1)T$, $t_1 = kT$, and by the trapezoidal integration rule we obtain

$$y((k+1)T) \cong \frac{u((k+1)T) + u(kT)}{2}T + y(kT) \tag{10.64}$$

After taking the Z-transform of eq. 10.64 and rearranging, we get

$$Y(z) = \frac{T}{2}\frac{z+1}{z-1}U(z)$$

Therefore, approximating the integral operation corresponds to

$$\frac{1}{s} \rightarrow \frac{T}{2}\frac{z+1}{z-1} \tag{10.65}$$

Recall from Chapter Eight that any proper $G(s)$ can be realized with the operations: addition, multiplication by a constant, and integration. Therefore, by eq. 10.65, we can obtain an $H(z)$ with

$$H(z) = G(s)\Big|_{s=\frac{2}{T}\frac{z-1}{z+1}} \tag{10.66}$$

Due to the form of this transformation, it is called a **bilinear transformation.**

Now, $H(e^{j\omega T})$ takes on the values of $G(s)$ as s varies along a path given by

$$s = \frac{2}{T}\frac{e^{j\omega T}-1}{e^{j\omega T}+1} = \frac{2}{T}\frac{e^{j\omega T/2}-e^{-j\omega T/2}}{e^{j\omega T/2}+e^{-j\omega T/2}}\frac{e^{j\omega T/2}}{e^{j\omega T/2}} = \frac{2}{T}\frac{j(e^{j\omega T/2}-e^{-j\omega T/2})/j2}{(e^{j\omega T/2}+e^{-j\omega T/2})/2}$$

$$s = j\frac{2}{T}\tan\left(\frac{\omega T}{2}\right) \tag{10.67}$$

Eq. 10.67 shows that the bilinear transformation given in eq. 10.66 maps the unit circle in the z-plane onto the $j\Omega$-axis in the s-plane. Therefore, $H(e^{j\omega T})$ takes on the values of $G(j\Omega)$. Recall that this is not possible with the forward or backward difference approximations.

The digital filter and analog filter input frequencies are related through

$$\Omega = \frac{2}{T}\tan\left(\frac{\omega T}{2}\right) \tag{10.68}$$

where for $\omega = 0$, $\Omega = 0$, and for $\omega = \omega_f$, $\Omega = \frac{2}{T}\tan\left(\frac{\omega_s T}{2\,2}\right) = \frac{2}{T}\tan\left(\frac{2\pi T}{2T\,2}\right) = \infty$. Therefore, as ω varies from $\omega = 0$ to $\omega = \omega_f$, $H(e^{j\omega T})$ takes on all the values of $G(j\Omega)$ as Ω varies from $\Omega = 0$ to $\Omega = \infty$, which is called the **warping effect**. Nevertheless, the bilinear transformation is useful for transforming any analog filter type. The extent to which the shape of $G(j\Omega)$ is preserved in $H(e^{j\omega T})$ through the nonlinear relationship given in eq. 10.68 will depend on T and the nature of $G(s)$.

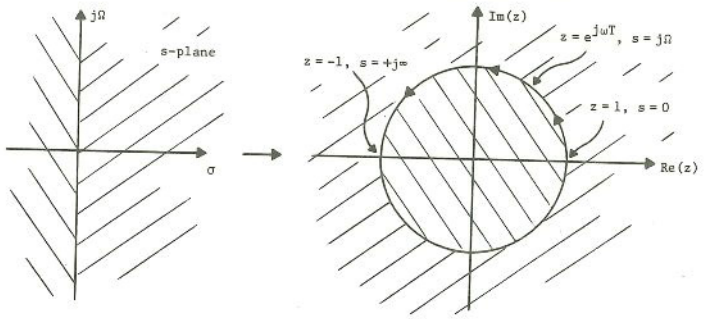


Fig. 10.29. Bilinear transformation s-plane to z-plane mapping.

By solving for z in terms of s from eq. 10.65, the poles of $H(z)$ can be found through

$$z = \frac{1+\frac{T}{2}s}{1-\frac{T}{2}s} = \frac{\frac{2}{T}+Re(s)+jIm(s)}{\frac{2}{T}-Re(s)-jIm(s)} \tag{10.69}$$

The magnitude $\|z\|$ of z in eq. 10.69 is given by

$$\|z\|^2 = \frac{\left(\frac{2}{T}+Re(s)\right)^2+(Im(s))^2}{\left(\frac{2}{T}-Re(s)\right)^2+(Im(s))^2} \tag{10.70}$$

In eq. 10.70, if $Re(s)$ is negative, then $\|z\| < 1$, and if $Re(s)$ is positive, then $\|z\| > 1$. The bilinear transformation maps the entire LH (RH) s-plane onto the inside (outside) of the unit circle in the z-plane. This is shown in Fig. 10.29, and we see that a stable $G(s)$ will result in a stable $H(z)$.

Example 10.11. For $G(s)$ given in Example 10.10, the bilinear transformation results in

$$H(z) = \frac{1}{\left(\frac{2}{T}\frac{z-1}{z+1}\right)^2 + \sqrt{2}\left(\frac{2}{T}\frac{z-1}{z+1}\right) + 1} = \frac{T^2(z^2+2z+1)}{(4+2T\sqrt{2}+T^2)z^2 - (8-2T^2)z + (4-2T\sqrt{2}+T^2)} \tag{10.71}$$

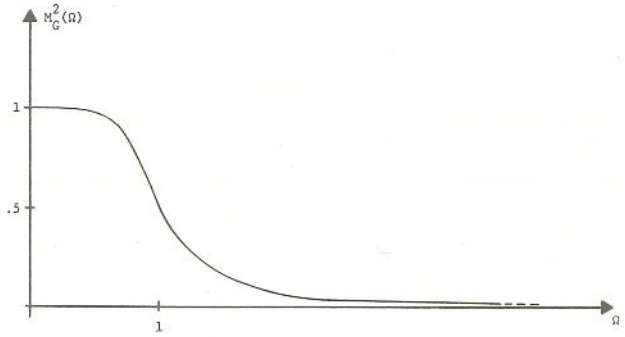


Fig. 10.30a. Analog filter magnitude frequency response.

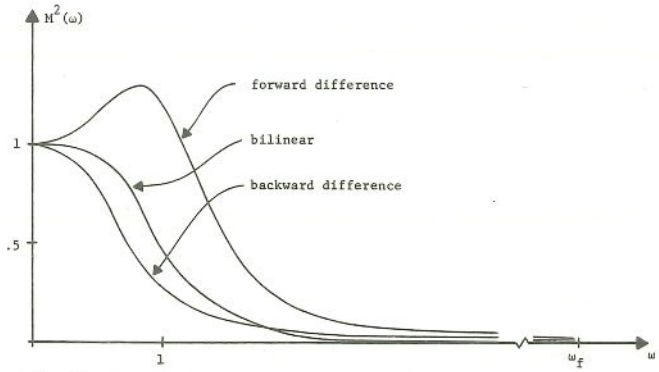


Fig. 10.30b. Digital filter magnitude frequency response.

The poles of $G(s)$ are at $s = (-1 \pm j)\sqrt{2}/2$. Let us compare the frequency response magnitudes of the digital filters we have obtained by the backward, forward, and bilinear transformations. For this, we must select a value for T. To satisfy eq. 10.63, T must be less than $\sqrt{2}$ secs., or $f_s > 1/\sqrt{2}$ Hz. Moreover, since $g(t) = L^{-1}(G(s))$ is not bandlimited, we must choose an f_s large enough so that

one period of $H(e^{j\omega T})$ can approximate $G(j\Omega)$. Since the bandwidth of $G(s)$ is $\Omega_c = 1$, let us try $f_s = 2$, so that $\omega_s = 4\pi$, and $T = 0.5$, which is also large enough so that we can readily discern the differences between the transformation methods. However, for practical purposes this f_s is too small. $M_G^2(\Omega)$ is shown in Fig. 10.30a, and the $M^2(\omega)$ for the $H(z)$ given in eqs. 10.55, 10.61, and 10.71 are shown in Fig. 10.30b.

Notice that with the bilinear transformation, $H(z)$ has a bandwidth of $\omega_c = 0.980$ rad/sec, which can be found by substituting $\Omega_c = 1$ into eq. 10.68. As T is decreased, $\omega_c \to \Omega_c$. However, the shape of $\| H(e^{j\omega T}) \|$ will always appear to be a squeezed version of $\| G(j\Omega) \|$ due to the warping effect.

Example 10.12. Suppose a signal $u(t)$, which is bandlimited to 200 Hz, is to be low-pass filtered by a second order digital filter with $f_c = 80$ Hz. The sampling frequency must be greater than 400 Hz. Let us use $f_s = 800$ Hz, and design $H(z)$ with the bilinear transformation. Now we face the problem of selecting an appropriate $G(s)$. Regardless of which $G(s)$ we use, if the bandwidth of $H(z)$ is to be $\omega_c = 160\pi \cong 502.65$ rad/sec, then by eq. 10.68 the bandwidth of $G(s)$ must be

$$\Omega_c = \frac{2}{1/800} \tan\left(\frac{(160\pi)(1/800)}{2} \right) \cong 519.87 \text{ rad/sec}$$

Then, when we transform a $G(s)$ with BW$=\Omega_c$ to $H(z)$ with the bilinear transformation, the value $\| G(j\Omega_c) \|^2 = 1/2$ will occur for $\| H(e^{j\omega T}) \|^2$ when $\omega = \omega_c$. Thus, $H(z)$ will have the desired BW.

We will consider the problem of selecting $G(s)$ in a short while. For now, since $G(s)$ in eq. 10.50 will yield a second order digital filter, let us use it. However, its bandwidth is not $\Omega_c = 519.87$. The bandwidth we need can be obtained, if in $G(s)$ of eq. 10.50 we replace s by

$$s \leftarrow \frac{s}{\Omega_c} \tag{10.72}$$

to obtain

$$G(s) = \frac{1}{\left(\frac{s}{\Omega_c}\right)^2 + \sqrt{2}\left(\frac{s}{\Omega_c}\right) + 1} = \frac{\Omega_c^2}{s^2 + \Omega_c\sqrt{2}\,s + \Omega_c^2} \tag{10.73}$$

Notice that for $G(s)$ given in eq. 10.73, $M_G^2(\Omega = \Omega_c) = 1/2$. In fact, since the bandwidth of $G(s)$ in eq. 10.50 is BW$=1$, it is called a **normalized** LP filter, and eq. 10.72 is a **normalized** analog LP filter to **unnormalized** analog LP filter transformation. Hereafter, we shall denote a normalized analog LP filter transfer function by $G_N(s)$, and $G(s)$ in eq. 10.73 is found with

$$G(s) = G_N(s)\,|_{s \leftarrow f(s)} \tag{10.74}$$

where the function $f(s)$, which is called a **frequency transformation**, is given by $f(s) = s/\Omega_c$. Finally, with eqs. 10.73 and 10.66, $H(z)$ is given by

$$H(z) = \frac{\Omega_c^2}{\left(\frac{2}{T}\frac{z-1}{z+1}\right)^2 + \Omega_c\sqrt{2}\left(\frac{2}{T}\frac{z-1}{z+1}\right) + \Omega_c^2} \tag{10.75}$$

which has the specified bandwidth $\omega_c = 160\pi \cong 502.65$ rad/sec.

The analog filter to digital filter transformations that we have developed so far are generally referred to as **numerical approximation methods**. There are numerous other numerical approximation methods that can be employed to discretize an analog system. See, for example, the method used in Example 8.30. In a short while, we will develop a few more methods for obtaining an $H(z)$ given a $G(s)$.

10-3.4 Analog Prototypes

In the previous example we saw that there are two aspects to designing a recursive digital filter $H(z)$ based on an analog prototype $G(s)$. First, we must convert the specifications for $H(z)$ to specifications for $G(s)$. This can depend on the discretization method that will be used to obtain $H(z)$ from $G(s)$. Second, we must determine a $G(s)$ that meets its specifications.

We will now obtain various forms of $G(s)$ based on achieving requirements of $M_G^2(\Omega)$. First of all, we note that

$$M_G^2(\Omega) = G(j\Omega)G^*(j\Omega) = G(j\Omega)G(-j\Omega)$$

and therefore $M_G^2(\Omega)$ is a ratio of polynomials in Ω^2 with real coefficients. Assuming $G(s)$ is stable, the magnitude frequency response is given by

$$M_G^2(\Omega) = G(s)G(-s)|_{s=j\Omega}$$

Denote the product $G(s)G(-s)$ by $T(s^2)$, which is a function of even powers of s. If $s = s_i$ is any pole (zero) of $G(s)$, then $s = -s_i$ is a pole (zero) of $G(-s)$. In general, the factors of $T(s^2)$ are:

$$(s+\alpha)(-s+\alpha)$$

$$(s^2+\alpha_1 s+\alpha_0)(s^2-\alpha_1 s+\alpha_0)$$

$$(s^2+\alpha)(s^2+\alpha)$$

which are due to a real pole or zero, a complex conjugate pair of poles or zeros, or a complex conjugate pair of imaginary zeros of $G(s)$, respectively, where all the poles of $G(s)$ must be in the LH s-plane. From the form of $T(s^2)$ we see that the poles and zeros of $T(s^2)$ are located symmetrically about the $j\Omega$-axis in the s-plane.

Given $M_G^2(\Omega)$, we form $T(s^2)$ with

$$T(s^2) = M_G^2(\Omega)|_{\Omega = s/j} \tag{10.76}$$

and then factor $T(s^2)$. To obtain $G(s)$ we use the LH s-plane poles of $T(s^2)$ and half of the zeros of $T(s^2)$ so that the remaining zeros and the zeros we are using form a symmetric pattern about the $j\Omega$-axis.

Now, we must select a suitable $M_G^2(\Omega)$. Since we expect to obtain $G(s)$ through eq. 10.74, it is more convenient to develop various forms for $M_N^2(\Omega) = G_N(j\Omega)G_N(-j\Omega)$ to obtain $G_N(s)$, which can then be unnormalized. We must choose a function $M_N^2(\Omega)$ that approximates the ideal LP filter characteristic shown in Fig. 10.31. In the literature concerned with analog filter design many suitable forms for $M_N^2(\Omega)$, which have various additional properties, have been reported. Here, we shall consider only two such forms for $M_N^2(\Omega)$.

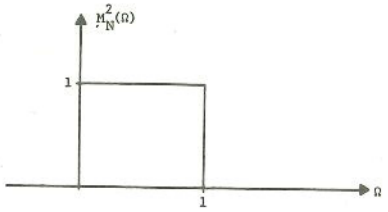


Fig. 10.31. Ideal LP filter magnitude characteristic.

Example 10.13. Suppose $M_N^2(\Omega)$ is chosen to be

$$M_N^2(\Omega) = \frac{1}{1+\Omega^4} \tag{10.77}$$

Notice that $M_N^2(\Omega = 0) = 1$, $M_N^2(\Omega = 1) = 1/2$, and $M_N^2(\Omega \to \infty) = 0$, and $M_N^2(\Omega)$ has the characteristic of an LP filter. By eq. 10.76, $T_N(s^2)$ becomes

$$T_N(s^2) = \frac{1}{1+\left(\frac{s}{j}\right)^4} = \frac{1}{1+s^4}$$

Now we must find the four roots of $s^4 + 1 = 0$, or $s^2 = \pm j$. For $s^2 = j$, we have

$$s^2 = j = e^{j\frac{\pi}{2}}, \quad s = \pm e^{j\frac{\pi}{4}}$$

For $s^2 = -j$, we have

$$s^2 = -j = e^{-j\frac{\pi}{2}}, \quad s = \pm e^{-j\frac{\pi}{4}}$$

Denote the four roots by $s_1 = -e^{-j\pi/4}$, $s_2 = -e^{j\pi/4}$, $s_3 = e^{-j\pi/4}$, and $s_4 = e^{j\pi/4}$. Using the LH s-plane poles of $T_N(s^2)$ results in

$$G_N(s) = \frac{1}{(s - s_1)(s - s_2)} = \frac{1}{s^2 + \sqrt{2}s + 1}$$

Because of the form we chose for $M_N^2(\Omega)$ in eq. 10.77, we know that this $G_N(s)$ has an LP filter characteristic with $\Omega_c = 1$.

A general form of eq. 10.77 is given by

$$M_N^2(\Omega) = \frac{1}{1 + (\Omega^2)^n} \tag{10.78}$$

which is shown in Fig. 10.32 for $n = 2$ and $n = 3$.

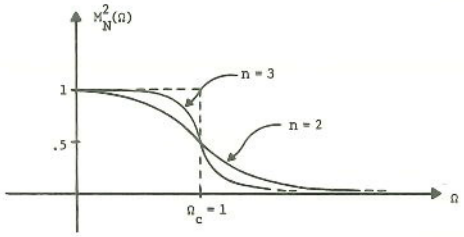


Fig. 10.32. Butterworth LP filter magnitude characteristic.

Notice that for any positive integer n, $M_N^2(\Omega = 1) = 1/2$, and that as n is increased we come closer to an ideal LP filter characteristic. $M_N^2(\Omega)$ given in eq. 10.78 is called a **Butterworth characteristic**, and since we have that

$$\frac{d^i}{d\Omega^i} M_N^2(\Omega)\,|_{\Omega=0} = 0$$

for $i = 1, \cdots, 2n - 1$, it is also called a **maximally flat characteristic**. The poles of $T_N(s^2)$ are the roots of $1 + (-s^2)^n = 0$, and the LH s-plane roots are given by

$$s_i = e^{j\left(\frac{2i-1}{2n}\pi + \frac{\pi}{2}\right)}$$

for $i = 1, \cdots, n$, which are all located on a circle of radius one in the s-plane. And, $G_N(s)$ is given by

$$G_N(s) = \prod_{i=1}^{n} \frac{1}{(s - s_i)} = \frac{1}{\alpha_n s^n + \cdots + \alpha_1 s + \alpha_0} \tag{10.79}$$

Since $G_N(s)$ given in eq. 10.79 has no finite zeros, it is called an **all-pole function**. Nevertheless, since $\lim_{s \to \infty} G_N(s) = 0$, we say that $G_N(s)$ has n zeros at infinity. For any n, the α_i, $i = 0, \cdots, n$ can be determined, and for $n = 1, \cdots, 5$ these coefficients are given in Table 10.1.

Table 10.1 Butterworth Filter Coefficients

n	α_0	α_1	α_2	α_3	α_4	α_5
1	1.0	1.0				
2	1.0	1.4142	1.0			
3	1.0	2.0	2.0	1.0		
4	1.0	2.6131	3.4142	2.6131	1.0	
5	1.0	3.2361	5.2361	5.2361	3.2361	1.0

Usually, the choice for n depends on a transition band specification on $M_N^2(\Omega)$, whereby we stipulate that $M_N^2(\Omega)$ shall remain less than some specified value for all Ω greater than some specified frequency.

Example 10.14. Let us find a Butterworth LP filter transfer function $G(s)$ with $\text{BW} = \Omega_c = 125$ rad/sec such that the gain is down at least 20 dB from the maximum gain by $\Omega = 275$ rad/sec. The term gain is used in referring to $M_G(\Omega)$. The maximum gain of 0 dB occurs at $\Omega = 0$, and the gain is -3 dB (or down 3 dB) at $\Omega = \Omega_c$.

To use Table 10.1 or eq. 10.79, we convert the above specifications to those of a normalized LP filter, i.e., $\text{BW} = 1$. This is done by using eq. 10.72 so that $M_N(\Omega)$ must be down at least 20 dB by $\Omega = 275/125 = 2.2$ rad/sec. Then, when s in $G_N(s)$ is replaced by $s/125$, the frequency 2.2 rad/sec, at which $M_N(\Omega)$ is down at least 20 dB, is transformed to 275 rad/sec, at which $M_G(\Omega)$ is down at least 20 dB.

For this normalized filter, the transition band specification requires that

$$10 \log M_N^2(2.2) \le -20, \text{ or } 20 \log M_N(2.2) \le -20 \tag{10.80}$$

$$-\log(1 + (2.2)^{2n}) \le -2$$

$$(4.84)^n \ge 10^2 - 1$$

The smallest integer that satisfies eq. 10.80 is $n = 3$. Of course, we can use a larger value of n, but this would unnecessarily increase the order of $G_N(s)$. Our goal is to satisfy the specification, for which $n = 3$ is adequate. From Table 10.1 we get

$$G_N(s) = \frac{1}{s^3 + 2s^2 + 2s + 1}$$

and after replacing s by $s/125$ we obtain the desired $G(s)$, i.e.

$$G(s) = \frac{1}{\left(\frac{s}{125}\right)^3 + 2\left(\frac{s}{125}\right)^2 + 2\left(\frac{s}{125}\right) + 1}$$

which satisfies the given specifications. Notice that $G(j275) = G_N(j2.2)$.

Another commonly used form for $M_N^2(\Omega)$ is given by

$$M_N^2(\Omega) = \frac{1}{1 + \varepsilon^2 C_n^2(\Omega)} \tag{10.81}$$

where ε is a parameter that we must select. If for $0 \le \Omega \le 1$, $C_n(\Omega)$ satisfies $0 \le C_n^2(\Omega) \le 1$, then $M_N^2(\Omega)$ satisfies $1/(1+\varepsilon^2) \le M_N^2(\Omega) \le 1$. And, if $C_n^2(\Omega)$ increases for $\Omega = 1$ to $\Omega = \infty$, then eq. 10.81 exhibits the behavior of an LP filter. A set of functions $C_n(\Omega)$, which meet the above requirements, are the Chebyshev polynomials, i.e.

$$C_1(\Omega) = \Omega$$
$$C_2(\Omega) = 2\Omega^2 - 1$$
$$C_3(\Omega) = 4\Omega^3 - 3\Omega$$
$$\vdots$$
$$C_{n+1}(\Omega) = 2\Omega C_n(\Omega) - C_{n-1}(\Omega)$$

for $n = 2, 3, \cdots$. For $n = 1, 2$, and 3, the $C_n(\Omega)$ are shown in Fig. 10.33a, and the resulting $M_N^2(\Omega)$ are shown in Fig. 10.33b.

The resulting filter is said to have a **Chebyshev characteristic**. In Fig. 10.33b we see that $\Omega = 1$ is the bandwidth if $\varepsilon = 1.0$. Instead, for any value of the parameter ε, Chebyshev filters are normalized to the ripple bandwidth $\Omega_r = 1$. A Chebyshev filter is also called an **equal-ripple filter**, because in the pass-band all maximum and minimum values of $M_N^2(\Omega)$ are 1 and $1/(1+\varepsilon^2)$,

respectively. The parameter ε determines the ripple minimum of $-10\log(1+\varepsilon^2)$ dB. Ideally, we want a small ripple. However, in eq. 10.81 we see that as we decrease ε, we must increase n to maintain a narrow transition band.

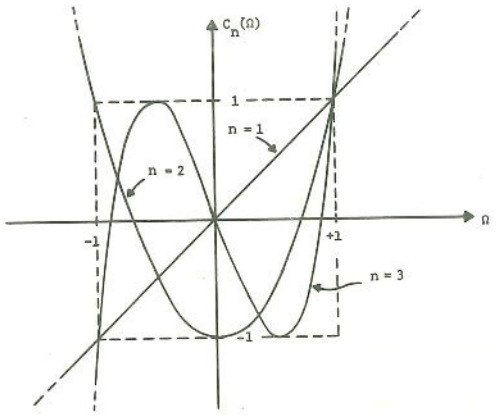


Fig. 10.33a. Chebyshev polynomials.

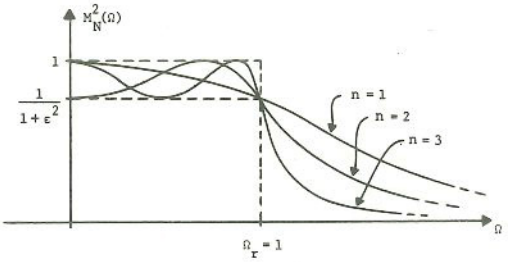


Fig. 10.33b. Chebyshev filter characteristic.

Another expression for the Chebyshev polynomials is given by

$$C_n(\Omega) = \cos(n\cos^{-1}(\Omega)), \quad |\Omega| \le 1 \tag{10.82a}$$

$$C_n(\Omega) = \cosh(n\cosh^{-1}(\Omega)), \quad |\Omega| > 1 \tag{10.82b}$$

For $\varepsilon < 1$, the bandwidth Ω_c is determined with

$$\frac{1}{1+\varepsilon^2\cosh^2(n\cosh^{-1}(\Omega_c))}=\frac{1}{2}$$

which yields

$$\Omega_c=\cosh\left(\frac{1}{n}\cosh^{-1}\left(\frac{1}{\varepsilon}\right)\right) \tag{10.83}$$

The poles of $T_N(s^2)$ are the roots of $1+\varepsilon^2C_n^2(s/j)=0$, which depend on both ε and n. The LH s-plane roots are given by

$$s_i=-\sinh(v)\sin(w_i)+j\cosh(v)\cos(w_i) \tag{10.84}$$

for $i=1,2,\cdots,n$, where $w_i=(2i-1)\pi/(2n)$ and $v=\frac{1}{n}\sinh^{-1}(1/\varepsilon)$. As for a Butterworth filter, it is convenient to compute the coefficients in eq. 10.79 using the poles given in eq. 10.84 just once, and then obtain them from a table. However, since the Chebyshev filter poles also depend on ε, the α_i, $i=0,1,\cdots,n$ required in eq. 10.79 are given in Table 10.2 only for a ripple trough of –0.5 dB, –1.0 dB, and –3.0 dB for $n=1,\cdots,5$. In the literature concerned with analog filter design, the reader will find more extensive tables of Butterworth and Chebyshev filter coefficients.

Table 10.2 Chebyshev Filter Coefficients

$-10\log(1+\varepsilon^2)=-0.5$ dB, $\varepsilon^2=0.1220$

n	α_0	α_1	α_2	α_3	α_4	α_5
1	1.0	0.3493				
2	1.0593	0.9960	0.6986			
3	1.0	2.1446	1.7506	1.3972		
4	1.0593	2.8656	4.7978	3.3461	2.7945	
5	1.0	4.2058	7.3192	10.8279	6.5530	5.5890

$-10\log(1+\varepsilon^2)=-1.0$ dB, $\varepsilon^2=0.2589$

n	α_0	α_1	α_2	α_3	α_4	α_5
1	1.0	0.5088				
2	1.1220	1.1172	1.0177			
3	1.0	2.5206	2.0117	2.0354		
4	1.1220	3.0230	5.9186	3.8787	4.0708	
5	1.0	4.7264	7.9331	13.7496	7.6272	8.1416

$-10\log(1+\varepsilon^2) = -3.0$ dB, $\varepsilon^2 = 0.9953$						
n	α_0	α_1	α_2	α_3	α_4	α_5
1	1.0	0.9976				
2	1.4125	1.2867	1.9953			
3	1.0	3.7046	2.3833	3.9905		
4	1.4125	3.2305	9.3308	4.6416	7.9810	
5	1.0	6.5126	8.7623	22.5895	9.1705	15.9645

Example 10.15. Let us find a Chebyshev LP filter with a ripple bandwidth of 125 rad/sec such that the gain is down at least 20 dB from the maximum gain by 275 rad/sec. The maximum gain of 0 dB occurs at the pass-band ripple peaks. Furthermore, suppose that a pass-band ripple trough of −1.0 dB is acceptable.

To use Table 10.2, we convert the above specifications to those of a normalized LP filter, i.e., $\Omega_r = 1$, and $M_N(\Omega)$ should be down at least 20 dB by $\Omega = 275/125 = 2.2$. First, we must determine ε^2, which can be found with

$$-10\log(1+\varepsilon^2) = -1.0$$

and $\varepsilon^2 = 0.2589$.

The normalized filter transition band specification requires that

$$-10\log(1+0.2589C_n^2(2.2)) \le -20 \tag{10.85}$$

$$C_n^2(2.2) \ge \frac{10^2-1}{0.2589} = 382.3870$$

Now we must check eq. 10.85 to find the smallest integer n that satisfies it. Since $C_2^2(2.2) = 75.3424$, and $C_3^2(2.2) = 1295.4241$, we choose $n = 3$, which is more than adequate. In fact, with $n = 3$, we could increase the pass-band ripple trough to

$$-10\log\left(1+\frac{10^2-1}{C_3^2(2.2)}\right) = -0.32\,\text{dB}$$

and still achieve the transition band specification. Moreover, with $n = 3$ and $\varepsilon^2 = 0.2589$, eq. 10.83 yields the normalized filter bandwidth of $\Omega_c = 1.0949$, and the gain is down 25.27 dB at $\Omega = 2.2$. The gain of the normalized Butterworth LP filter found in Example 10.14 is down 20.58 dB at $\Omega = 2.2$ for $n = 3$. From this comparison we see that if we can accept the pass-band ripple, then a Chebyshev filter can provide more stop-band attenuation than does a comparable Butterworth filter.

From Table 10.2 we get

$$G_N(s) = \frac{1}{2.0354s^3 + 2.0117s^2 + 2.5206s + 1.0}$$

and after replacing s by $s/125$ we obtain the desired $G(s)$. The ripple bandwidth of $G(s)$ is $\Omega_r = 125$, and the bandwidth of $G(s)$ is $\Omega_c = (1.0949)(125)$.

On the other hand, if we want $G(s)$ to have a 3 dB bandwidth of 125, then we must unnormalize $G_N(s)$ by replacing s by $s/(125/1.0949)$, and the gain $M_G(\Omega)$ will be down even more than 25.27 dB at $\Omega = 275$.

10-3.5 Analog Frequency Transformations

So far we have only found a $G(s)$ that performs as an LP filter. To design digital BP, BS and HP filters, we must also be able to obtain analog BP, BS, and HP filter transfer functions, which are then discretized to find $H(z)$. It is possible to obtain a $G(s)$ that exhibits the behavior of any of these filter types by an appropriate choice for the frequency transformation $f(s)$ in eq. 10.74.

We have been using the symbol ω for the digital filter $H(z)$ frequency variable, and for an unnormalized analog filter $G(s)$ frequency variable we have been using the symbol Ω. As we obtain additional frequency transformations it will be useful to distinguish between the normalized analog LP filter $G_N(s)$ frequency response and that of $G(s)$. Let us use the symbol p for the Laplace variable in G_N, and write $G_N(p)$ instead of $G_N(s)$. Also, for the frequency response of $G_N(p)$, we will use λ for the frequency variable, i.e., $p = j\lambda$. Now, eq. 10.74 becomes

$$G(s) = G_N(p)\big|_{p=f(s)} \tag{10.86}$$

and $f(s)$ is called a normalized analog LP filter to unnormalized analog filter **frequency transformation**.

For example, in Example 10.14 we would write $G_N(p) = 1/(p^3 + 2p^2 + 2p + 1)$, $\lambda_c = 1.0$, $\Omega_c = 125$, and $f(s) = s/\Omega_c$, and then obtain $G(s)$ with eq. 10.86. Then, the frequency responses of $G(s)$ and $G(p)$ are obtained with $G(j\Omega)$ and $G_N(j\lambda)$, respectively. With $p = s/\Omega_c$, the normalized LP filter frequency variable and unnormalized LP filter frequency variable are related through $\lambda = \Omega/\Omega_c$. Thus, $\Omega = \Omega_c \rightarrow \lambda_c = 1$, and $\Omega = 275 \rightarrow \lambda = 2.2$.

Let us consider another frequency transformation $f(s) = \Omega_c/s$. For the frequency response of $G(s)$ we evaluate $G_N(p)$ for

$$p = \frac{\Omega_c}{j\Omega} = -j\frac{\Omega_c}{\Omega}$$

and we see that $f(s)$ maps the $j\Omega$-axis in the s-plane onto the $j\lambda$-axis in the p-plane, which is required of any $f(s)$ that we might choose. With $p = j\lambda$, we have

$$\lambda = -\frac{\Omega_c}{\Omega} \tag{10.87}$$

and we can relate the λ and Ω frequencies as follows.

$$\lambda = -\infty \rightarrow \Omega = 0^+$$

$$\lambda = -\lambda_c = -1.0 \rightarrow \Omega = +\Omega_c$$

$$\lambda = -0^+ \rightarrow \Omega = +\infty$$

$$\lambda = 0^+ \rightarrow \Omega = -\infty$$

$$\lambda = +\lambda_c = 1.0 \rightarrow \Omega = -\Omega_c$$

$$\lambda = +\infty \rightarrow \Omega = -0^+$$

Therefore, $G(j0^+)$, $G(j\Omega_c)$, and $G(j\infty)$ take on the values $G_N(-j\infty) = 0$, $G_N(-j1)$, and $G_N(j0^-)$, respectively, resulting in $M_G^2(\Omega)$ as shown in Fig. 10.34.

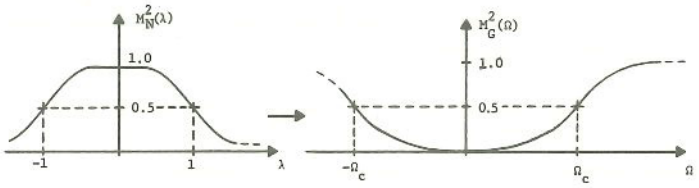


Fig. 10.34. Normalized LP to unnormalized HP transformation.

In Fig. 10.34 we see that $f(s) = \Omega_c/s$ transforms $G_N(p)$ into an HP filter with cut-off frequency $\Omega = \Omega_c$. If we use just $f(s) = 1/s$, then we would obtain a normalized HP filter, which can also be unnormalized.

Example 10.16. Let us find a Butterworth HP filter $G(s)$ with cut-off frequency $\Omega_c = 50$ rad/sec such that the gain is down at least 40 dB by $\Omega = 20$ rad/sec.

We must first convert these specifications to those of a normalized LP filter. By eq. 10.87, $\Omega_c = 50$ and $\Omega = 20$ transform to $\lambda_c = -1.0$ and $\lambda = -50/20 = -2.5$, respectively. Since $M_N(\lambda)$ (and $M_G(\Omega)$) is an even function, the gain of $G_N(p)$ must be down at least 40 dB by $\lambda = +2.5$. Now, the reader should proceed as in Example 10.14 to obtain $G_N(p)$, and then with eq. 10.86 $G(s)$ is given by

$$G(s) = \frac{s^4}{s^4 + 130.655s^3 + 8535.5s^2 + 326637.5s + (50)^4}$$

Notice that the transfer function of an HP filter is not a strictly proper function.

———

The LP to HP transformation $f(s) = 1/s$ is useful for obtaining yet another type of function $M_N^2(\lambda)$ in addition to those given in eqs. 10.78 (Butterworth) and 10.81 (Chebyshev). If we subtract $M_N^2(\lambda)$ given in eq. 10.81 from 1, then we get

$$1 - \frac{1}{1+\varepsilon^2 C_n^2(\lambda)} = \frac{\varepsilon^2 C_n^2(\lambda)}{1+\varepsilon^2 C_n^2(\lambda)} \tag{10.88}$$

which, for $n = 5$, is shown in Fig. 10.35a.

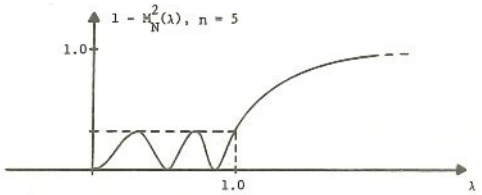


Fig. 10.35a. Equal ripple stop-band HP filter.

The characteristic shown in Fig. 10.35a is that of an HP filter that can be transformed into an LP filter characteristic by replacing λ by $1/\lambda$, resulting in

$$M_N^2(\lambda) = \frac{\varepsilon^2 C_n^2(1/\lambda)}{1+\varepsilon^2 C_n^2(1/\lambda)} \tag{10.89}$$

which, for $n = 5$, is shown in Fig. 10.35b. This normalized LP filter characteristic possesses the equal ripple property in the stop-band, and it is called an **inverse Chebyshev** characteristic. As the reader might suspect, there are **elliptic** filters, which possess the equal ripple property in both the stop-band and the pass-band. For the further development of inverse Chebyshev and elliptic filters, the reader is referred to the literature on analog filter design.

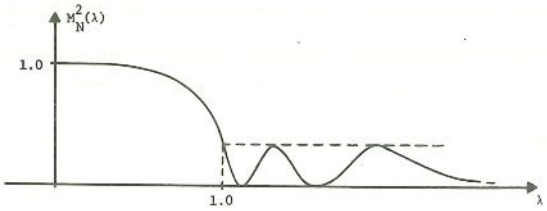


Fig. 10.35b. Normalized inverse Chebyshev LP filter characteristic for $n = 5$.

Let us expand our repertoire of methods for generating a $G(s)$ for different filter types by investigating some additional frequency transformations. Consider the transformation $f(s) = (s^2 + \Omega_0^2)/(\Omega_b s)$, where Ω_0 and Ω_b are constants that will be specified later. For the frequency response of $G(s)$ we evaluate $G_N(p)$ for

$$p = \frac{(j\Omega)^2 + \Omega_0^2}{\Omega_b j\Omega} = j\frac{1}{\Omega_b}\frac{\Omega^2 - \Omega_0^2}{\Omega}$$

With $p = j\lambda$, we have

$$\lambda = \frac{1}{\Omega_b}\frac{\Omega^2 - \Omega_0^2}{\Omega} \tag{10.90}$$

and we can relate the λ and Ω frequencies as follows.

$$\lambda = -\infty \rightarrow \Omega = -\infty, \Omega = 0^+$$

$$\lambda = -0^+ \rightarrow \Omega = -\Omega_0^+, \Omega = \Omega_0^-$$

$$\lambda = 0^+ \rightarrow \Omega = -\Omega_0^-, \Omega = \Omega_0^+$$

$$\lambda = +\infty \rightarrow \Omega = -0^+, \Omega = +\infty$$

Therefore, $G(j0^+)$, $G(j\Omega_0^-)$, $G(j\Omega_0^+)$, and $G(j\infty)$ take on the values $G_N(-j\infty)$, $G_N(-j0^+)$, $G_N(+j0^+)$, and $G_N(j\infty)$, respectively. This results in an $M_G^2(\Omega)$ as shown in Fig. 10.36, which is a BP filter characteristic.

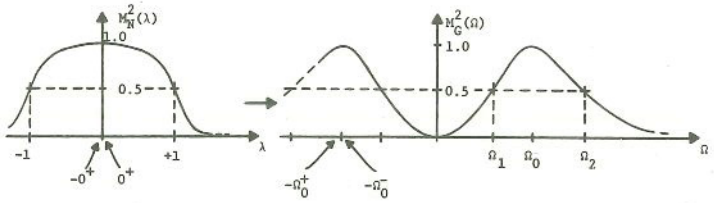


Fig. 10.36. Normalized LP to unnormalized BP transformation.

For $M_G^2(\Omega)$, Ω_1 and Ω_2 are the lower and upper, respectively, cut-off frequencies, which we want to come from $\lambda = -\lambda_c = -1.0$ and $\lambda = \lambda_c = 1.0$, respectively, and therefore we have

$$-1 = \frac{1}{\Omega_b}\frac{\Omega_1^2 - \Omega_0^2}{\Omega_1} \tag{10.91a}$$

$$1 = \frac{1}{\Omega_b}\frac{\Omega_2^2 - \Omega_0^2}{\Omega_2} \tag{10.91b}$$

Eliminating Ω_b from eqs. 10.91 results in

$$\Omega_1(\Omega_2^2 - \Omega_0^2) = \Omega_2(\Omega_0^2 - \Omega_1^2)$$

$$\Omega_1\Omega_2(\Omega_1+\Omega_2)=\Omega_0^2(\Omega_1+\Omega_2)$$

$$\Omega_0=(\Omega_1\Omega_2)^{1/2} \tag{10.92a}$$

Substituting eq. 10.92a into either eq. 10.91a or 10.91b yields

$$\Omega_b=\Omega_2-\Omega_1 \tag{10.92b}$$

Therefore, Ω_b is the bandwidth of the BP filter $G(s)$, and $f(s)$ transforms a normalized LP filter into an unnormalized BP filter. Notice that Ω_0 is the geometric mean of Ω_1 and Ω_2 and not the arithmetic mean.

Example 10.17. Let us determine a Butterworth BP filter transfer function $G(s)$ with cut-off frequencies at $\Omega_1=400$ rad/sec and $\Omega_2=600$ rad/sec, which is down at least 20 dB at $\Omega_3=300$ rad/sec and $\Omega_4=700$ rad/sec. We refer to the set of frequencies $\Omega_1,\Omega_2,\Omega_3$, and Ω_4 as the **critical frequencies**. First, we normalize the critical frequencies with eq. 10.90, resulting in

$$\lambda_1=\frac{1}{600-400}\frac{400(400-600)}{400}=-1.0$$

$$\lambda_2=\frac{1}{200}\frac{600(600-400)}{600}=1.0$$

$$\lambda_3=\frac{1}{200}\frac{(300)^2-(400)(600)}{300}=-2.500$$

$$\lambda_4=\frac{1}{200}\frac{(700)^2-(400)(600)}{700}=1.786$$

Since $M_N^2(\lambda)$ is an even function, which decreases monotonically, the normalized LP filter must satisfy the 20 dB down requirement by $\lambda=1.786$ (This will also satisfy the 20 dB down requirement by $\lambda=\pm2.5$.) resulting in

$$-10\log(1+(1.786)^{2n})\le -20 \quad\rightarrow\quad 1+(1.786)^{2n}\ge 100$$

This requires $n=4$. From Table 10.1 we obtain $G_N(p)$, and then $G(s)$ can be found with

$$G(s)=G_N(p)\big|_{p=(s^2+24000)/(200s)}$$

Notice that the order of the LP filter is $n=4$, while the order of the resulting BP filter is $2n=8$.

To obtain a band-stop filter with cut-off frequencies at Ω_1 and Ω_2, we replace $f(s)$ by $1/f(s)$ in the LP to BP transformation, resulting in the normalized LP to unnormalized BS transformation given by

$$G(s) = G_N(p)\big|_{p=(\Omega_2-\Omega_1)s/(s^2+\Omega_1\Omega_2)}$$

By means similar to how the normalized LP and BP filter characteristics were related, the reader should investigate the LP $\rightarrow$ BS filter transformation.

The frequency transformations we have investigated are summarized in Table 10.3. For any $f(s)$ that the reader may invent, recall that $f(s)$ must map the $j\Omega$-axis onto the $j\lambda$-axis. Furthermore, the LH p-plane poles of $G_N(p)$ must map to LH s-plane poles, and $G(s)$ must be a proper function.

Table 10.3. Normalized LP Filter to $G(s)$ Frequency Transformations

$G(s) = G_N(p)\big\|_{p=f(s)}$	
$f(s)$	$G(s)$
$\dfrac{s}{\Omega_c}$	LP, bandwidth $= \Omega_c$
$\dfrac{\Omega_c}{s}$	HP, cut-off freq. $= \Omega_c$
$\dfrac{1}{\Omega_2-\Omega_1}\dfrac{s^2+\Omega_1\Omega_2}{s}$	BP, bandwidth $= \Omega_2-\Omega_1$
$(\Omega_2-\Omega_1)\dfrac{s}{s^2+\Omega_1\Omega_2}$	BS, pass-band $= \begin{cases} 0 \rightarrow \Omega_1 \\ \Omega_2 \rightarrow \infty \end{cases}$

Now that we know how to determine a $G(s)$ with various frequency selective properties, let us develop a few more methods for obtaining an $H(z)$ given a $G(s)$.

10-3.6 Impulse Invariant Method

Let $g(t) = L^{-1}(G(s))$ denote the impulse response of an analog filter (system) with transfer function $G(s)$. The first method we will consider is called the **impulse invariant method**, whereby $H(z)$ is obtained with $Z(g(kT))$. The unit pulse response $h(k)$ of the resulting digital filter will be determined by the impulse response of the analog filter sampled at $t = kT$.

By the Poisson summation formula (eq. 9.2c) we have

$$\sum_{k=0}^{\infty} g(kT)e^{-j\omega kT} = \frac{1}{2}g(0^+) + \frac{1}{T}\sum_{m=-\infty}^{\infty} G(j(\omega - m\omega_s))$$

Now consider $Z(g(kT))$, which is given by

$$Z(g(kT)) = \sum_{k=0}^{\infty} g(kT)z^{-k}$$

and therefore

$$Z(g(kT))\,|_{z=e^{j\omega T}} = \frac{1}{2}g(0^+) + \frac{1}{T}\sum_{m=-\infty}^{\infty} G(j(\omega - m\omega_s))$$

Our goal is to find an $H(z)$ such that $H(e^{j\omega T})$ is comparable to $G(j\omega)$, and then $H(z)$ will exhibit frequency selective properties similar to those of $G(s)$. To achieve this goal, f_s must be large enough such that $G(s)$ can satisfy

$$G(j\omega)|_{|\omega| > \omega_s/2} \cong 0 \qquad \textbf{(10.93a)}$$

which is required to avoid aliasing error. Furthermore, by eq. 9.2c we also require that

$$g(0^+) = 0 = \lim_{s \to \infty} sG(s) \qquad \textbf{(10.93b)}$$

which means that the order of the numerator polynomial of $G(s)$ must be less than the order of the denominator polynomial by at least two. Therefore, the impulse invariant method is not useful for discretizing analog filters such as HP or BS filters.

If $G(s)$ satisfies eqs. 10.93, then by the Poisson summation formula we have

$$Z(g(kT))\,|_{z=e^{j\omega T}} \cong \frac{1}{T}G(j\omega)$$

for $|\omega| < \omega_s/2$, and to approximate $G(j\omega)$ we use

$$H(z) = TZ(g(kT)) \qquad \textbf{(10.94)}$$

If eqs. 10.93 are satisfied, then the impulse invariant design method produces an $H(z)$ that approximates both the magnitude and phaseshift characteristic of $G(s)$. Notice that $h(k) = Tg(k)$, and the digital filter unit pulse response follows samples of the analog filter impulse response.

Let us write $G(s) = P(s)/Q(s)$. If $G(s)$ has only simple poles, then its partial fraction expansion is given by

$$G(s) = \frac{P(s)}{Q(s)} = \sum_{i=1}^{n} \frac{K_i}{(s - p_i)}$$

where now the p_i, $i = 1, \cdots, n$, denote the n poles of $G(s)$, and $g(t)$ is given by

$$g(t) = \sum_{i=1}^{n} K_i e^{p_i t} u_{-1}(t)$$

Substituting the Z-transform of $g(kT)$ into eq. 10.94 results in

$$H(z) = T \sum_{i=1}^{n} \frac{K_i}{1 - e^{p_i T} z^{-1}} \tag{10.95}$$

In eq. 10.95 we see that the poles of $H(z)$ can be found through the relationship $z = e^{sT}$, which maps the LH s-plane onto the interior of the unit circle in the z-plane. Therefore, if $G(s)$ is stable, then $H(z)$ in eq. 10.94 will also be stable.

There is no restriction that $G(s)$ have only simple poles. If $G(s)$ has multiple poles, then we perform an appropriate partial fraction expansion and proceed as above to obtain an $H(z)$.

Example 10.18. Consider again the digital filter design problem of Example 10.12, where a signal, which is bandlimited to 200 Hz, is to be LP filtered by a digital filter with bandwidth $\omega_c = 160\pi$. With the impulse invariant design method ω_c is also used as the bandwidth of $G(s)$. In fact, all of the critical frequencies of $H(z)$ are used as the critical frequencies of $G(s)$ to meet transition band requirements. Let us try a Butterworth characteristic, and suppose that $n = 2$ is sufficient to meet some transition band requirement. Unnormalizing $G_N(p)$ given in eq. 10.50, which we now recognize to be a Butterworth filter, with $f(s) = s/\omega_c$ yields the desired $G(s)$, as given in eq. 10.73. Since the bandwidth of $G(s)$ is $f_c = 80$ Hz, then $f_s = 800$ Hz, as used in Example 10.12, should be large enough to incur only a small aliasing error with eq. 10.94. This will allow us to compare the $H(z)$ as found in Example 10.12 with the bilinear transformation to the $H(z)$ that we will obtain in this example.

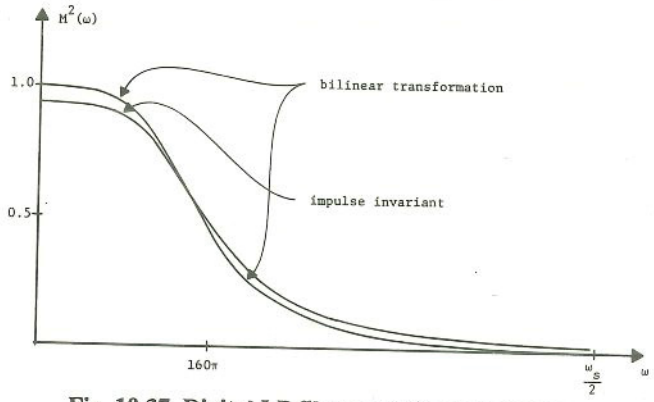


Fig. 10.37. Digital LP filter magnitude response.

By eq. 10.95, $H(z)$ turns out to be

$$H(z) = \frac{2\alpha e^{-\alpha} \sin(\alpha) z}{z^2 - 2e^{-\alpha}\cos(\alpha) z + e^{-2\alpha}} \tag{10.96}$$

where $\alpha = \omega_c T\sqrt{2}/2 = \pi\sqrt{2}/10$. The $M^2(\omega)$ of the $H(z)$ given in eqs. 10.75 and 10.96 are shown in Fig. 10.37 for $0 \le \omega < \omega_s/2$.

Notice that with the bilinear transformation $M^2(\omega_s/2) = M_G^2(\infty)$ and $M^2(0) = M_G^2(0)$, which will occur regardless of the value of T. However, if we decrease f_s, then with the impulse invariant method, $M^2(\omega_s/2)$ will increase due to aliasing error. With $f_s = 800$, both methods yield magnitude responses similar to $M_G^2(\omega)$. The final choice for an $H(z)$ will also depend on additional factors such as the phaseshift characteristic, and if necessary, how readily it can be corrected with an all-pass equalizer to approximate a linear phaseshift in the pass-band. Also, from an implementation viewpoint, the differing arithmetic and memory requirements necessary to run the difference equation corresponding to each $H(z)$ may play a deciding role.

10-3.7 Modified Impulse Invariant Method

Suppose we write $G(s)$ as

$$G(s) = \frac{P(s)}{Q(s)} = G_0 \frac{\prod_{i=1}^{m}(s - z_i)}{\prod_{i=1}^{n}(s - p_i)} \tag{10.97}$$

where G_0 is some constant, and the z_i, $i = 1, \cdots, m$ are the zeros of $G(s)$. If n is not significantly greater than m, then aliasing error will occur with the impulse invariant method. Instead, let us define the functions given by

$$G_1(s) = \frac{G_0}{\prod_{i=1}^{n}(s - p_i)}, \quad G_2(s) = \frac{1}{\prod_{i=1}^{m}(s - z_i)}$$

so that $G(s) = G_1(s)/G_2(s)$. Both $G_1(s)$ and $G_2(s)$ are all-pole functions. If m and n are greater than one, then $g_1(0^+) = 0$ and $g_2(0^+) = 0$. Now choose T such that

$$G_1(j\omega)|_{|\omega| > \omega_s/2} \cong 0, \quad G_2(j\omega)|_{|\omega| > \omega_s/2} \cong 0$$

and by the impulse invariant method obtain $H_1(z)$ and $H_2(z)$, i.e.

$$H_1(z) = TZ(g_1(kT)), \quad H_2(z) = TZ(g_2(kT))$$

Therefore, for $|\omega| < \omega_s/2$, $H_1(e^{j\omega T}) \cong G_1(j\omega)$, and $H_2(e^{j\omega T}) \cong G_2(j\omega)$. Finally, $H(z)$ is obtained with

$$H(z) = \frac{H_1(z)}{H_2(z)} = \frac{Z(g_1(kT))}{Z(g_2(kT))} \tag{10.98}$$

This technique is called the **modified impulse invariant method**, where both the poles and zeros of $G(s)$ are impulse invariant discretized. If $G(s)$ has any zeros in the RH s-plane, then $G_2(s)$ will not be stable. This problem can be avoided by first replacing the RH s-plane zeros $s = z_i$ of $G(s)$ by $s = -z_i$, which will not change $\|G(j\omega)\|$, and then proceed to obtain $H(z)$. The poles of $H(z)$ are due to the poles of $H_1(z)$, which come from the poles of $G(s)$, and the zeros of $H_2(z)$. If $H_2(z)$ has any zeros on or outside the unit circle in the z-plane, then $H(z)$ will not be stable. This problem can also be avoided by replacing the zeros of $H_2(z)$ that are outside the unit circle by their reciprocals, which, according to eq. 10.12, will not change the shape of $\|H(e^{j\omega T})\|$. Also, the magnitudes of any zeros on the unit circle can be slightly reduced. Finally, we expect that $M^2(\omega) \equiv M_G^2(\omega)$. However, the unit pulse response of $H(z)$ will not match $g(kT)$. Nevertheless, the major disadvantage of this method is that the order of $H(z)$ will be greater than the order of a filter obtained by some other method such as the bilinear transformation.

10-3.8 Unit Step Invariant Method

A design method that is similar to the impulse invariant method is called the **unit step invariant method**. By this technique we match the unit step response of the digital filter $H(z)$ to samples of the unit step response of the analog filter $G(s)$. Therefore, $H(z)$ is obtained with

$$\frac{H(z)}{1-z^{-1}} = Z\left(\left(L^{-1}\left(\frac{G(s)}{s}\right)\right)\Big|_{t=kT}\right) \tag{10.99}$$

which requires that $G(s)$ is a strictly proper function. By this design method we preserve the transient behavior of the analog filter.

Example 10.19. Suppose $G(s) = 1/(s+a)$, where $a > 0$. The unit step response $y(t)$ is given by

$$y(t) = L^{-1}\left(\frac{1}{s(s+a)}\right) = \frac{1}{a}(1-e^{-at})u_{-1}(t)$$

By eq. 10.99, the unit step invariant method yields

$$H(z) = (1-z^{-1})\left(\frac{1}{a}\left(\frac{1}{1-z^{-1}} - \frac{1}{1-z^{-1}e^{-aT}}\right)\right) = \frac{1}{a}(1-e^{-aT})\frac{1}{z-e^{-aT}}$$

Based on a state variable description of an analog system with transfer function $G(s)$, the unit step invariant method was developed in the time domain in Chapter Eight, and it was used to discretize an analog Butterworth LP filter in Example 8.20. Recall that in Chapter Eight we obtained this method by approximating the input with a piecewise constant function.

Due to aliasing error, this technique is not useful for discretizing BS and HP analog filters. However, because of the added factor $1/s$ in eq. 10.99, the aliasing error will be less than with the impulse invariant method.

10-3.9 Matched Z-Transform Method

A technique that simply attempts to match the peaks and troughs of $M_G^2(\omega)$ for $G(s)$ given in eq. 10.97 is called the **matched Z-transform method**. By transforming poles and zeros of $G(s)$ according to $z = e^{sT}$, $H(z)$ is obtained with

$$H(z) = (1+z^{-1})^{(n-m)} G_0 \frac{\prod_{i=1}^{m}(1-e^{z_i T}z^{-1})}{\prod_{i=1}^{n}(1-e^{p_i T}z^{-1})} \tag{10.100}$$

where, as usual, $m \le n$. The extra zeros at $z=-1$ are added to $H(z)$ for the following reason. The frequency response $G(j\omega)$ is obtained as ω varies from $\omega=0$ to $\omega=\infty$, and for large ω, $G(j\omega)$ behaves as $G_0/(j\omega)^{n-m}$. If $n > m$, then $G(j\infty)=0$. For a digital filter $H(z)$, the frequency response $H(e^{j\omega T})$ is obtained as ω varies from $\omega=0$, i.e., $z=1$, to $\omega=\omega_f=\omega_s/2=\pi/T$, i.e., $z=e^{j\omega_f T}=-1$. To force a correspondence between the high frequency behavior of $G(j\omega)$ as $\omega\to\infty$ and $H(e^{j\omega T})$ as $\omega\to\omega_f$, the extra zeros are added to $H(z)$. This method is useful for discretizing any type of analog filter. However, it does not preserve detailed characteristics of $G(s)$.

10-3.10 Design Summary

Each of the discretization methods we have considered has its own advantages and disadvantages. Often, designing a digital filter requires a considerable amount of guess and try numerical experimentation to arrive at an acceptable $H(z)$. However, because of its simplicity and wide applicability, the bilinear transformation is most commonly used to obtain a digital filter based on an analog prototype. Let us summarize the steps involved in determining a digital filter transfer function $H(z)$. We start with a specification of constraints on the digital filter frequency response, and then:

(1) convert these constraints to those of an analog prototype. This will require prewarping the critical frequencies as with a bilinear transformation, i.e., eq. 10.68,

(2) normalize the analog prototype critical frequencies to those of a normalized analog LP filter,

(3) select an LP filter characteristic, if a characteristic has not already been specified, and determine parameter values such that $G_N(p)$ satisfies specifications,

(4) unnormalize $G_N(p)$ through a frequency transformation to obtain $G(s)$,

(5) select a discretization method, if a method has not already been selected, and obtain $H(z)$ from $G(s)$, and

(6) evaluate the frequency and transient response of the resulting $H(z)$, and if necessary repeat steps (1) through (5).

With the above procedure we will be successful in designing a recursive digital filter that meets magnitude frequency response requirements. Although the extent to which the phaseshift is not linear varies from one LP filter characteristic to the next, we have no direct control over the resulting phaseshift. A further possibility is to use a normalized analog LP filter prototype that already approximates a linear phaseshift characteristic such as the **Bessel filter**, which has a maximally flat group delay characteristic. For this, the reader is referred to the literature on analog filter design. If a nearly constant pass-band group delay is necessary, then a phase equalizer such as the all-pass function given in eq. 10.15a can be used. The problem is that, other than guess and try procedures, there are no relatively straightforward methods for determining the equalizer pole locations to achieve an overall nearly constant group delay.

10-3.11 Phase Equalization

We will now develop a, albeit, computer intensive procedure for phaseshift equalizer design. For this, we shall continue with the equalizer design discussion that was initiated in Example 10.3.

Example 10.20. Assume that we have designed a digital filter such as the BP filter of Example 10.2, which we now denote by $H_1(z)$, i.e.

$$H_1(z) = \frac{\frac{1}{2}\gamma z}{(z - \gamma e^{j\omega_0 T})(z - \gamma e^{-j\omega_0 T})}$$

where $\gamma = 0.95$, $\omega_0 = 4\pi/3$, and $T = 1/8$. The cut-off frequencies are $\omega_1 = 3.75$ and $\omega_2 = 4.55$. The group delay $\tau_1(\omega)$ is given in Example 10.3, and it is repeated here for convenience, i.e.

$$\tau_1(\omega) = T\left(1 - \frac{\gamma^2 - \gamma\cos((\omega - \omega_0)T)}{1 + \gamma^2 - 2\gamma\cos((\omega - \omega_0)T)} - \frac{\gamma^2 - \gamma\cos((\omega + \omega_0)T)}{1 + \gamma^2 - 2\gamma\cos((\omega + \omega_0)T)}\right)$$

We shall arbitrarily try two all-pass functions as given in eq. 10.15a, so that $H_{EQ}(z)$ has the form

$$H_{EQ}(z) = \prod_{i=1}^{2} \frac{(1 - p_i z)(1 - p_i^* z)}{(z - p_i^*)(z - p_i)}$$

The overall transfer function will be $H_2(z) = H_1(z)H_{EQ}(z)$, and $\tau_2(\omega) = \tau_1(\omega) + \tau_{EQ}(\omega)$. We expect to achieve an equalizer design as is illustrated in Fig. 10.6d.

The equalizer design procedure is based on finding the p_1 and p_2 that minimize the square of the difference between $\tau_2(\omega)$ and some constant group delay τ_0, i.e.

$$e^2(\omega, p_1, p_2) = (\tau_2(\omega) - \tau_0)^2 = (\tau_1(\omega) - (\tau_0 - \tau_{EQ}(\omega)))^2$$

over some frequency range. Here, $\tau_1(\omega)$ is given, and τ_0, p_1, and p_2 must be found. We could also specify τ_0, but we shall leave it as a variable, the value of which is to be determined by minimizing

e^2. The phaseshift equalizer can only add to the group delay of $H_1(z)$. We shall think of e^2 as a function of one independent variable, i.e., ω, and five parameters, i.e., τ_0, α_1, β_1, α_2, and β_2, where $p_1 = \alpha_1 e^{j\beta_1}$ and $p_2 = \alpha_2 e^{j\beta_2}$.

Minimizing e^2 is a formidable task, and an inspection of Fig. 10.6d reveals that we should approximate a linear phaseshift characteristic over a restricted frequency range that extends from about $\omega = \omega_3$ to about $\omega = \omega_4$. Practically, phase distortion in the stop-band is not an issue. Therefore, let us select I frequency points within this range at which we shall minimize e^2, and minimize the sum of the errors squared, i.e.

$$e^2(p_1, p_2) = \sum_{i=1}^{I} w_i(\tau_1(x_i) - (\tau_0 - \tau_{EQ}(x_i)))^2 \tag{10.101}$$

where the x_i, $i = 1, \cdots, I$, are the frequency points, and the w_i are positive numbers called **weights**, which allow us to attribute more significance to minimizing e^2 at some frequency points than at others. If it is equally important to minimize e^2 at every point, then we set $w_i = 1.0$, $i = 1, \cdots, I$. $\tau_1(x_i)$ is known at every frequency point $\omega = x_i$, and it is the data to which we must fit the function $f(x_i, \tau_0, p_1, p_2) = (\tau_0 - \tau_{EQ}(x_i, p_1, p_2))$.

Let the array P denote the parameter set $(\tau_0, \alpha_1, \beta_1, \alpha_2, \beta_2)$, where $P(1) = \tau_0$, $P(2) = \alpha_1$, etc., and write the function f as $f(x_i, P)$. Now, we have cast the equalizer design problem into that of fitting a function to data by minimizing the sum of the errors squared, which is given by

$$e^2(P) = \sum_{i=1}^{I} w_i(\tau_1(x_i) - f(x_i, P))^2 \tag{10.102}$$

Numerous methods have been developed for minimizing functions. Most minimization methods require either analytically defined or numerically computed partial derivatives of the function to be minimized with respect to each of the variables, which in our problem is the parameter set P. We shall employ a method that does not require partial derivatives. There is no function minimization method that is guaranteed to find the global minimum of a function as opposed to finding some local minimum of the function (See Fig. 10.38.), unless the function has only one local minimum, which is then the global minimum. Therefore, we must provide an initial guess for P that is in the vicinity of that $P = P_{min}$, where e^2 takes on its global minimum value.

A good initial guess requires some knowledge of the problem at hand. A function minimization method is then expected to adjust the initial guess to a value for which e^2 takes on a local minimum value, which may also be the global minimum. In Appendix E is a subroutine that performs this task. The function minimization method that is implemented by this subroutine is called the **simplex algorithm**. For a detailed description of this algorithm the reader is referred to the literature that is cited at the end of Appendix E.

To use the subroutine given in Appendix E, we must provide a main program that calls this subroutine, and we must provide the data $\tau_1(x_i)$ and x_i, $i = 1, \cdots, I$, an initial guess for P, and a subroutine that evaluates the function e^2, which is to be minimized.

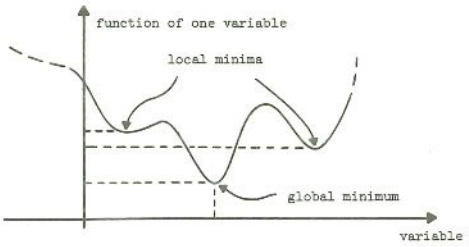


Fig. 10.38. A function with several minima.

To be more specific, let us try $I = 21$ frequency points, which are given by

$$x_i = \omega_3 + (\omega_4 - \omega_3)\frac{i-1}{I-1}$$

so that $x_1 = \omega_3$ and $x_{21} = \omega_4$. We will use a computer to calculate the data $\tau_1(x_i)$. For the initial guess of P, let $P(1) = 2.4$ secs., which is the peak value of $\tau_1(\omega)$ (See Fig. 10.6c.), $P(3) = \omega_3 T$, $P(5) = \omega_4 T$, which initially places the equalizer peaks at ω_3 and ω_4, respectively (See eq. 10.15b.), and $P(2) = P(4) = \gamma$ so that the extent of the equalizer peaks are the same as that of $\tau_1(\omega)$. Fig. 10.39 shows the main program and all necessary support subprograms to apply subroutine MINMUM given in Appendix E.

```
C       THIS IS THE MAIN PROGRAM FOR FINDING THE PARAMETERS
C       OF A PHASE EQUALIZER.
        IMPLICIT REAL*8 (A-H,O-Z)
        REAL*8 NAME
        REAL*4 GDELAY(1024),FREQ(1024)
        LOGICAL OUTPUT
        EXTERNAL ERSQR
        DIMENSION X(100,5),WGT(100),Y(100),GUESS(20),P(20)
        COMMON /POINTS/X,NVAR/VALUES/WGT,Y,NPTS
        DATA NAME/'-ERSQR--'/
        CALL DAT
        CALL INIT(GUESS)
        DO 1 I=1,20
    1   P(I)=GUESS(I)
        OUTPUT=.FALSE.
        CALL MINMUM(ERSQR,F,P,NAME,OUTPUT)
C       PLOTTING THE OVERALL GROUP DELAY
        PI=3.1415926
        T=1./8.
        WF=PI/T
        GAMMA=.95
        W0=4.*PI/3.
        N=256
        DW=WF/N
        DO 2 I=1,N
        W=(I-1)*DW
```

```
      FREQ(I)=W
    2 GDELAY(I)=TAU1(W,GAMMA,W0,T)+TAUEQ(W,P(2),P(3),T)+
    1 TAUEQ(W,P(4),P(5),T)
      CALL PLOT('------GROUP-DELAY-------',N,
    1 GDELAY,'--SECS.-',FREQ,'-RAD/SEC')
      STOP
      END

      SUBROUTINE DAT
C     THIS SUBROUTINE PROVIDES THE POINTS AND DATA.
C     UP TO NPTS=100 DATA POINTS CAN BE SPECIFIED.
C     THE DATA AND FUNCTION CAN DEPEND ON UP TO
C     NVAR=5 INDEPENDENT VARIABLES.
      IMPLICIT REAL*8 (A-H,O-Z)
      DIMENSION X(100,5),WGT(100),Y(100)
      COMMON /POINTS/X,NVAR/VALUES/WGT,Y,NPTS
C     SPECIFYING THE NUMBER OF INDEPENDENT VARIABLES
      NVAR=1
C     SPECIFYING H1(Z) PARAMETERS
      PI=3.1415926
      W1=3.75
      W2=4.55
      W3=2.7
      W4=5.3
      GAMMA=.95
      W0=4.*PI/3.
      T=1./8.
C     SPECIFYING THE NUMBER OF DATA POINTS
      NPTS=21
C     PROVIDING THE DATA AND WEIGHTS
      DO 1 I=1,NPTS
      X(I,1)=W3+(W4-W3)*(I-1)/(NPTS-1)
      W=X(I,1)
      WGT(I)=I**2
      IF(I.GT.(NPTS+1)/2) WGT(I)=(NPTS+1-I)**2
    1 Y(I)=TAU1(W,GAMMA,W0,T)
      WRITE(6,901)
      WRITE(6,902) (I,I=1,NVAR)
      DO 2 I=1,NPTS
    2 WRITE(6,903) WGT(I),Y(I),(X(I,J),J=1,NVAR)
      RETURN
  901 FORMAT(2X,'WEIGHTS',4X,'DATA',8X,'INDEPENDENT',
    1 1X,'VARIABLE(S)')
  902 FORMAT(24X,5(I3,9X))
  903 FORMAT(1X,7(1PD10.3,2X))
      END

      FUNCTION TAU1(W,GAMMA,W0,T)
      IMPLICIT REAL*8 (A-H,O-Z)
      C1=GAMMA*DCOS((W-W0)*T)
      C2=GAMMA*DCOS((W+W0)*T)
      C3=GAMMA**2
      C4=(C3-C1)/(1.+C3-2.*C1)
      C5=(C3-C2)/(1.+C3-2.*C2)
```

```
      TAU1=T*(1.-C4-C5)
      RETURN
      END

      SUBROUTINE INIT(GUESS)
C     THIS SUBROUTINE PROVIDES THE INITIAL GUESS FOR
C     THE PARAMETERS.
      IMPLICIT REAL*8 (A-H,O-Z)
      DIMENSION GUESS(20)
      GUESS(1)=2.4
      GAMMA=.95
      W3=2.71
      W4=5.29
      T=1./8.
      GUESS(3)=W3*T
      GUESS(5)=W4*T
      GUESS(2)=GAMMA
      GUESS(4)=GAMMA
      RETURN
      END

      SUBROUTINE ERSQR(F,PARMS,NPARMS)
C     THIS SUBROUTINE COMPUTES THE SUM OF
C     THE WEIGHTED ERRORS SQUARED.
      IMPLICIT REAL*8 (A-H,O-Z)
      DIMENSION WGT(100),Y(100),PARMS(20)
      COMMON /VALUES/WGT,Y,NPTS
      F=0.0
      DO 1 I=1,NPTS
    1 F=F+WGT(I)*(Y(I)-FUNK(PARMS,I,NPARMS))**2
      RETURN
      END

      FUNCTION FUNK(PARMS,I,NPARMS)
C     THIS FUNCTION SUBPROGRAM EVALUATES THE USER SPECIFIED
C     FUNCTION TO BE FITTED TO DATA. THE FUNCTION CAN DEPEND
C     ON UP TO NVAR=5 INDEPENDENT VARIABLES, AND UP TO
C     NPARMS=20 PARAMETERS.
      IMPLICIT REAL*8 (A-H,O-Z)
      DIMENSION PARMS(20),X(100,5)
      COMMON /POINT/X,NVAR
      DATA DELTA/1.D-06/
C     SPECIFYING THE NUMBER OF PARAMETERS
      NPARMS=5
C     LIMITING THE PARAMETER RANGE
      IF(PARMS(1).LE.0.0) PARMS(1)=DELTA
      IF(PARMS(2).LE.0.0) PARMS(2)=DELTA
      IF(PARMS(2).GE.1.0) PARMS(2)=1.0-DELTA
      IF(PARMS(4).LE.0.0) PARMS(4)=DELTA
      IF(PARMS(4).GE.1.0) PARMS(4)=1.0-DELTA
C     EVALUATING THE FUNCTION IN TERMS OF THE PARAMETERS
C     AND THE INDEPENDENT DATA POINTS
```

```
      W=X(I,1)
      T=1./8.
      FUNK=PARMS(1)-TAUEQ(W,PARMS(2),PARMS(3),T)-
     1 TAUEQ(W,PARMS(4),PARMS(5),T)
      RETURN
      END
      FUNCTION TAUEQ(W,A,B,T)
C     EVALUATES EQ. 10.15B
      IMPLICIT REAL*8 (A-H,O-Z)
      C1=A*DCOS(W*T-B)
      C2=A*DCOS(W*T+B)
      C3=A**2
      C4=(C3-C1)/(1.+C3-2.*C1)
      C5=(C3-C2)/(1.+C3-2.*C2)
      TAUEQ=2.*T*(1.-C4-C5)
      RETURN
      END
```

Fig. 10.39. Program listing for equalizer design.

Referring to Fig. 10.39, subroutine DAT provides the data, subroutine INIT provides the initial guess, subroutine function TAU1 evaluates $\tau_1(\omega)$, and subroutine function FUNK evaluates $f(x_i, P)$. The output of the program is shown in Fig. 10.40, from which we get $\alpha_1 = 0.9315$, $\beta_1 = 0.4074$, $\alpha_2 = 0.9327$, and $\beta_2 = 0.6397$.

WEIGHTS	DATA	INDEPENDENT VARIABLE(S) 1
1.000D+00	1.818D-01	2.700D+00
4.000D+00	2.131D-01	2.830D+00
9.000D+00	2.536D-01	2.960D+00
1.600D+01	3.071D-01	3.090D+00
2.500D+01	3.792D-01	3.220D+00
3.600D+01	4.789D-01	3.350D+00
4.900D+01	6.198D-01	3.480D+00
6.400D+01	8.230D-01	3.610D+00
8.100D+01	1.117D+00	3.740D+00
1.000D+02	1.527D+00	3.870D+00
1.210D+02	2.018D+00	4.000D+00
1.000D+02	2.395D+00	4.130D+00
8.100D+01	2.373D+00	4.260D+00
6.400D+01	1.971D+00	4.390D+00
4.900D+01	1.482D+00	4.520D+00
3.600D+01	1.083D+00	4.650D+00
2.500D+01	7.985D-01	4.780D+00
1.600D+01	6.020D-01	4.910D+00
9.000D+00	4.655D-01	5.040D+00
4.000D+00	3.686D-01	5.170D+00
1.000D+00	2.981D-01	5.300D+00

STARTING THE MINIMIZING PROCEDURE FOR THE FUNCTION **ERSQR** OF 5 VARIABLES

INTERATION	FUNCTION VALUE	VARIABLES 1	2	3	4	5
0	4.320D+02	2.400D+00	9.500D-01	3.388D-01	9.500D-01	6.612D-01
CONVERGED						
402	6.071D+01	4.011D+00	9.315D-01	4.074D-01	9.327D-01	6.397D-01

Fig. 10.40. Equalizer design program output.

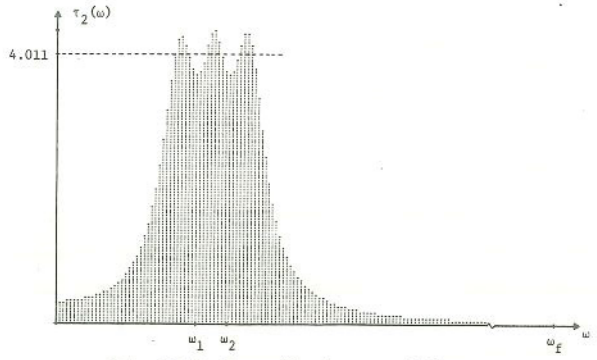


Fig. 10.41. Equalized group delay.

With these equalizer poles, the overall group delay $\tau_2(\omega)$ is shown in Fig. 10.41, where we see that within the pass-band of $H_1(z)$, the group delay of $H_1(z)$ has been corrected to remain within $\pm 10\%$ of $\tau_0 = 4.011$ secs. It is very likely that with more frequency points and additional all-pass sections we can achieve an even better phase equalizer. This will require further numerical experimentation.

SECTION 10-4 Summary

We have considered the design of two types of digital filters. These are the recursive form as in eq. 10.1, and the nonrecursive or convolutional form as in eq. 10.2. We started our study of digital filter design techniques by first showing that to achieve a real LTI digital filter, $M(\omega)$ and $\phi(\omega)$ in $H(e^{j\omega T}) = M(\omega)e^{j\phi(\omega)}$ must be even and odd, respectively, real periodic functions of frequency. Then we described the ideal frequency response of standard filter types, i.e., LP, BP, HP, and BS filters, and showed that an ideal filter must have a linear phaseshift characteristic or constant group delay. We also showed that an ideal magnitude characteristic cannot be achieved with a causal and finite duration unit pulse response filter. Since in general, we cannot expect to achieve an ideal response characteristic, digital filter design becomes an approximation problem given specifications on allowed maximum deviations away from an ideal characteristic. Typically, such specifications are imposed on the magnitude frequency response, and we showed that the settling time of a filter is inversely proportional to its bandwidth. While we can approximate an ideal magnitude frequency response as closely as we like, we cannot in general also achieve a linear phaseshift characteristic.

A linear phaseshift characteristic can be obtained with a nonrecursive form if the unit pulse response satisfies certain symmetry conditions. Such symmetry conditions were incorporated into two FIR filter design methods. The first method we considered is called the Fourier series method, which approximates a desired continuous frequency response with a Fourier series to eventually yield the finite duration unit pulse response of the filter. The second method we considered is called the frequency sampling method, which yields a filter with a frequency response that passes through samples of a desired frequency response. However, the computational requirements of running a nonrecursive form are greater than those of a comparable (in the magnitude response) recursive form.

Several recursive digital filter design methods were developed and compared. All of these methods are based on discretizing an analog prototype transfer function, and basically, they fall into two categories. The first category consists of methods for numerically approximating a continuous time system with an LTI difference equation. Among these methods, we considered the first order forward and backward difference approximations and the bilinear transformation. There are numerous other numerical approximation methods. However, because of its simplicity and suitable properties, the bilinear transformation is commonly used. The second category consists of methods whereby we obtain an $H(z)$ such that $H(e^{j\omega T})$ matches as closely as possible $G(j\omega)$. Of course, the methods in the first category also have this goal. However, methods such as the impulse and unit step invariant methods, modified impulse invariant method, and matched Z-transform method are more direct in attempting to match the frequency response of the analog prototype.

It is convenient to require only a few tables of precomputed normalized analog LP function coefficients to arrive at a variety of other analog prototypes. For this, normalized LP to LP, BP, HP, and BS frequency transformations were used. An alternative would be to discretize a normalized analog LP function, and then employ digital filter frequency transformations to obtain a final $H(z)$ (See Problems 10.33 and 10.34.).

In the next chapter, we will utilize four distinctly different microprocessors to implement a digital filter. This will require knowledge of digital system hardware design and programming in addition to an understanding of the intended application in order to select an appropriate microprocessor and develop a digital signal processing system.

REFERENCES

Digital Signal Processing

(1) Antoniou, A., *Digital Filters: Analysis and Design*, McGraw-Hill, New York, N.Y., 1979.

(2) Beauchamp, K. and Yuen C., *Digital Methods For Signal Analysis*, George Allen & Unwin, London, U.K., 1979.

(3) Bogner, R.E. and Constantinides, A.G., (eds.), *Introduction to Digital Filtering*, Wiley, New York, N.Y., 1975.

(4) Candy, J.V., *Signal Processing: The Modern Approach*, McGraw-Hill, New York, N.Y., 1988.

(5) Cappellini, V., Constantinides, A.G., and Emiliani, P., *Digital Filters and Their Applications*, Academic Press, London, U.K., 1978.

(6) Chen, C.T., *One-Dimensional Digital Signal Processing*, Marcel Dekker, Inc., New York, N.Y., 1979.

(7) Childers, D. and Durling, A., *Digital Filtering and Signal Processing*, West Pub., St. Paul, Minn., 1975.

(8) DeFatta, D.J., Lucas, J.G., and Hodgkiss, W.S., *Digital Signal Processing: A System Design Approach*, Wiley, New York, N.Y., 1988.

(9) Gold, B. and Rader, C.M., *Digital Processing of Signals*, McGraw-Hill, New York, N.Y., 1969.

(10) Hamming, R.W., *Digital Filters*, Prentice-Hall, Englewood Cliffs, N.J., 1977.

(11) Helms, H.D., Kaiser, J.F., and Rabiner, L.R. (eds.), *Literature in Digital Signal Processing*, IEEE Press, New York, N.Y., 1975.

(12) IEEE Proc., *Special Issue on Digital Signal Processing*, vol. 63, no. 4, 1975.

(13) IEEE Trans., Acoustics, Speech, and Signal Processing, *Special Issue on Digital Signal Processing*, vol. ASSP-23, no.3, 1975.

(14) Jackson, L.B., *Digital Filters and Signal Processing*, Kluwer Academic Pub., Boston, Mass., 1989.

(15) Jones, N.B. (ed.), *Digital Signal Processing*, Peter Peregrinus Ltd., U.K., 1982.

(16) Jong, M.T., "A FORTRAN Program For Designing Elliptic Digital Filters," in *Methods of Discrete Signal and System Analysis*, McGraw-Hill, New York, N.Y., 1982.

(17) Johnson, J.R., *Introduction To Digital Signal Processing*, Prentice-Hall, Englewood Cliffs, N.J., 1989.

(18) Kuc, R., *Introduction To Digital Signal Processing*, McGraw-Hill, New York, N.Y., 1988.

(19) Ludeman, L.C., *Fundamentals of Digital Signal Processing*, Harper & Row, New York, N.Y., 1986.

(20) Lam, H., *Analog and Digital Filters: Design and Realization*, Prentice-Hall, Englewood Cliffs, N.J., 1979.

(21) McClellan, J.H., Parks, T.W., and Rabiner, L.R., "A Computer Program for Designing Optimum FIR Linear Phase Digital Filters," IEEE Trans. in Audio and Electroacoustics, vol. AU-21, no. 6, pp. 506-526, Dec., 1973.

(22) Oppenheim, A.V. and Schafer, R.W., *Digital Signal Processing*, Prentice-Hall, Englewood Cliffs, N.J., 1975.

(23) Oppenheim, A.V. and Schafer, R.W., *Discrete-Time Signal Processing*, Prentice-Hall, Englewood Cliffs, N.J., 1989.

(24) Oppenheim, A.V. (ed.), *Applications of Digital Signal Processing*, Prentice-Hall, Englewood Cliffs, N.J., 1978.

(25) Proakis, J.G. and Manolakis, D.G., *Introduction To Digital Signal Processing*, Macmillan, New York, N.Y., 1988.

(26) Rabiner, L.R. and Gold, B., *Theory and Application of Digital Signal Processing*, Prentice-Hall, Englewood Cliffs, N.J., 1975.

(27) Rabiner, L.R., and Rader, C.M. (eds.), *Digital Signal Processing*, IEEE Press, New York, N.Y., 1972.

(28) Roberts, R.A. and Mullis, C.T., *Digital Signal Processing*, Addison-Wesley, Reading, Mass., 1987.

(29) Stanley, W.D., Dougherty, G.R., and Dougherty, R., *Digital Signal Processing*, Reston, Reston, Va., 1984.

(30) Stearns, S.D., *Digital Signal Analysis*, Hayden, Rochelle Park, N.J., 1975.

(31) Strum, R.D. and Kirk, D.E., *First Principles of Discrete Systems and Digital Signal Processing*, Addison-Wesley, Reading, Mass., 1988.

(32) Terrell, T.J., *Introduction to Digital Filters*, Wiley, New York, N.Y., 1980.

(33) Tretter, S.A., *Introduction to Discrete-Time Signal Processing*, Wiley, New York, N.Y., 1976.

(34) Williams, C.S., *Designing Digital Filters*, Prentice-Hall, Englewood Cliffs, N.J., 1986.

Analog Filter Design

(35) Balabanian, N., *Network Synthesis*, Prentice-Hall, Englewood Cliffs, N.J., 1958.

(36) Budak, A., *Passive and Active Network Analysis and Synthesis*, Houghton Mifflin, Boston, Mass., 1974.

(37) Van Valkenburg, M.E., *Introduction to Modern Network Synthesis*, Wiley, New York, N.Y., 1967.

(38) Weinberg, L., *Network Analysis and Synthesis*, McGraw-Hill, New York, N.Y., 1962.

PROBLEMS

10.1 For a discrete time system with transfer function

$$H(z)=\frac{1-z^{-2}}{1+0.64z^{-2}}$$

obtain $M^2(\omega)$ (Use eq. 10.10.), $\phi(\omega)$, and $\tau(\omega)$. Verify that the real and imaginary parts of $H(e^{j\omega T})$ are even and odd, respectively, periodic functions.

10.2 For an all-pass digital filter with a transfer function as given in eq. 10.15a, verify that $M^2(\omega)=1$.

10.3 Consider the averaging algorithm given by

$$y(k)=\frac{1}{N}\sum_{i=0}^{N-1}x(k-i)$$

Obtain $H(z)$, and expressions for $M^2(\omega)$ and $\tau(\omega)$. For $f_s=10$ Hz and $N=3$ and 4, sketch $M^2(\omega)$ and $\phi(\omega)$ for $\omega=0$ to ω_s.

10.4 By a procedure similar to that used to obtain the unit pulse response of an ideal BP filter as given in eq. 10.17, obtain the unit pulse response $h_{HP}(k)$ of an ideal HP filter. Sketch $h_{HP}(k)$.

10.5 Consider the block diagram shown in Fig. P10.5, where a digital filter is used to obtain another one. If $H(z)$ is an ideal LP filter with BW $=\omega_c$, then sketch the magnitude frequency response of $Y(z)/U(z)$. What kind of filter has been achieved, and is it also an ideal filter?

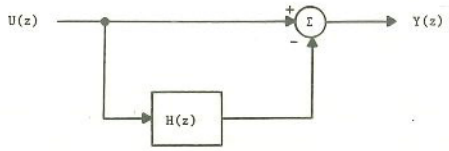


Fig. P10.5. Filter derived from another filter.

10.6 A BP filter can be achieved by cascading an LP filter and an HP filter. Assume we have ideal filters with nonzero group delays. The BP filter cut-off frequencies are to be ω_1 and ω_2. Specify the characteristics of the LP and HP filters to obtain a BP filter, and show the cascade connection. What will be the group delay of the BP filter?

10.7 Suppose that a discrete time signal $u(k)$ is represented by a finite number of points, which have been recorded, i.e., stored in computer memory. Now off-line processing is possible with a digital filter $H(z)$ to obtain $N+1$ points for the output $v(k)$ as shown in Fig. P10.7a.

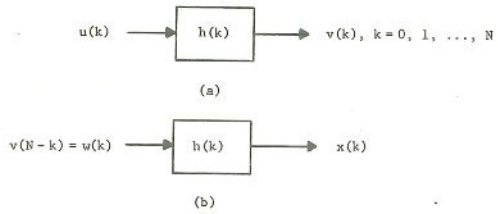


Fig. P10.7. Zero phaseshift filter.

Suppose N is large enough so that we have a good representation for $v(k)$. Now define $w(k)$ to be the time reversed $v(k)$, i.e., $w(k) = v(N-k)$, $k = 0, 1, \cdots, N$, and let $x(k)$ be the response of the filter $H(z)$ to $w(k)$ as shown in Fig. P10.7b. If the final output is $y(k)$, which is $x(k)$ time reversed, then show that the phaseshift from $u(k)$ to $y(k)$ is zero. Also, find $Y(z)/U(z)$ in terms of $H(z)$. If $H(z)$ has an ideal BP filter magnitude frequency response with cut-off frequencies at ω_1 and ω_2 and arbitrary phaseshift characteristic, then what filtering activity is achieved as we go from $u(k)$ to $y(k)$?

10.8 Two digital filters have transfer functions given by

$$H_1(z) = \frac{1+2z^{-1}}{1-.8z^{-1}}, \quad H_2(z) = \frac{2+z^{-1}}{1-.8z^{-1}}$$

For each filter obtain and sketch the magnitude squared frequency response for $\omega = 0$ to ω_s. Now obtain and sketch the unit step response of each filter. What, if any, is the basis for the difference in their transient responses? Are the phaseshift characteristics the same?

10.9 Some digital filter design procedure has yielded the following transfer function.

$$H(z) = \frac{1+z^{-1}+1.25z^{-2}}{1-2.2z^{-1}+1.22z^{-2}}$$

Is this filter stable? If not, then obtain a stable digital filter transfer function with the same magnitude frequency response as that of $H(z)$.

10.10 The unit pulse response of a digital filter is given by

$$h(kT) = (\gamma)^k \sin\left(\frac{\pi}{4}kT\right) u_{-1}(kT)$$

If $T = 1$ sec., then what is the settling time of the filter for $\gamma = 0.5$ and 0.9? Sketch a pole-zero plot for each value of γ.

10.11 Suppose that the unit pulse response $h(k)$ of an LTI discrete time system is greater than or equal to zero for all k. Explain why the unit step response of this system cannot exhibit any oscillatory behavior. Hint: consider eq. 10.18.

10.12 It takes a computer $\tau = 0.4$ msecs. to process each input sample by a particular digital filter algorithm. An amount of 0.1 msecs. is required to perform a sample and hold and A/D conversion. Can this system perform real-time processing of signals bandlimited to 1250 Hz? If it can, then obtain a flowchart similar to Fig. 10.14, which describes the sequence of events. If it cannot, then what is the input bandwidth limit? And, obtain an appropriate flowchart. Hint: consider the situation where the 0.1 msecs. duration tasks take place while the computer is executing the algorithm. Now suppose τ has been reduced to $\tau = 0.04$ msecs. What is the resulting input bandwidth restriction? If necessary, obtain a revised flowchart.

10.13 A signal is bandlimited to 500 Hz. Use the Fourier series design method to approximate the ideal magnitude characteristic shown in Fig. P10.13a, and obtain a linear phaseshift and causal FIR LP filter with $f_c \doteq 250$ Hz.

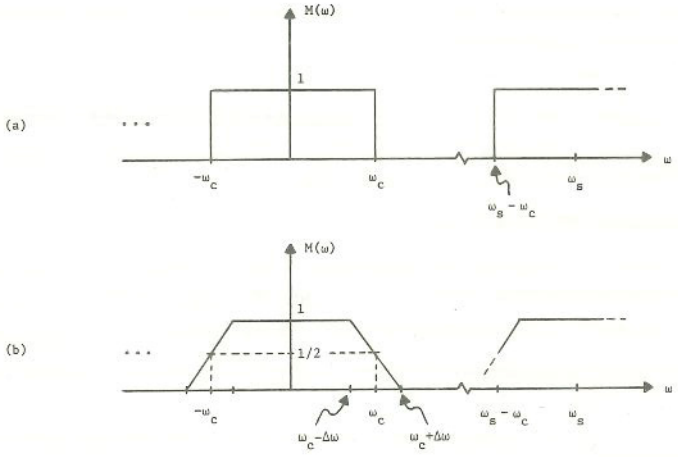


Fig. P10.13. LP filter characteristic.

Assume $f_s = 1000$ Hz, and truncate the series with $K = 5$. Will the resulting filter phaseshift characteristic be linear in the stop-band?

10.14 Repeat Problem 10.13 with $f_s = 2000$ Hz.

10.15 Repeat Problem 10.14, but use the characteristic shown in Fig. 10.13b with $\Delta\omega = 100\pi$ rad/sec. How does the addition of a transition band affect Gibbs' oscillation?

10.16 A signal is bandlimited to 500 Hz. By the Fourier series design method, design a constant group delay and causal FIR filter that approximates

$$H_d(e^{j\omega T}) = \begin{cases} j\omega, & 0 \le \omega < 500\pi \\ 0, & 500\pi < \omega < \omega_s - 500\pi \end{cases}$$

Assume $f_s = 2000$ Hz, and truncate the series with $K = 5$. Sketch the resulting $h(k)$ and magnitude frequency response.

10.17 For $f_s = 2000$ Hz, use the Fourier series design method to obtain a linear phaseshift and causal FIR filter, which approximates an ideal BP filter with lower and upper cut-off frequencies at $f_1 = 250$ Hz and $f_2 = 500$ Hz, respectively. Use $K = 10$. For this resulting filter, what will the cut-off frequencies be if f_s is changed to $f_s = 4000$ Hz? Finally, obtain a direct form simulation diagram, which uses the least number of multipliers.

10.18 Repeat Problem 10.13, and use the Hann window to reduce Gibbs' oscillation.

10.19 Repeat Problem 10.13, and use the Bartlett window. Does the resulting filter magnitude characteristic exhibit any Gibbs' oscillation?

10.20 The zeros of an FIR filter are: $-1, +1, 0.75 \pm j0.25$, and $1.2 \pm j0.4$. Does this filter have a linear phaseshift characteristic?

10.21 Verify eqs. 10.44 and 10.47.

10.22 For the frequency sampling FIR filter design method, specify $M_d(n)$ and $\phi_d(n)$ for the LP filter described in Problem 10.13. Use $N = 5$. Obtain a simulation diagram based on eqs. 10.43. Sketch the resulting $M(\omega)$ for $\omega = 0$ to ω_s.

10.23 Repeat Problem 10.22 for $N = 6$.

10.24 For the frequency sampling FIR filter design method, specify $M_d(n)$ and $\phi_d(n)$ for the LP filter described in Problem 10.15. Use $N = 64$. Specify any additional parameters so that a power of two FFT algorithm can be used to obtain $h(k)$.

10.25 If $h(k)$ is to be antisymmetrical about $t = (N-1)T/2$, then, for N even or odd, give an expression for $\phi_d(n)$, as in eqs. 10.45 for a symmetrical $h(k)$. Can the specification for $M_d(n)$ be the same as for the symmetrical case? Can an LP FIR filter be realized with an antisymmetrical $h(k)$?

10.26 With the frequency sampling method, repeat Problem 10.16.

10.27 Assume a signal $u(k)$ has a time varying spectrum $U_k(n)$. Suppose the contribution of only one frequency component to the signal is of interest, i.e., $n = i$ or $\omega_i = 2\pi i/T_0$. At any time k, the spectrum at ω_i is to be computed using the samples $x(k), x(k-1), \cdots, x(k-(N-1))$. Design an FIR discrete time system, the output of which is $y(k) = U_k(i)$. Hint: take the Z-transform of the DFT of the N points $x(k-l)$, $l = 0, \cdots, (N-1)$. Draw a block diagram of the resulting FIR system.

10.28 Consider discretizing a continuous time system with transfer function $G(s) = 10/(s+10)$ by the forward difference approximation. What is the maximum value for T so that the resulting digital filter $H(z)$ will be stable? Sketch the resulting $M^2(\omega)$ for $T = 0.05$ and 0.1, and compare this to $M_G^2(\Omega)$.

10.29 A time function is bandlimited to 20 Hz. Design a recursive digital LP filter with BW = 5 Hz, such that the gain is down at least 20 dB at 10 Hz. Use the bilinear transformation method on a Butterworth analog prototype. Assume $f_s = 40$ Hz. Write the resulting difference equation for running the filter.

10.30 Repeat Problem 10.29, but obtain a Chebyshev digital LP filter with a ripple bandwidth of 5 Hz. Let the peak to peak ripple be 1 dB.

10.31 Starting with eq. 10.82a, obtain the Chebyshev polynomial recursion formula. Hint: use the identity, $\cos((n+1)x) = 2\cos(x)\cos(nx) - \cos((n-1)x)$. Sketch $C_4(\Omega)$, and $C_5(\Omega)$, and the resulting $M_N^2(\Omega)$.

10.32 Study the transformation $s = (z+1)/(z-1)$ for obtaining a digital filter from an analog LP prototype. What kind of digital filter results? Derive an expression that relates the analog filter and digital filter input frequencies.

10.33 Suppose that by any of several methods a digital LP filter $H_1(z)$ with BW = 1 Hz has been designed. Consider obtaining another digital filter $H_2(z)$ with

$$H_2(z) = H_1(z)|_{z \leftarrow f(z)}$$

where $f(z) = -z$. Show that $H_2(z)$ is the transfer function of a digital HP filter, and determine the cut-off frequency, if $f_s = 10$ Hz.

10.34 Suppose that $f(z) = -z^2$ is used in Problem 10.33 to obtain $H_2(z)$. What type of filter results? Sketch $M_2^2(\omega)$ for $\omega = 0$ to ω_s.

10.35 Find the transfer function of an analog Butterworth LP filter with BW = 100 Hz, such that the gain is down at least 20 dB at 400 Hz. With $f_s = 2000$ Hz, use the bilinear transformation to obtain a digital LP filter such that the gain of the digital filter at 100 Hz is the same as that of the analog filter at 100 Hz. What is the bandwidth of the resulting digital filter?

10.36 Use the bilinear transformation to design a digital BP filter with cutoff frequencies at 1500 Hz and 2500 Hz such that the gain is down at least 20 dB at 500 Hz and 5000 Hz. Use a Butterworth prototype, and assume that $f_s = 20$ KHz.

10.37 The bilinear transformation is based on the trapezoidal integration formula, which is one of many numerical integration formulas. Another numerical integration formula is Simpson's rule, which is given by

$$y(k+1) = y(k-1) + \frac{T}{3}(u(k+1) + 4u(k) + u(k-1))$$

Obtain a transformation based on Simpson's rule for discretizing an analog system described by $G(s)$. Determine an expression that relates the analog and digital filter input frequencies. Does this transformation map the $j\Omega$-axis in the s-plane onto the unit circle in the z-plane? Will it always yield a stable digital filter from a stable analog filter? Now use

$G_N(p) = 1/(p+1)$ as a normalized analog LP filter prototype to obtain $H_1(z)$ using the bilinear transformation and to obtain $H_2(z)$ using the transformation based on Simpson's rule. The bandwidth of both $H_1(z)$ and $H_2(z)$ is to be 1 Hz, where $f_s = 10$ Hz. Sketch both $M_1^2(\omega)$ and $M_2^2(\omega)$. Which digital filter provides more stop-band attenuation?

10.38 Design a digital HP filter based on an analog Chebyshev LP filter prototype with a 1 dB peak to trough ripple. With $f_s = 200$ Hz, the digital filter cut-off frequency should be 80 Hz, and the gain should be down at least 20 dB for frequencies less than 50 Hz. Use the bilinear transformation method.

10.39 Design a digital BS filter with cut-off frequencies at 40 Hz and 80 Hz, such that the gain is down at least 20 dB for frequencies greater than 50 Hz and less than 70 Hz. Apply the bilinear transformation to a Butterworth analog prototype, and use $f_s = 400$ Hz.

10.40 With $f_s = 5$ Hz, use the impulse invariant method to discretize an analog system with transfer function $G(s) = s/(s^2+s+1)$. Sketch $M_G^2(\omega)$ and $M^2(\omega)$. What is the major cause for the difference between the analog and digital filter frequency responses?

10.41 Using the modified impulse invariant method, design a digital HP filter based on a second order Butterworth analog filter prototype. The sampling frequency is $f_s = 1000$ Hz, and the digital HP filter cut-off frequency should be 200 Hz.

10.42 Repeat Problem 10.40, but use the unit step invariant method.

10.43 A third order analog Butterworth LP filter with $\omega_c = 1$ is described by $G(s) = 1/((s+1)(s^2+s+1))$. Using the matched Z-transform method, obtain a digital filter $H(z)$ from $G(s)$. The digital and analog filter should have the same zero frequency gain. Use $f_s = 10$ Hz, and write the resulting difference equation. Sketch $M^2(\omega)$ for $\omega = 0$ to ω_s.

10.44 Suppose the following transformation, i.e.

$$s = \frac{z^2 - 2z\cos(\omega_0 T) + 1}{z^2 - 1}$$

is used to obtain a discrete time system with transfer function $H(z)$ from an analog LP filter $G(s)$ with BW $= \Omega_c$. Show that $H(z)$ is a BP filter, and that $H(z)$ will be stable if $G(s)$ is stable. Obtain an expression that relates the analog and digital filter input frequencies. If ω_1 and ω_2 are the lower and upper digital filter cut-off frequencies, respectively, which must map to $-\Omega_c$ and $+\Omega_c$, respectively, then show that ω_0 is determined with

$$\cos(\omega_0 T) = \frac{\sin((\omega_1 + \omega_2)T)}{\sin(\omega_1 T) + \sin(\omega_2 T)}$$

Now, apply this transformation to obtain a digital BP filter with $\omega_1 = 20$ Hz, $\omega_2 = 40$ Hz, and $f_s = 200$ Hz. Base the design on a normalized analog prototype filter with $G_N(p) = 1/(p+1)$. Sketch the magnitude frequency response $M^2(\omega)$ for $\omega = 0$ to ω_s.

10.45 Assume that $H_1(z)$ is a digital LP filter with BW $= \omega_c$. Show that if ω_0 is sufficiently greater than ω_c, then $H_2(z)$, as obtained with

$$H_2(z) = H_1\left(ze^{j\omega_0 T}\right) + H_1\left(ze^{-j\omega_0 T}\right)$$

is a BP filter. Let $H_1(z) = a(1+z^{-1})/((1+a)-(1-a)z^{-1})$, where $a = \tan(\pi/16)$, which is an LP filter with $\omega_c = \omega_s/16$. For this $H_1(z)$, obtain $H_2(z)$ with $\omega_0 = \omega_s/4$, and sketch $M_2^2(\omega)$ for $\omega = 0$ to ω_s. What happens to $M_2^2(\omega)$ as ω_0 is decreased?

10.46 The transfer function $H_1(z)$ of a digital LP filter with $\omega_c = 2\pi$ when $f_s = 16$ is given by

$$H_1(z) = \frac{0.2(1+z^{-1})}{1.2-0.8z^{-1}}$$

Determine and sketch the group delay $\tau(\omega)$ for $\omega = 0$ to ω_s. Consider cascading $H_1(z)$ with one second order all-pass section $H_{EQ}(z)$ as given in eq. 10.15a. In terms of the poles $p = \alpha e^{\pm j\beta}$ of the all-pass section, write an expression for the overall group delay $\tau_2(\omega)$, where $H_2(z) = H_1(z)H_{EQ}(z)$. Now, by guess and try, specify values for α and β such that a reasonably constant group delay $\tau_2(\omega)$ occurs in the frequency range $\omega = 0$ to 4π. Sketch the overall group delay for $\omega = 0$ to ω_s.

10.47 Consider a linear phaseshift FIR filter for which $H(z) = (1+az^{-1})(1+(1/a)z^{-1})$. Two possible realizations are shown in Fig. P10.47.

Let us investigate what happens to the frequency response of the filter due to representing coefficient multipliers with a finite number of binary digits (bits). Let $a = 0.8$, and obtain and sketch $M^2(\omega)$ for $\omega = 0$ to ω_s. Now, suppose we must represent each coefficient with only two integer bits and two fractional bits, which are obtained by rounding off the binary representation, i.e., add $(0.001)_2$ to the binary representation and truncate to two fractional bits. Therefore, $c_1 \equiv (00.11)_2 = (0.75)_{10}$, $c_2 = (01.01)_2 = (1.25)_{10}$, and $c_3 \equiv (10.00)_2 = (2.0)_{10}$. Which realization, i.e., the cascade or direct, preserves the linear phaseshift characteristic? Now, for each realization write $M^2(\omega)$ in terms of the coefficient multipliers c_1, c_2, and c_3. An indicator of the gain sensitivity to coefficient multiplier quantization error is $\partial M^2/\partial c_i$. For example, show that

$$\left.\frac{\partial M^2}{\partial c_1}\right|_{c_1 = 0.80,\, c_2 = 1.25} = (1.6 + 2\cos(\omega T))\,(2.5625 + 2.5\cos(\omega T))$$

Also, obtain the gain sensitivities with respect to c_2 and c_3. In general, these sensitivities depend on the input frequency. Which realization is less gain sensitive to coefficient multiplier quantization errors?

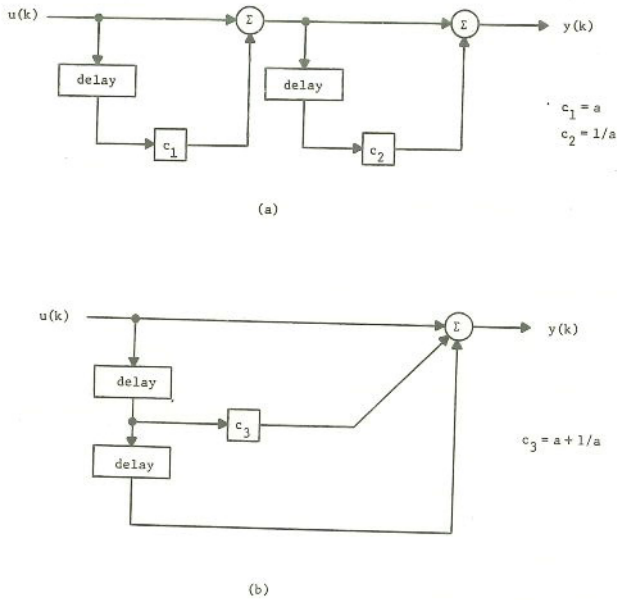


Fig. P10.47. Two realizations for $H(z)$.

10.48 Consider the digital LP filter

$$y(k) = 0.05u(k) + 0.95y(k-1)$$

where $y(-1)$ is the initial condition and $u(k)$ is the input. Let us investigate what happens due to quantizing the result of a multiply accumulate operation. It will be arithmetically convenient if we let $u(k) = u_{-1}(k)$, and then, ideally, the steady-state response for any initial condition is 1.0. However, suppose that each $y(k)$, $k = 0, 1, \cdots$ is rounded off to two fraction digits, i.e., add 0.005 and truncate to two fraction digits, before it is used to process the next input sample to obtain the next output. For example, if $y(-1) = 0.83$, then $y(0) = 0.8575$. But, due to rounding off, $y(0) = 0.86$ will be used to obtain $y(1)$, which is rounded off to obtain $y(2)$, etc. Manually, compute $y(k)$, $k = 0, 1, \cdots$ until steady-state conditions for two fraction digits have been reached for each of the initial conditions: $y(-1) = 0.80, 0.85, 0.90, 0.95, 1.05, 1.15$, and 1.25. What happened for initial conditions less than 0.91 and greater than 1.11? This phenomenon is called the **deadband effect**, to which digital filters are susceptible.

COMPUTER PROJECTS

10.49 Write a main program that uses subroutine FILTER given in Fig. 10.8 to obtain the response of a BP filter with transfer function given by

$$H(z)=\frac{z^2-\frac{5}{3}z+\frac{2}{3}}{z^2-\frac{4}{3}z+\frac{8}{9}}$$

Let $f_s = 16$ Hz.

(a) Suppose the input is $u(k)=\sin(\omega_a kT)+\sin(\omega_b kT)$, where $\omega_a = 2\pi(2)$ and $\omega_b = 2\pi(4)$. Obtain 128 point plots, which should be sufficient to discern the steady-state response, of the input and output. Assume zero initial conditions.

(b) Now let the input be $u(k)=\sin(\omega kT)$, and obtain plots of the output for $\omega = 2\pi, 30\pi$, and 34π. Explain any differences and similarities between these outputs.

10.50 Modify the main program of Problem 10.49 to implement the procedure described in Problem 10.7. The program should first obtain a 256 point response to $u(k)=\sin(\omega kT)$, where $\omega = 2\pi$, for $k = 0, 1, \cdots, 127$, and $u(k) = 0$, for $k = 128, 129, \cdots, 255$, of the filter in Problem 10.49. The program should plot $y(k)$, $k = 0, 1, \cdots, 255$. For what range of k have we achieved a zero phaseshift BP filter? Repeat the above for $\omega = 8\pi$.

10.51 Modify the main program of Problem 10.49 to implement a filter, which consists of the $H(z)$ given in Problem 10.49 cascaded with itself. Now repeat parts (a) and (b) of Problem 10.49. It may be necessary to increase the number of points to discern the steady-state response.

10.52 Write a main program that uses the following subroutine to compute and plot the frequency response of the FIR filters resulting from Problems 10.13, 10.18, and 10.19. Obtain the frequency responses for $K = 10$ and 50. Without windowing, is the amplitude of Gibbs' oscillation reduced as K is increased? Now consider the desirable attributes of a window function as arrived at from eqs. 10.32, and make up a window function $w_{reader}(i)$. Use this window function to obtain the frequency response for $K = 5$, 20, and 50. In all cases, be careful to use the proper window width. Does $w_{reader}(i)$ reduce the amplitude of Gibbs' oscillation without increasing the transition bandwidth too much?

```
      SUBROUTINE SYMFIR (T,H,K,N)
      DIMENSION H(128),AMP(1024),W(1024)
      FF=(1./T)/2.
      DW=2.*3.1415926*FF/N
      DO 1 J=1,N
      W(J)=(J-1)*DW
      AMP(J)=H(K+1)
      DO 1 I=1,K
      M=I-1
    1 AMP(J)=AMP(J)+2.*H(I)*COS((K-M)*T*W(J))
      CALL PLOT('FIR-FILTER-FREQ-RESPONSE',N,
```

```
1 AMP,'--MAG---',W,'RAD/SEC-')
  RETURN
  END
```

This subroutine implements eq. 10.36a, and computes and plots N points of the magnitude frequency response. The array H contains the unit pulse response, i.e., $H(1) = h(0), \cdots, H(K+1) = h(K)$.

10.53 Modify the subroutine given in Problem 10.52 to compute and plot $\hat{H}(e^{j\omega T})$ according to eq. 10.36b, and write a main program to obtain the frequency response of the FIR differentiator resulting from Problem 10.16. Do this for $K = 5, 20$, and 50. What happens to Gibbs' oscillation as K is increased? Repeat the above, but use the Hann and Bartlett windows. Does either of these windows prevent sign changes in $\hat{H}(e^{j\omega T})$ for $0 \le \omega < \omega_s/2$?

10.54 Write a main program that uses the DFT as computed with the FFT algorithm to determine the unit pulse response of a linear phaseshift FIR filter by the frequency sampling method. Do this for the LP filter specified in Problem 10.13 (See Fig. P10.13a.) with 8 and 32 frequency samples. Also, modify the subroutine in Problem 10.52 to obtain the frequency response according to eq. 10.38a. For each case, obtain plots of the FIR filter unit pulse response and a 128 point frequency response. Does increasing the number of frequency samples reduce oscillations in the frequency response? Repeat the above for the LP filter given in Fig. 10.13b ($\Delta\omega = 100\pi$). Does introducing a transition band reduce oscillations in the frequency response? Is $\Delta\omega = 100\pi$ necessarily the best transition band width for the least frequency response oscillations?

10.55 With $f_s = 5$ Hz, obtain 1 Hz ripple bandwidth digital LP filters from a second order 1 dB ripple analog Chebyshev LP filter by the bilinear transformation, the impulse invariant method, and the matched Z-transform method. Write a main program, which uses the FFT algorithm, to compute and plot a 256 point frequency response for each of the resulting digital filters. Which filter has the best stop band attenuation? Which filter incurs the most aliasing error? Which filter best preserves the equal ripple characteristic of the analog filter?

10.56 Write a main program and support subroutines similar to the programs given in Example 10.20 that will determine the poles of the all-pass phase equalizer for the LP filter described in Problem 10.46. Also, obtain 256 point plots of the original and equalized group delay. Try both 11 and 21 frequency points over the frequency range $\omega = 0$ to 4π. Use the result of Problem 10.46 as the initial guess for the poles.

10.57 Consider again the digital BP filter given in Problem 10.49 as it would be implemented with finite word length digital hardware, where the input, filter coefficients, and addition and multiplication results must be quantized to a finite number of bits. Also, addition or multiplication may produce a result that is outside the range of numbers that can be represented with the given number of bits. This is called **overflow**, in which case the result is replaced with the largest positive or negative value that can be represented with the given number of bits, i.e., the **saturated value**. It would be convenient to be able to simulate binary round off quantization on a general purpose computer. For this, the following function subprogram QUANT is useful. It accepts a number X in base 10, performs a binary round off to NF fractional bits, and returns the binary quantized number in base 10. Also, if X is outside the

range $[-QMAX, QMAX]$, where $QMAX = 2^{NI} - 2^{-NF}$, and NI is the number of integer bits, then X is rounded off to the saturated value $\pm QMAX$. For example, if X = –4.196, then Y=QUANT(X,3,2) yields Y = –4.25, while Y=QUANT(X,2,3) yields the saturated value Y = –3.875. With NI large enough, saturation can be avoided. NI and NF cannot be less than zero, and NI and NF cannot both be zero.

```
      FUNCTION QUANT(X,NI,NF)
      QUANT=0.
      IF(NI.LT.0.OR.NF.LT.0) RETURN
      IF(NI.EQ.0.AND.NF.EQ.0) RETURN
      IF(X.EQ.0.) RETURN
      AX=ABS(X)
      SIGN=1.
      IF(X.LT.0.) SIGN=-1.
      IX=AX
      FX=AX-IX
      TWOPNI=FLOAT(2**NI)
      TWOMNF=1./FLOAT(2**NF)
      QFX=0.
      IF(NF.EQ.0) GO TO 2
      DO 1 I=1,NF
      FX=2.*FX
      IF(FX.LT.1.) GO TO 1
      FX=FX-1.
      QFX=QFX+1./FLOAT(2**I)
1     CONTINUE
2     FX=2.*FX
      IF(FX.GE.1.) QFX=QFX+TWOMNF
      QX=IX+QFX
      QMAX=TWOPNI-TWOMNF
      IF(QX.GT.QMAX) QX=QMAX
      QUANT=SIGN*QX
      RETURN
      END
```

Write a main program that uses subroutine FILTER given in Fig. 10.8. Add NI and NF to the argument list of subroutine FILTER, and replace the statement

```
SUM=SUM+C(INDEX)*Y(INDEX)
```

with

```
CY=C(INDEX)*Y(INDEX)
X=SUM+QUANT(CY,NI,NF)
SUM=QUANT(X,NI,NF)
```

With variations of the above replacement, product only and sum of products only quantization can also be simulated. In the main program, use statements such as B0=QUANT(B0,NI,NF) to quantize the filter coefficients.

(a) Obtain 256 point plots of the unit step response of the BP filter given in Problem 10.49 for NI=3 and NF=12, 8, 4, and 2. Use zero initial conditions. Ideally, the steady-state unit step response is zero. However, what happens to the transient and

the steady-state response as the number of binary fraction bits is reduced? Is the filter stable for every case? Does the steady-state response settle to a constant value for every case? Repeat the above for NI=1.

(b) Now, suppose the input is $u(k) = A \sin(8\pi kT)$, where $f_s = 16$, and NI and NF are fixed at NI=1 and NF=6. Notice that the input must also be quantized. What is the maximum input amplitude to avoid digital filter input saturation? With this maximum input amplitude, obtain and plot the filter response for zero initial conditions. Does the output ever become saturated? If it does saturate, then scale $H(z)$ to obtain a response that does not saturate. Give reasons for why the steady-state response is not a pure sinusoid.

10.58 Modify the function subprogram QUANT to perform quantization by truncation, and repeat Problem 10.57.

About the book

This book presents the fundamentals of continuous and discrete time signal processing. It is intended for the reader with little or no background in this subject. The emphasis is on development from basic principles.

The first chapter gives an overview of some applications of signal processing. Then, this book presents topics such as: system properties, convolution, periodic continuous and discrete time signals, the discrete Fourier transform (DFT) and its applications, the Fourier transform, the fast Fourier transform (FFT), correlation analysis, the Laplace transform, the Z-transform, state variable methods for describing and analyzing continuous and discrete time linear and time invariant systems, the design of digital filters, and the application of special purpose microprocessors for real-time digital signal processing.

Some features of this book are:

1) gradual and step-by-step development of the mathematics for signal processing,
2) numerous examples and homework problems,
3) many examples of using the computer for applying the theory,
4) emphasis on the relationship between continuous and discrete time signal processing,
5) computer based assignments to gain practical insight,
6) a set of computer programs to aid the reader in applying the theory.

With this book the reader can become knowledgeable about both the theoretical and practical aspects of digital signal processing.

About the author

Roland Priemer received the Ph.D. degree in Electrical Engineering from the Illinois Institute of Technology in 1969. Presently, he is a member of the faculty in the Department of Electrical Engineering and Computer Science at the University of Illinois at Chicago. Dr Priemer's research interests are in optimal and adaptive digital signal processing. He has published papers on topics in graph theory, estimation theory, and microprocessor based applications of digital signal processing. He is a consultant to industry generally in areas such as biomedical signal processing, digital system hardware and software design, and process control.

0864 sc

ISBN 9971-50-920-2 (pbk)